Design and Synthesis of Dual-active Heterocyclic Hybrid Inhibitors for β-Hematin and *Plasmodium falciparum N*-Myristoyltransferase

by
Jonathan Bruce Hay

Thesis presented in partial fulfilment of the requirements for the degree of Master of Science at Stellenbosch University

Supervisor: Dr Margaret A. L. Blackie
Co-supervisor: Dr Katherine A. de Villiers

Department of Chemistry and Polymer Science
Faculty of Science

March 2016

DECLARATION

By submitting this thesis electronically, I declare that the entirety of the work contained therein is my own, original work, that I am the sole author thereof (save to the extent explicitly otherwise stated), that reproduction and publication thereof by Stellenbosch University will not infringe any third party rights and that I have not previously in its entirety or in part submitted it for obtaining any qualification.

March 2016

ABSTRACT

The current project focused on the design and synthesis of a novel antiplasmodial dual-active conjugate hybrid compound based on an indole scaffold and known antiplasmodial quinolines. The two scaffolds were chosen to target independent pathways in the malaria parasite, namely *N*-myristoylation and hemozoin formation.

Initially, a novel indole compound, ethyl 4-(piperidin-4-yloxy)-1*H*-indole-2-carboxylate, which would possibly function as a *Plasmodium N*-myristoylation inhibitor, was synthesised. This would also function as the precursor to the proposed hybrid compound. The synthetic methodology that was employed included the synthesis of starting materials, 2-(benzyloxy)benzaldehyde and ethyl 2-azidoacetate, utilizing well-known benzyl protection and substitution reactions. These compounds were condensed into an azide cinnamate, (*Z*)-ethyl 2-azido-3-[2-(benzyloxy)phenyl]acrylate, via the Knoevenagel condensation reaction. An alternative method was investigated to obtain the same azide compound via an Arbuzov ylide formation and Horner-Wadsworth-Emmons Wittig-type reaction to obtain an *E*-stereospecific cinnamate, (*E*)-ethyl 3-[2-(benzyloxy)phenyl]acrylate, followed by a cerium ammonium nitrate mediated azide addition to afford the azide cinnamate. The azide cinnamate was later subjected to a Hemmetsberger thermal cyclization to form the indole scaffold, ethyl 4-(benzyloxy)-1*H*-indole-2-carboxylate, followed by a Mitsunobu reaction to afford the novel indole compound. Saponification yielded the carboxylic acid indole derivative, 4-(benzyloxy)-1*H*-indole-2-carboxylic acid, which was to function as a precursor to the hybrid compound, since an amidation reaction was considered as a possible method for coupling the indole and quinoline scaffolds.

Later, 4,7-disubstituted quinoline derivatives were targeted as these would function as the second heterocyclic scaffold for the intended hybrid compound. These were synthesized according to the Gould-Jacobs, Skraup and Doebner-Miller methods, using simple *m*-substituted anilines as starting materials. The Gould-Jacobs reaction provided the desired 4-chloro-7-substituted quinolines (7-Br, -F, -NO_2, -$CH_3$and -OCH_3), however, the Skraup and Doebner-Miller reactions only provided the 7-substituted quinolines (7-Br, -CH_3 and -OCH_3) and required the use of a subsequent oxidation reaction to yield quinoline *N*-oxides that were later chlorinated to give the desired 4-chloro-7-substituted quinolines. Following the synthesis of the desired quinoline substructures, the 4-chloro-7-substituted quinolines were converted to the desired quinoline pendant groups, N^1-7-X-quinolin-4-yl)ethane-1,2-diamine (X = CF_3 and Cl), via a chloride substitution reaction using diamino ethane.

Preliminary investigations were carried out to obtain the proposed hybrid compound and to ascertain whether an amidation reaction was suitable for the coupling of the two heterocyclic scaffolds. Given time constraints towards the end of the project, only an *N*, *N*′-carbonyldiimidazole (CDI) facilitated amidation was investigated. Unfortunately, the approach was not successful. The challenge remains

therefore, to utilize the methodologies optimized in this project to investigate heterocyclic hybrid compounds as novel resistance reversers in the treatment of malaria

UITTREKSEL

Die huidige projek het gefokus op die ontwerp en sintese van 'n nuwe, unieke antiplasmodiale, dubbel geaktiveerde hibriedverbinding wat as uitgangspunt op 'n indoolbasis en bekende antiplasmodiale kinoliene gerig is. Twee weë is gekies om onafhanklike roetes in die malaria-parasiet, naamlik *N*-miristoïelisasie en hemosoïenvorming, te teiken.

Aanvanklik was 'n nuwe indool-verbinding, gesintetiseer, etiel 4- (piperidien-4-ieloksi)-1*H*-indool-2-karboksilaat, wat moontlik sou kon funksioneer as 'n *Plasmodium N*-myristoylation inhibeerder. Dit sou ook kon dien as die uitgangsverbinding tot die voorgestelde hibriedverbinding. Die sintese metodiek wat in gebruik was, was onder meer, die sintese van die uitgangsverbindings, 2-(bensieloksi) bensaldehied en etiel 2-asidoasetaat, deur die gebruik van bekende bensiel-beskerming en substitusie-reaksies. Hierdie verbindings was verander na ‘n asiedsinnamaat, (*Z*)-etiel-2-asido-3-[2-(bensieloksi)feniel]akrilaat, deur die Knoevenagel kondensasie-reaksie. 'n Alternatiewe metode was ook ondersoek om dieselfde asiedverbinding te verkry deur 'n Arbuzov iliedvormings reaksie en’n Horner-Wadsworth-Emmons-Wittig-tipe reaksie om 'n *E*-stereospesifieke sinnamaat te verkry, (*E*)-etiel 3-[2-(bensieloksi)feniel]akrilaat , gevolg deur 'n serium-ammoniumnitraat bemiddelde asied byvoeging om die asiedsinnamaat te verkry. Om die gewenste indool bousteen te berei en dan die nuwe unieke indoolverbinding te verkry, was die asiedsinnamaat onderworpe aan 'n Hemmetsberger termiese siklisasie om etiel 4-(bensieloksi)-1*H*-indool-2-karboksilaat te verkry en gevolg deur 'n Mitsunobu-reaksie. Verseeping lewer die karboksielsuur-indool-afgeleide, 4-(bensieloksie)-1H-indool-2-karboksielsuur.Hierdie verbinding sou as 'n voorloper dien vir die sintese van die hibriedverbinding aangesien 'n amidasie-reaksie as 'n moontlike koppelings metode vir die indool- en kinolien-boustene, om die hibriedverbinding te vorm, oorweeg was.

Later was 4,7-digesubstiteerde kinolien-afgeleides gebruik omdat dit as die tweede heterosikliese bousteen sou kon funksioneer vir die beoogde hibriedverbinding. Hierdie verbindings was gesintetiseer volgens die Gould-Jacobs, Skraup en Doebner-Miller metodes, deur die gebruik van eenvoudige *m*-gesubstiteerde aniliene as uitgangsverbindings. Die Gould-Jacobs reaksie het die gewenste 4-chloor-7-gesubstiteerde kienoliene (7-Br, -F, -NO2, -CH_3 en -OCH_3) gelewer. Die Skraup en Doebner-Miller reaksies het slegs die 7-gesubstiteerde kinoliene (7-Br, -CH_3 en -OCH_3) gelewer en het die gebruik van 'n daaropvolgende oksidasie-reaksie vereis om kinolien *N*-oksiede te berei, wat later gechlorineer was om die verlangde 4-chloor-7-gesubstiteerde kinoliene te gee. Na aanleiding van die sintese van die vereiste kinolien-substrukture, was die 4-chloor-7-gesubstiteerde kinoliene omgeskakel na die gewenste kinolien sygroepe, N^1-7-X-(kinolien-4-iel)etaan-1,2-diamien (X = CF3 en Cl), deur 'n chloried gesubstitusie-reaksie met behulp diaminoetaan.

ACKNOWLEDGEMENTS

I would like to acknowledge Stellenbosch University for giving me the opportunity to have done this masters project. This institution is truly one of the best and those of us who have been blessed to have spent any length of time here, know that this university is a unique and special place. It becomes a part of you which you carry with you for the rest of your life.

I wish to humbly thank my supervisors, Dr Margaret A.L. Blackie and Dr Katherine A. de Villiers. Thank you for your support and guidance the last few years. You've given me the opportunity to further my chemistry studies and for that I thank you both. You are both very dear to me and are brilliant chemists and supervisors, and no one could have asked for a better pair of ladies to work for. You've pushed me to do my best and exceed expectations and words cannot express the gratitude I feel for everything you have done for me.

I would also like to acknowledge the National Research Foundation and Dr. Katherine de Villiers for their generous financial support, without which I wouldn't have been able to have done this amazing project.

To Monica Clement, I extended a very special thank you. You are the best friend I could ask for, thank you for all your help and guidance these past two months, and, the 22 before that. You've made lab life a joy for me, especially when you have to listen to me and my special ability of taking song lyrics and turning them into something the song writers never thought possible, my temporary moments of insanity when my fume hood became the stage for World War Three when reactions end up failing, or just generally listening to me talk about the most random subject know too humankind. We've had some good times and some bad, but mostly good. Thank you for everything you've done for me and with me, these last two years getting to know you have been a blessing and I hope we remain friends for many more years to come.

It would be foolish of me if I don't give a warm and heartfelt thank you to Raymond, Mubarrick and 'auntie' Mary, our technical staff. Thank you all for the good times we've spent chatting but most importantly I say thank you for all your assistance in the laboratory with timely deliveries of chemicals and equipment which assisted me in keeping to my schedules. You are truly special to me and you can be sure I hold you very dear to my heart.

To my colleagues in the Group of Medicinal and Organic Chemistry thank you for the friendship, advice and the all-round joking that we do during lunch breaks to keep ourselves entertained. You are all exceptional people and chemists to boot. I would also like to say thank you to Elsa Malherbe and Dr. Jaco Brand for your assistance with running NMR analysis for me, especially Elsa, you are truly an expert and a wonderful person, thank you. Thank you Dr. Marietjie Stander at CAF MS unit for

running the ton of MS samples that I had sent in during this write-up and getting the results to me so quickly, it was much appreciated. I'd also like to give a special thank you to Mr. Johan Malherbe for his assistance with corrections of the afrikaans abstract.

Last, but never the least, to my family, Kevin, Anna-Marie and Christopher Hay. I thank you with all the love I possess and more. You have watched this boy grow into a man and supported me through my life with everything I've done. Thank you for your assistance during this write-up, it is truly appreciated. You've been there through the thick and thin, the unconditional love and support you give helps me through anything and everything. I love you all and thank you.

CONFERENCE ATTENDANCE

Bi-national Organic Chemistry Conference (BOCC) **2014**, Stellenbosch, South Africa

Poster: *Design and Synthesis of Novel Dual-activity Inhibitors for Plasmodium and β-Hematin*

"*Perseverance - when obstacles arise, you change your direction to reach your goal, you do not change your decision to get there*." – Zig Ziglar

TABLE OF CONTENTS

PREFACE

ABBREVIATIONS

3D7	Chloroquine-sensitive *Plasmodium* parasite
ACT	Artemisinin-based combination therapy
ADQ	Amodiaquine
ART	Artemisinin
Asym	Asymmetric
ATV	Atovaquone
CAN	Cerium(IV) ammonium nitrate
CDI	*N*,*N*′-Carbonyldiimidazole
CG	Cycloguanil
cm^{-1}	Reciprocal centimeters
CQ	Chloroquine
CRT	Chloroquine resistance transporter
Cytb	Cytochrome b
Cytc1	Cytochrome c1
DBAD	Di-*tert*-butyl azidocarboxylate
DBU	Diazabicycloundecene
DCM	Dichloromethane
DHA	Dihydroartemisinin
DHF	Dihydrofolate
DHFR	Dihydrofolate reductase
DHPS	Dihydropteroate synthase
DMF	Dimethyl formamide
DMSO	Dimethyl sulphoxide
DMSO-d_6	Deuterated dimethyl sulfoxide
DNA	Deoxyribonucleic acid
ES (-/+)	Electro-spray ionization (negative/positive)
ETFA	Ethyl trifluoroacetate
EtOAc	Ethyl acetate
FPT	Freeze-pump-thaw
FTIR	Fourier-transform Infrared spectroscopy
Hb	Hemoglobin
Hex	Hexane

HPPK	Hydroxymethylpterin pyrophosphokinase
HRMS	High resolution mass spectrometry
HWE	Horner-Wadsworth-Emmons
Hz	Hertz
IC_{50}	Half maximum inhibitory concentration
IMC	Inner-membrane complex
IRS	Insecticide residual spraying
ITN	Insecticide-treated bed nets
K1	Chloroquine-resistant *Plasmodium* parasite
LL-PTC	Liquid-liquid phase transfer catalysis
M	Molar concentration
m/z	Mass-to-charge ration
MDG	Millenium development group
MDR	Multi-drug resistant
MeCN	Acetonitrile
MHz	Megahertz
mM	Millimolar
Myr-CoA	Myristoyl-coenzyme A
nM	Nanomolar
nm	Nanometers
NMR	Nuclear magnetic resonance
NMT	*N*-myristoyltransferase
P.	*Plasmodium*
Pf	*Plasmodium falciparum*
PG	Proguanil
Pv	*Plasmodium vivax*
PYR	Pyrimethamine
QN	Quinine
RBC	Red blood cell
RBM	Roll back malaria
R_f	Retention factor
SDX	Sulfadoxine
S_N2	Nucleophilic substitution second-order reaction
Str.	Stretching vibration
TBAHS	Tetrabutylammonium hydrogensulfate
THF	Tetrahydrofuran

TLC	Thin layer chromatography
TOF	Time-of-flight
WHO	World Health Organization

CHAPTER 1: INTRODUCTION

1.1 INTRODUCTION

Malaria, a disease caused by a protozoan parasite, is one of the world's most serious public health challenges.[1] The World Health Organization (WHO) estimates that 3.3 billion people are at risk globally of being infected with malaria (WHO World Malaria Report 2014).[2,3] The most prevalent burden is placed on sub-Saharan Africa, with an estimated 90% of all deaths occurring in that region, 78% of which are children aged under 5 years.[2,3] The latest estimates indicate that 198 million cases occurred globally in 2013 with approximately 584 000 deaths (uncertainty of 367 000-755 000) having occurred during that year.[2] On a more positive note, since 2000, decreases in malaria cases and mortality of 30% and 60%, respectively, have been recorded by the WHO.[2] This can, in part, be attributed to the establishment of the Roll Back Malaria (RBM) initiative in 1998, and the Millennium Development Goals (MDG) in 2000.[3,4] The RBM initiative identified the increasing burden that malaria was placing on the poorest people in the world and that greater resources had to be allocated to reducing the malaria burden.[4] The MDG extended the objectives of the RBM to the year 2015 with emphasis on halting and reversing the spread of malaria and other diseases.[3] In 2015 this goal was reached for malaria and a significant portion of the global population is now at lower risk of contracting the disease, as well as having access to more effective resources for control, prevention and chemotherapy.[2,3,5-7]

1.2 MALARIA – A BRIEF HISTORY AND IMPACT

Since ancient times, malaria has played an important role in the movements of population, outcome of wars and the rise and decline of nations.[8,9] As early as 2700 BC, both the Egyptians and Chinese mentioned a disease with deadly periodic fevers and splenomegaly (enlargement of the spleen) in their writings, suggesting that it may have been malarial.[8] Ever since, malaria has impacted world history on a scale that no other infectious disease has and it continues to plague humanity to this day.[8] Alexander the Great's campaign of the Indian subcontinent in 323 BC came to a halt because he died of what is believed to be malaria.[9] Malaria appeared in Rome in 200 BC and spread throughout Europe during the 12th century. Even before the spread of malaria was understood, military commanders developed a crude but effective strategy to avoid 'marsh fever' by not conducting operations in marshy areas, where infections in the troops were observed to drastically increase.[9] More recently, during the United States Naval campaign of the Southwest Pacific in World War II, immense losses in

battle strength were suffered as a result of malarial infections in the troops during conflicts in the tropical regions of the Pacific islands.[9]

However, it is not only in military theatres of war where malaria is recorded to have been an infectious affliction to mankind, but also during times of peace and infrastructural expansion by the global civilization.[10] During the construction of the Panama Canal in the latter part of the 19th century and start of the 20th century, malaria impacted the progress as a result of the drastic increase in the number of infections in the work force.[10]

Alphonse Laveran, in 1880, discovered that protozoa were responsible for malaria infections, but his findings were dismissed by leading malariologists that believed that bacteria was responsible for the infections.[10] The malariologists who had dismissed the findings by Laveran were later proven wrong by scientists and clinicians who confirmed Lavaren's results.[10] Shortly after Lavaren, Ronald Ross in 1887, identified the anopheline mosquitoes as the vectors (carriers) of the parasite. He went on to advocate vector control measures to reduce the population of mosquitoes on and around the construction site at the Panama Canal which proved to be a successful strategy.[10] The completion of the Panama Canal in 1914 justified the use of vector control measures proposed by Ross, which became the dominant method of malaria control for the following 50 years. The approach remains a cornerstone in the fight against malaria today.[10] Together with chemotherapy and case management, vector control makes up the three standards of the WHO recommended control of malaria, with each being as important as the other.[2,5]

Throughout the 20th century, since Ross had first identified the mosquito as the vector of the parasite's transmittance, the debate of vector- versus clinically-based control has continued.[10] The WHO's annual report on malaria sheds some light on the situation in Africa (and the world) regarding the use of vector versus clinical methods of control.[2] The current control methods consist of Insecticide Residual Spraying (IRS), Insecticide-Treated bed Nets (ITN) and Artemisinin-based Combination Therapy (ACT), all of which have shown impressive increases in the prevention of malaria incidents, but there are still millions that are under high risk of infection.[2,3,6] Although ITN and IRS intervention methods make up the foundation of the efforts to reduce infections, they are merely the first stage in combating the epidemic.[3,6] Quinine, first isolated in 1820 from the bark of the *Cinchona* tree, replaced the use of the crude bark as treatment for malaria.[11,12] With quinine and related drugs, such as the synthetic derivative chloroquine, becoming obsolete because of parasite resistance, the use of combination therapies is currently the preferred method for the clinical control of malaria.[6] Certain compounds have been rendered ineffective by excessive and repeated use and as a direct result thereof, the parasite has developed a resistance to some classes of compounds.[5,13,14] This unfortunate drawback has opened the door to further the study into the design and synthesis of new, more effective and resistant drugs to combat the malaria parasite.

1.3 THE PLASMODIUM PARASITE - SPECIES AND LIFE CYCLE

The malaria parasite (protozoa) belongs to the genus *Plasmodium* (*P.*) and the infection of human hosts is associated with four of the five species of the parasite namely, *P. falciparum*, *P. vivax*, *P. ovale* and *P. malariae*.[2,3,15] Of these four species, *P. falciparum* and *P. vivax* are the most prevalent and responsible for the majority of severe infections and mortality.[2] *P. falciparum* is the most dangerous of the disease, with 90% of annual cases, mostly in sub-Saharan Africa, leading to severe infection and death.[2,16] *P. vivax* is the most geographically distributed species in Asia and Americas with approximately 80% of the reported cases being attributed to it.[17] Although *P. vivax* accounts for the majority of infections, the death toll is much lower in comparison to the more infectious and deadly *P. falciparum*.[17] The parasites are transmitted to humans by infected female mosquitoes belonging to the genus *Anopheles*[2,13,18] that transfers the parasite to the host when the mosquito takes a blood meal.

Although many studies of the parasite life cycle have been carried out,[15,18-25] the complexity thereof has made it difficult to completely understand the finer intricacies.[15,18] Nevertheless, research has been fruitful and a universal understanding of the life cycle has been obtained that aids in creating better, more effective and efficient intervention methods.[2,3,6,19] The complex life cycle of the malaria parasite, in this case *P. falciparum*, can be simplified into three stages of development: **1**, **2** and **3** (Figure 1).[15,18,20] The first stage (**1**), occurs with the invasion of the liver cells (hepatocytes) in the human-host by the sporozoites secreted from the salivary glands of the female mosquito vector and circulated to the liver in the blood stream.[18,19,21]

Once the sporozoites have invaded the hepatocytes, development and division occurs, and depending on the parasite species, this stage takes between 6 and 15 days (6 days for *P. falciparum*).[19] At this stage it is worth mentioning, that for the *P. vivax* and *P. ovale* parasites a portion of the parasite population (hypnozoites) remain dormant in the liver cells and can remain so for months or even years.[26] These species are then able to cause a relapse at a later stage by entering a cycle of asexual reproduction of sporozoites causing clinical symptoms without the patient having been exposed to another infected mosquito bite, giving the disease the name “relapsing malaria”.[26]

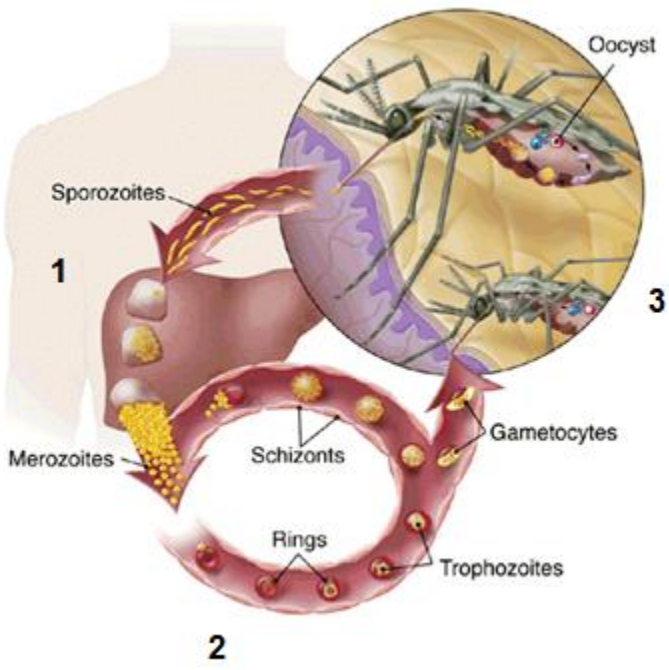

Figure 1 – Simplified representation of the *P. falciparum* malaria parasite life cycle with the three main stages of development; liver cells **1**, red blood cells **2** of human host and tissue cells **3** of mosquito-vector.[18]

Once maturation within the hepatocytes has been reached, they burst and release mature merozoites into the blood stream, where they rapidly attach to and invade human erythrocytes (red blood cells, RBCs). Here they develop through the blood cycle **2** into rings and thereafter into trophozoites.[19,21] The trophozoite stage is the most active metabolic phase of the parasites' life cycle, during which time the trophozoites consume and degrade hemoglobin from the RBCs.[18,27] The trophozoites then mature into schizonts, which divide into daughter cells and, following eruption of the RBC wall, merozoites are again released into the bloodstream repeating the cycle of RBC invasion.[27] This blood cycle repeats every 48 hours until either the immune system of the host responds, chemotherapy is introduced or the patient succumbs to the disease.[19] Following eruption of the RBCs, some merozoites differentiate into gametocytes (sexual form), which are then ingested by another mosquito (female) during a blood meal from the human-host **3**.[19] The gametocytes mature into male (macro) and female (micro) gametes, which after fertilization form diploid zygotes and further transformation forms ookinetes.[19,21] These ookinetes penetrate the midgut walls to finally develop into oocysts, where meiotic division occurs forming sporozoites.[19,21] Rupturing of the oocysts releases the sporozoites that migrate to the salivary glands from where the cycle, described above, can be repeated on the mosquito's next blood meal.[21]

1.4 ANTIMALARIAL DRUGS, DRUG TARGETS AND PARASITE DRUG RESISTANCE

It is during the parasite's blood stage, or intra-erythrocytic phase **2**, that the majority of antimalarial drugs are active. Each class of compounds targets different bio-pathways within the parasite.[28] For the purpose of this thesis, the major classes of drugs, the pathways they target, the mode of action the drugs have and finally parasite resistance towards the drugs will be discussed. The three major pathways that currently-used drugs target are heme detoxification, nucleic acid metabolism, and oxidative stress.[28,29]

1.4.1 Heme-detoxification – Blood Schizontocydes

The blood schizontocydes are quinoline- and artemisinin-containing compounds that act on intra-erythrocytic parasites (*Plasmodium*) both in the asexual and partially in the sexual stages of the life cycle.[29] It is believed that the primary target of the compounds is the food vacuole of the parasite where they exert their inhibitory effects.[27,29-32] The blood schizontocydes are divided into two groups, the first is the Type 1 and Type 2 quinoline-containing drugs and the second is the endoperoxide-containing artemisinin-type drugs. Each group will be briefly discussed according to the drugs in the group, followed by their targeted pathway and finally the parasite resistance applicable to each group.

Group 1 – Type 1 and 2 Quinoline-containing Drugs

This group of antimalarials is the most commonly used and many of the compounds in the group currently experience the highest drug resistance by all the *Plasmodium species*.[2,3,14,28,33] Quinine (Figure 2) was first isolated from the *Cinchona* tree, more specifically the bark of the tree, and has been used as an antimalarial drug since 1820.[11,12] Many structural analogues of quinine have been synthesized over the years and used as antimalarial compounds and have subsequently been grouped into Type 1 and Type 2 drugs, both of which function as inhibitors of hemozoin formation which will be discussed further on in this section. Each of the two types, although similar, functions by a slightly different pathway.[29] Examples of the quinoline-containing drugs are given in Figure 2.

Type 1 drugs all contain the 4-aminoquinoline as substructure and include chloroquine, amodiaquine, ferroquine and ruthenoquine that are all hydrophilic weak bases that are deprotonated at neutral pH.[29] The Type 2 drugs consist of the quinoline methanol's such as mefloquine, halofantrine and the

Cinchona alkaloids (quinine and quinidines amongst others), which are weaker bases than the Type 1 drugs and consequently are protonated at neutral pH making them more lipid soluble.[29] There is however, a third type that can also be grouped into this class of quinoline-containing drugs, namely the organometallic antimalarials. These quinoline-containing drugs incorporate transition metals into the structure (ferroquine and ruthenoquine, Figure 2) that have a mechanism of inhibition similar to Type 1 drugs and show some excellent results towards inhibition.[27,34]

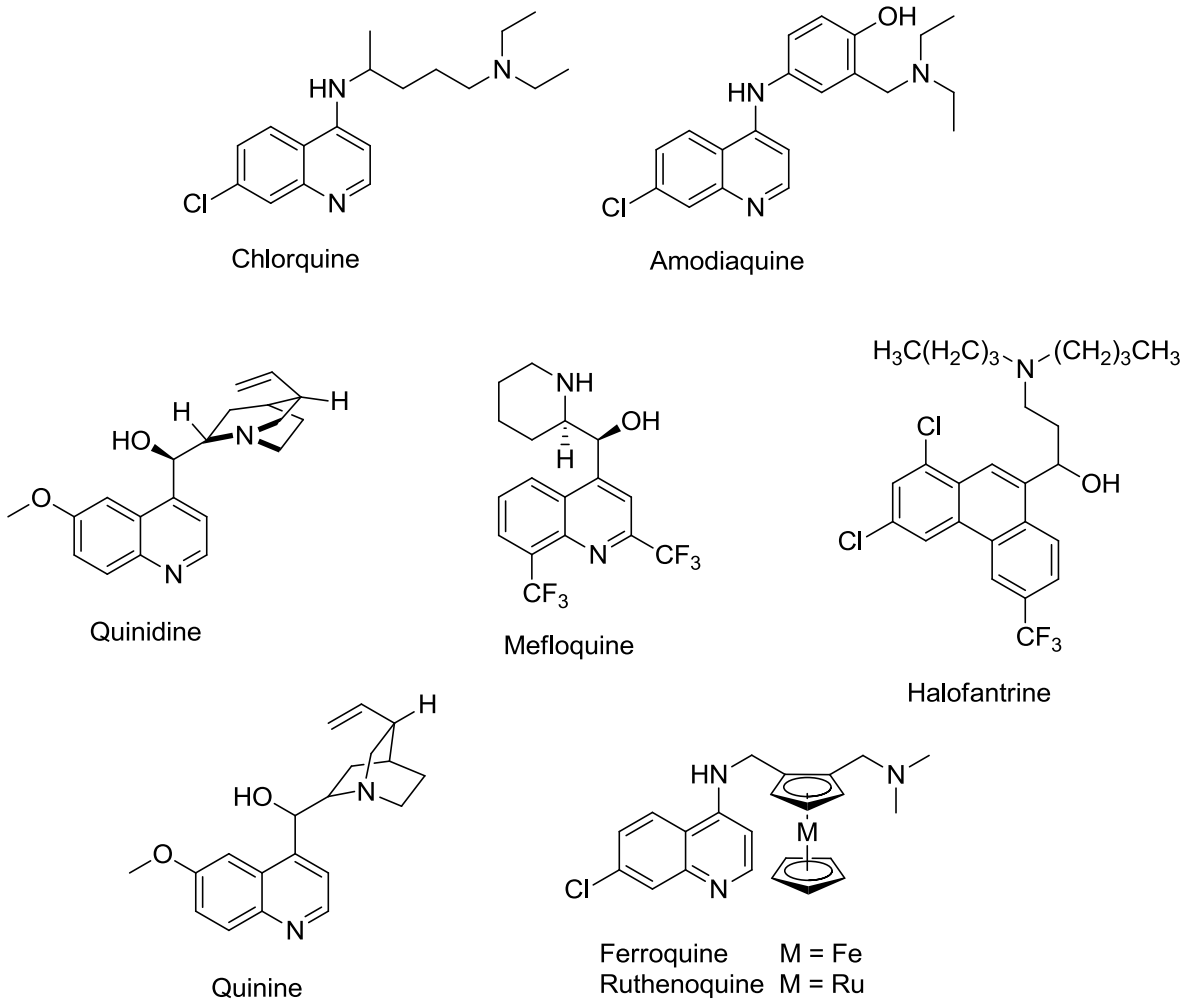

Figure 2 – Representative compounds of the quinoline-containing drugs. [29]

As previously mentioned in the parasite life cycle, the formation of trophozoites is the most active phase of the cycle, occurring within the RBCs with the ingestion and degradation of the host hemoglobin (Hb).[15,27,32] Hemozoin formation is an important step in the process of the parasite's breakdown of the host Hb, with heme and globin being released as by-products from the digestion process.[27,30-32] The release of four equivalents of heme, iron(II) protporphyrin IX (Fe(II)PPIX), per unit of Hb creates a unique problem for the parasite.[32,35] The reason is that the Fe(II)PPIX is released

into the acidic food vacuole, and is oxidized to Fe(III)PPIX, which is toxic to the parasite and if allowed to accumulate, could cause parasite death.[20,31] This is because Fe(III)PPIX is able to generate reactive oxygen-derived species that can induce oxidative stress on the vacuole membrane. This leads to cell lysis and ultimately death of the parasite.[20,32] It is this process of hemozoin formation that Type 1 and 2 drugs target.

To overcome this toxicity problem, the parasite possesses an effective method of detoxification that converts at least 95% of the toxic Fe(III)PPIX to a non-toxic crystalline solid material, known as hemozoin.[36] Synthetically made hemozoin, known as *β*-hematin, was determined to be structurally identical to hemozoin by experimental analysis carried out using X-ray diffraction by Slater *et al*. in 1991.[37] Although the mechanism is not yet fully understood, many theories have been suggested to explain the formation of malaria pigment, hemozoin.[15,20,27,32,38] However, it is generally accepted that the mechanism of formation occurs via a biomineralization process in the food vacuole.[30,31] The host-Hb is transported to the acidic food vacuole where Hb is digested by a series of protease enzymes to release Fe(II)PPIX (Figure 3 - **A**).[20,31] The Fe(II)PPIX is then rapidly oxidized to Fe(III)PPIX (Figure 3 - **B**), which undergoes a process of dimerisation via a μ-propionato coordination forming an Fe(III)PPIX cyclic dimer.[36,39] A biomineralization occurs that forms the crystalline hemozoin (Figure 3 - **C**) by Fe(III)PPIX dimers hydrogen bonding directly to one another and via the propionic acid groups attached to each of the porphyrin.[36] It is not until the pigment is formed that the parasite is free of intoxification by the Fe(III)PPIX.[31]

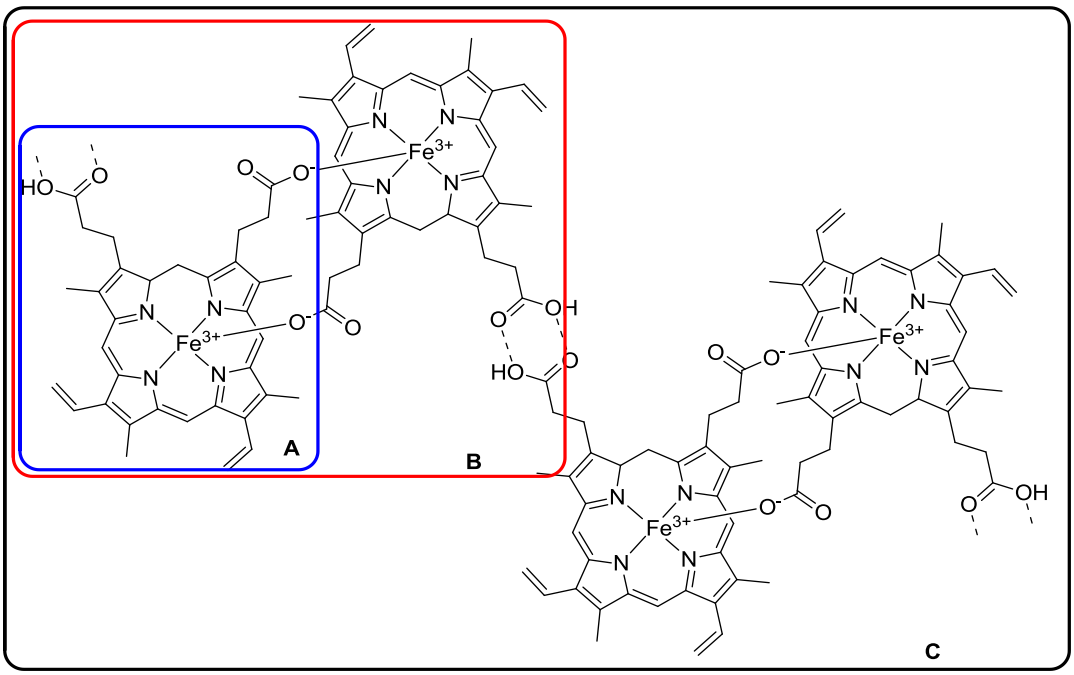

Figure 3 – Structural representation of hematin (**A** - blue), cyclic dimer (**B** – red) and the hemozoin (**C** – black) consisting of the cyclic dimers hydrogen bonded to form the malaria pigment. [20,31]

Antimalarial drugs such as the quinoline-containing *β*-hematin inhibitors target this process of heme-detoxification by inhibiting the formation of hemozoin causing a toxic accumulation of Fe(III)PPIX in the food vacuole that kills the parasite.[31]

All of the antimalarials of this class are based on the *N*-heterocyclic system of a quinoline and tertiary amines, which makes them all able to transverse the vacuolar membrane, where they become protonated in the acidic food vacuole of the parasite and accumulate in large quantities.[14,29] Once protonated, the compound is essentially trapped within the parasite and leads to the observed mM levels of compound in the vacuole compared to nM level outside the parasite membrane.[14,40] However, it is not solely the quinoline substructure that gives the compounds their efficacy, but rather the combination of quinoline and substituents that make these compounds effective antimalarials.[38] Although the mechanism for the inhibition of hemozoin is not fully understood, Figure 4 demonstrates a proposed model for the structure-activity relationship for quinoline-containing compounds. This model, to some extent, can explain how the mechanism for these compounds may possibly proceed and is supported by many other studies.[28,29,14,38,41,42]

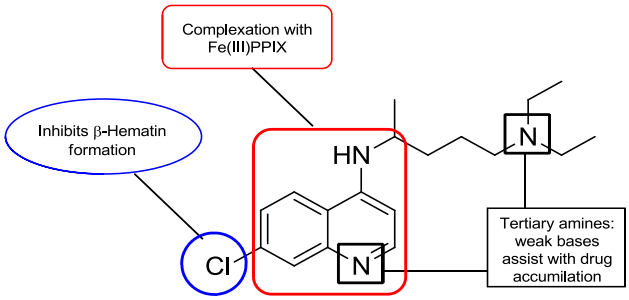

Figure 4 – Representation of the structure-activity relationships of the different moieties of chloroquine and similar quinoline based antimalarial compounds.[38]

Egan *et al.*[38] proposed, that the quinoline nitrogen together with other tertiary amine moieties, are responsible for assisting in membrane cross over into the parasite food vacuole and via pH trapping accumulation of the drug occurs.[38] The aminoalkyl side-chain is required in the compound as it too assists in drug accumulation by trapping of the compound via pH trapping.[38] The 4-aminoquinoline ring system is responsible for the compounds complexing to the Fe(III)PPIX group (formed by Hb digestion) in the vacuole, and is suggested to be the crucial component for hematin binding.[38,43] Once complexed, the 7-position group is required for the correct charge distribution and is responsible for the majority of inhibition of the hemozoin formation, and thus the buildup of toxic heme effectively kills the parasite.[14,28,29,38] It has been reported that stronger electron-withdrawing groups at the 7-position results in a decrease of the pK_a of the quinoline nitrogen that causes a lower accumulation of the compound in the vacuole, thus decreasing the activity. If strong electron-donating groups are substituted onto the 7-position, it was observed that a similar effect occurs.[44] However, it was found that the halogens (bromine, iodine and chlorine) have the most favorable electronic properties for the

compounds to effectively accumulate in the food vacuole, with the chlorine analogues proving to be the most effective at binding with the heme (Fe(III)PPIX).[44]

Resistance towards the quinoline-containing compounds, especially chloroquine, is of great concern in many parts of the world. Efficacy of these drugs is slowly declining and in some cases made completely ineffective (Indo-China) toward many of the *Plasmodium* species.[2,13,40] Many theories have suggested that the resistance towards chloroquine is a result of pH changes in the food vacuole or alterations in membrane permeability.[40] Currently, studies have indicated that the loss in efficacy seems to be a result of the decrease in drug accumulation within the food vacuole, which points to a transport problem.[40] The chloroquine resistance transport protein in *P. falciparum* (*Pf*crt) is associated with a transmembrane protein located on the membrane of the food vacuole and mutations of the *Pf*crt at K76T and the A220S gene can cause the decrease in drug transport into the digestive vacuole and thus reduced drug efficacy.[33,40] Studies have also shown that mutations of the multi-drug resistance 1 gene (*Pf*mdr1), also plays a role in the drug resistance towards the chloroquine, and also the amino alcohols such as mefloquine.[33] However, this has not been entirely confirmed and is still under investigation.[33]

Group 2 – Endoperoxides

Quighaosu, first extracted in 1979 from the quighao plant (*Artemisia annua*, sweet wormwood), was first reported in China by unidentified authors in the *Chinese Medicinal Journal* to cure patients suffering from malaria, but the chemotherapeutic effects of the plant extracts on malaria have been known for centuries in traditional Chinese medicine.[28,45,46] Recently (2015), the coveted Nobel Prize in Physiology or Medicine *"for her discoveries concerning a novel therapy against Malaria"* was awarded to Professor Youyou Tu for her key role in determining the unusual structure of Quinhaosu, and the breakthrough made in the treatment of malaria.[47] Quinhaosu was later named artemisinin (ART), and became an ever more relevant antimalarial drug as chloroquine (CQ) and amodiaquine (ADQ) drugs began to show that drug resistance was manifesting in the parasite during treatment.[28]

Currently, artemisinin-based combination therapy (ACT) is the WHO recommended standard for the treatment of uncomplicated and severe forms of malaria as well as for the treatment of drug-resistant species.[2,3,29,32,33] ART is used as either the extracted natural form, artemisinin, or as semi-synthetic derivatives of artemisinin such as dihydroartemisinin (DHA) (Figure 5).[29] ART and its derivatives are all highly effective and fast-acting and show activity in all phases of the asexual intra-erythrocytic schizogonic cycle, as well as acting on the initial sexual form of young gametocytes.[29] This class of antimalarials are fast-acting endoperoxide-type (peroxide-bridge containing) compounds and have

consistently shown higher levels of parasite deaths across all the antimalarial classes currently in use.[2,3,33]

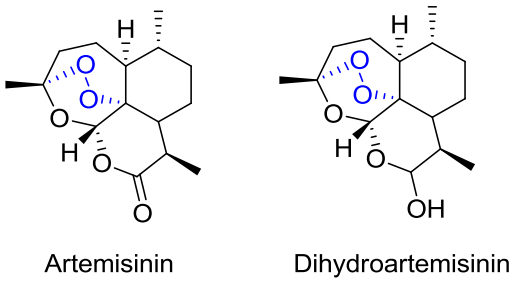

Figure 5 – Structural representations of the natural form of artemisinin and the semi-synthetic derivative, dihydroartemisinin. Highlighted in blue are the peroxide-bridges characteristic to the endoperoxide compounds.[33]

The mode of action of ART is currently under debate, as it is unclear as to how the complex endoperoxide mechanism works.[28] However, the endoperoxides have a multipart mechanism of action and is thought to cause multiple inhibitory effects in the *Plasmodium* parasites.[33] There is general consensus that the endoperoxides have several effects on the *Plasmodium* parasites.[14,28,29,33] It is believed by many that the activity of ART is related to the interaction with the Fe(III)PPIX in the food vacuole derived from the ingestion and degradation of Hb by the parasite.[14,28,29,33] Studies have indicated that the endoperoxide bridge within the compounds can be cleaved by a reductive process with the Fe(II) that is provided, either by the Fe(II)PPIX or by other exogenous (external iron species) and forms one or more radical species that may be able to alkylate or modify malarial proteins in some way.[14,48,49] Another study has also indicated that there is a similarity to the mechanism of quinoline-type drugs, whereby ART is also able to accumulate in the food vacuole of the parasite and interact with the heme detoxification process.[50] However, there are conflicting reports that do not agree with the findings that ART does, in fact, inhibit the formation of hemozoin and so the debate over the exact mechanism continues.[14,51,52]

Recently, the emergence of ART resistance has been recorded in northwestern Thailand and western Cambodia during clinical trials on parasites collected from participants.[28] Up until now, resistance towards artemisinin-based compounds has been of little significance and only sequestered to small regions of the world. The resistance is characterized by the delayed parasite clearance that is observed in patients treated with ART with no clear molecular markers that can be identified to assist in ART-resistance surveillance.[14] However, the WHO still recommends the use of ART in combination therapy together with other antimalarial compounds to lower the risk of possible drug resistance developing.[2,3]

1.4.2 Nucleic Acid Metabolism

This class of antimalarials form part of the nucleic acid inhibitors that, in contrast to the other classes, are responsible for the reduced levels of DNA, methionine and serine formation. This class is sub-divided into two types of compounds, namely the folate antagonists and the naphthoquinones, that exert their activity throughout the growing asexual erythrocytic cycle (host RBC stage)[29] of the parasite.

The Antifolates

The major drugs of this class used against malaria are: Type 1 – sulfa-drugs of which the sulfonamides, such as sulfadoxine (SDX), are the most important, and Type 2 – pyrimethamine (PYR) and proguanil (PG, metabolized to cycloguanil [CG]).[28] It was discovered that during a detailed study of bacterial systems in the 1940's and onwards, that PYR and CG drugs targeted the activity of dihydrofolate reductase (DHFR) in the parasites bifunctional DHFR-thymidylate synthase protein, whilst the sulfa-drugs targeted dihydropteroate synthase (DHPS) activity of the parasite's bi-functional hydroxymethylpterin pyrophosphokinase (HPPK)-DHPS protein.[28] Figure 6 illustrates the structures of the major drugs mentioned and to which group, Type 1 or Type 2, they belong to.[33]

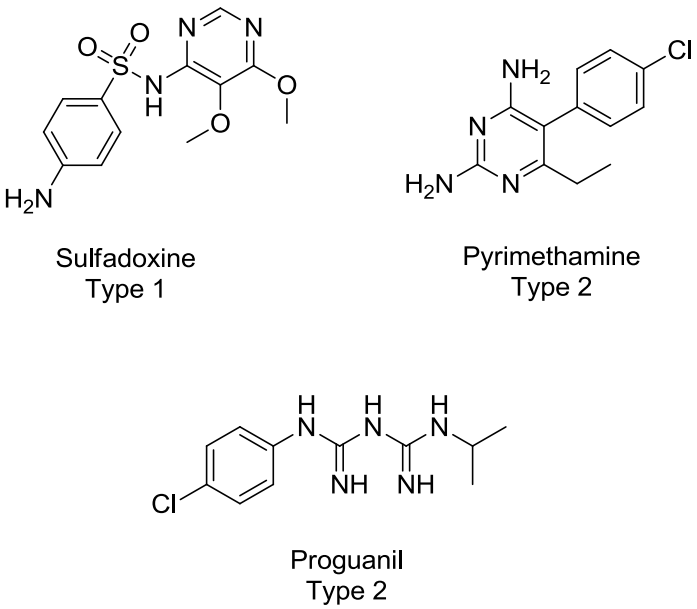

Figure 6 – Structures of antifolate Type 1 and 2 drugs.[33]

In both Type 1 and Type 2 antifolates, the inhibitors target catalytic enzymes (DHPS or DHFR) to impede the folate biosynthesis pathways and inhibit the formation of essential cofactors for the

parasites survival.[29,33] Sulfadoxine (Type 1) acts as an inhibitor by mimicking *p*-aminobenzoic acid and out competing it for the active site on the DHPS.[28] Once bound to the DHPS, the DHPS is no longer able to catalyze the reaction between *p*-aminobenzoic acid and hydroxymethyldihydropterin and thus the formation of dihydropteroate is impeded.[28] DHPS enzyme is only found in the parasite which makes it highly suitable target for inhibition.[28] A similar mode of action occurs in the case of the pyrimethamine drugs but the target is DHFR.[28] The pyrimethamine is a mimic compound of dihydrofolate (DHF) and is able to fit into the hydrophobic pocket of the DHFR enzyme and forms hydrogen bonds just as the DHF would.[29,33] The blockage of DHF impedes the formation of tetrahydrofolate as the DHF can no longer interact with the DHFR.[29,33] However, DHFR is present in both the parasite and the host as it is required for virtually all organisms to maintain the constant production of tetrahydrofolate.[29,33] Although the parasite is able to salvage tetrahydrofolate from the host, the activity of DHFR is still an essential part of the parasite's survival.[29,33]

The antifolates class of drugs is one of the most highly prescribed antimalarials, however the rapid emergence of widespread clinical resistance has made monotherapy significantly less effective in most regions of the world.[29,33] The appearance of resistance to drug treatment in both DHFR and DHPS is attributed to the accumulation of point mutations in the genes of each of the enzymes, and have been characterized in clinical isolates.[14,28,33] For DHFR, the quadrupole mutation in the genes N51I, C95R, S108N and I64L have led to the identification of highly resistant strains with the S108N gene being a sufficient mutation to confer drug resistance.[14,28,33] The most common mutations responsible for the resistance in DHPS towards SDX are the A437G and K540E gene alterations.[14,28,33] Alterations of all the aforementioned genes essentially cause an alteration of the enzymes that impede the drugs, PYR for DHFR and SDX for DHPS, from being able to effectively bind to the enzyme thus preventing inhibition.[14,28,33] Nevertheless, the use of sulfadoxine-pyrimethamine combination therapy is still recommended and shows improvement in the treatment outcomes of pregnant women when given in intermittent preventative therapy.[14,28,33]

Atovaquones

Atovaquone (ATV), is currently the only antimalarial drug in clinical use that functions as an inhibitor of mitochondrial cytochrome *bc*1 and impedes the biosynthesis of pyrimidine (Figure 7).[28,33] It was initially tested and used against murine infections before being identified as an effective antiparasitic drug.[28] It was identified during a study that was specifically focused on the respiratory chain-linker electron transport between the human host and *Plasmodium* by making use of menoctone, a lead compound and a ubiquinone antagonist.[28] ATV was described to be a broad-spectrum antiparasitic drug, that when administered as a chemoprophylaxitic for malaria, would collapse the mitochondrial

membrane potential.[28,33] Today, the drug is used in combination therapy with proguanil (PG), an antifolate-group drug, due to its unfortunate susceptibility to rapid drug resistance developing and is marketed under the brand name Malarone™.[28,33] The structure of ATV is comprised of a hydroxynaphthoquinone that is substituted to act as a derivative of coenzyme Q found in the respiratory chain (Figure 7).[28,33]

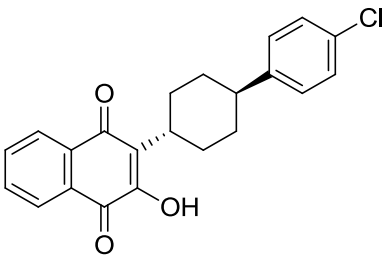

Atovaquone

Figure 7 – Molecular structures of Atovaquone.[33]

ATV mode of action inhibits the movement of iron-sulfur protein subunits of cytochrome *b* (*Cytb*), that are essential for the preservation of effective transfer of electrons from unihydroquinone to *Cytc1*.[28,33] Prevention of electron transfer in the mitochondrion results in the loss of membrane potential, but also impedes the biosynthesis of pyrimidine, known to be essential for parasite survival, thus leading to death of the parasite.[28,33] The biosynthesis of pyrimidine is essential due to the fact that the parasite is unable to salvage pyrimidine from the host, thus forcing the parasite to synthesize its own. Once inhibition is initiated by ATV, the parasite relies on its own source of pyrimidine, depleting it until the parasite dies.[28,33]

The approach of targeting the mitochondrion is in fact a very promising approach. Antibiotics such as the tetracyclines target the 30S ribosome of the mitochondrion and are highly successful and have been successfully used against the CQ-resistant parasites.[28,29,33] However, targeting of only a single protein has the drawback of rapid drug resistance developing, with a single point mutation being enough to render a drug ineffective as is the case with ATV.[28,29,33] There is currently clinical evidence that resistance towards ATV is developing in the parasite resulting in an increase of mortality cases as a direct result of resistance at single or double point mutations at codon 268 (Y268C or Y268S) of *Cytb*.[33,53] The implementation of the combination therapy using PG together with ATV was to prevent, or at least slow, the further development of drug resistance.[28,29,33] The use of PG along with ATV results in a synergistic effect, whereby the PG probably does not function as an antifolate (previously discussed), but rather exerting an effect directly on the mitochondrial membrane potential and thus assisting the ATV.[28,33] However, the combination therapy of these two drugs have not

entirely prevented resistance from developing in the parasite towards ATV and failures in treatment using the drug have been reported, but these are in isolated cases.[28,33] Malarone™ remains a useful malaria treatment due to its effectiveness in both the liver and blood stages of the disease and the WHO still recommended its use in areas where artemisinin resistance is emerging in the *Plasmodium falciparum* parasite.[33,53]

1.5 A DIFFERENT APPROACH - *N*-MYRISTOYLATION

The *N*-myristoyltransferase (NMT) is an enzyme that is essential and exclusive to eukaryotes and is a critical component of signaling pathways, regulation of membrane localization and complex protein assembly.[1,54,55] NMT is ubiquitous in many eukaryotes and has been isolated and characterized for yeast and fungi, parasitic protozoa, plants, mammals and insects, with variations occurring between the various species.[55,56] This has been beneficial to drug development as selective drugs for specific species can be developed. The NMT enzyme catalyses the process of *N*-myristoylation by transferring a C_{14} saturated fatty acid (myristic acid), from myristoyl-coenzyme A (myr-CoA), to a wide variety of protein substrates containing an *N*-terminal site (Scheme 1).[17,55-58]

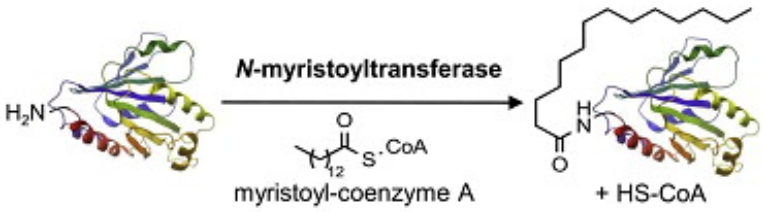

Scheme 1 – Simple representation of *N*-Myristoylation of a target protein containing an *N*-terminal site (left) to give the *N*-myristoylated protein (right).[57]

It has been hypothesized by Wright *et al.*[56] that the inhibition of NMT could lead to multiple adverse effects on the biological pathways within the *Plasmodium* parasite and could ultimately lead to parasite death.[56] The investigation into NMT of parasitic protozoa led to the identification of a single NMT gene in the species *Plasmodium*, and the partial inhibition thereof caused rapid and irreversible failure of the parasite's ability to invade RBCs, and ultimately parasite death.[56] In addition Wright *et al.*[56] and Yu *et al.*[58] both determined that the structures of *Plasmodium vivax* (*Pv*) and *Plasmodium falciparum* (*Pf*) NMT shared more than 80% of their sequence identities with one another.[56,58] Both Yu *et al.*[58] and Goncalves *et al.*[17] separately studied the effects of synthesized inhibitor compounds on *Pv*NMT and *Pf*NMT and observed similar inhibition levels for both structures.[17,58] Wright *et al.*[56] recently (2013) reported promising results confirming the structural findings by Yu *et al.*[58] and

Goncalves *et al*.[17] (Figure 8).[56] They determined that by binding a surrogate myristoyl group, tetradec-13-ynoic acid, to both *Pv*NMT and *Pf*NMT, the two enzymes would be susceptible to the inhibitory effects of a common structure.[56] These results indicate that the identification of effective inhibitor compounds for one species enzyme, namely *Pv*NMT, may possibly be effective towards the *Pf*NMT enzyme.

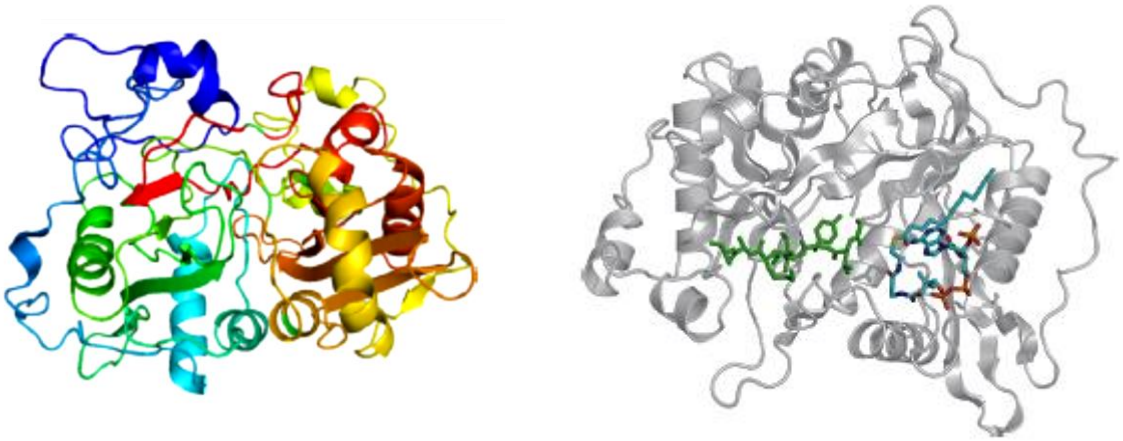

Figure 8 – Ribbon structure of *Plasmodium vivax* NMT (*Pv*NMT) left, and *Plasmodium falciparum* NMT (*Pf*NMT) right.[59]

The myristoylation of proteins can have a number of effects, including enhancing interactions of the protein with organelle or plasma membranes (changing protein stability) and may also stabilize any protein-protein interactions.[55] The reaction mechanism (Figure 9) for the myristoylation of a peptide proceeds via 2-step sequential interaction where the myr-CoA substrate first binds to the NMT enzyme (Blue circle) to form a myristoyl-CoA:NMT binary complex (Figure 9).[59] This is followed by a conformational change in the NMT enzyme creating a peptide binding pocket that is able to accept peptide substrates.[55,60,61] The peptide substrate then proceeds to bind to the NMT enzyme forming a myristoyl-CoA:NMT-peptide ternary complex.[59,60] The transformation by catalysis then occurs whereby the myristate transfers from the CoA to the peptide substrate.[59,60] Following the transfer, the CoA is released, after which the newly formed myristoylated peptide is also released from the NMT.[59,60] Finally, the NMT enzyme undergoes a conformation change to return to its original form with a myr-CoA binding pocket and no peptide binding pocket. The NMT is then able to undergo another catalytic cycle for myristoylation of another peptide.[55,60]

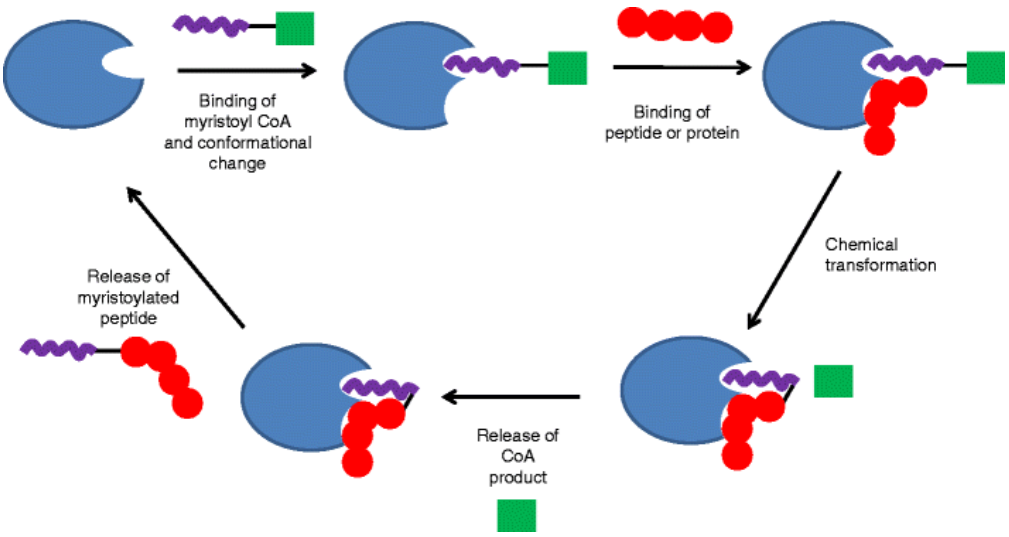

Figure 9 – Illustration by Wright *et al*. of the bi-bi reaction mechanism of *N*-Myristoylation that occurs between NMT (Blue), Myr-CoA (Purple-Green) and the peptide substrate (Red).[56]

In a recent study carried out by Wright *et al*.,[56] it was demonstrated that NMT is an important chemically-compliant target in the malaria parasite.[56] Myristoylation of the parasite proteins results in increased lipophilicity that facilitates their association with cellular membranes (RBCs) and allows the parasite to transverse the RBC membrane.[56,59] It has been shown that selective inhibition of the *N*-myristoylation process caused irreversible failure in the parasite's ability to form an inner-membrane complex (IMC), which was essential in the life cycle of the parasite.[56] The IMC played an important role and was responsible for the critical assembly of the molecular motor apparatus by which the parasite was able to invade RBCs.[56,58] Therefore, disruption of the process by removal or inhibition of the NMT enzyme from the parasite cycle, has made this enzyme the most recent viable chemotherapeutic target for research and development of new antiplasmodial compounds that specifically target *Plasmodium* NMT.[17,56,58]

In this regard, benzofuran, benzothiophene and indole structures have gained attention in the quest for novel antiplasmodial agents. Studies carried out by Yu *et al*.[58], Sheng *et al*.[62] and Rackham *et al*.[54], incorporated the abovementioned heterocyclic substructures and showed promising results as inhibitors of various species of NMT. Figure 10 illustrates some of the recent compounds that were synthesized by Yu *et al*.[58] and Sheng *et al*.[62], and that provide a valuable starting point for further research into NMT inhibitors.

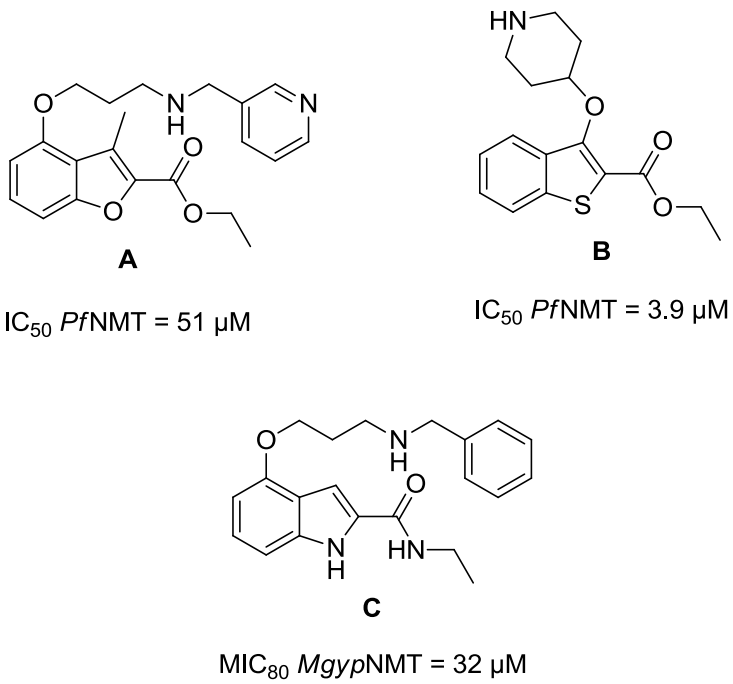

Figure 10 – Representative structures of current NMT inhibitory compounds for *Plasmodium* NMT (**A** and **B**) and *Fungal* NMT (**C**).[54,58,62]

Although the research is still in its infancy, Yu *et al*.[58] carried out structural investigations identifying points of modification that can serve as guidelines for future NMT drug design using benzofuran, benzothiophene and indole (Figure 11).[58] The first point of modification was the C-4 side chain (**L**), where incorporation of a trimethylene linker was an optimal length for the chain and that a secondary amine (**X**) was preferred for improved selectivity of NMT.[58] The second investigation was on the C-2 side chain (**R**^{2}), identifying that larger aromatic side chains gave increased enzyme inhibition, and that the incorporation of an ester group with a methylene linker indicated that flexibility in the C-2 side chain played a key role in increasing potency.[58]

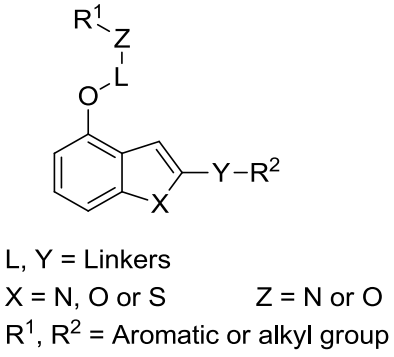

Figure 11 – Structural representation of benzofuran to illustrate the positions of investigated groups.[58]

The last point of modification was the linker group (**Y**), that indicated the introduction of heteroatoms improved enzyme affinity with the ester functionality showing the best results with a marked improvement in potency.[58] On the basis of the current research into NMT, valuable results were obtained as a starting point for the development of *Plasmodium* NMT inhibitory compounds, and more importantly, the results enforce that the *Plasmodium* NMT enzyme remains a target for continued drug development.

1.5.1 Difficulties in New Drug Development and Hybrid Compounds

It has become apparent that it is more and more difficult to develop new and effective drugs to combat the growing resistance posed by the malaria parasite.[64] The reason for this is that the parasite possesses an effective ability to circumvent the efficacy of currently available drugs by rapidly developing resistance, due to the overuse and incorrect use of current drugs and the use of substandard drugs (lower drug concentration per recommended dose).[26,63-67] Owing to the increasing drug resistance within the parasite, studies for virtually all the available antimalarial drugs currently in use have reported drug resistance, and the most powerful weapon artemisinin will also eventually succumb to drug resistance developing in the parasite towards artemisinin.[26,63-67] Certain drugs such as the artemisinin-type endoperoxides are still highly effective antimalarial agents, and although reports have been made of resistance, the resistance is sequestered to small regions of south-east Asia.[14,28,29,33,40]

Although, the WHO 'gold standard' treatment of using artemisinin-combination therapy for malaria has started to show some decreases in efficacy due to drug resistance by the parasite, it is still recommended by the WHO but in combination with two or more other drugs to hinder the development of resistence.[2,3,5] Another factor, apart from resistance, is the difficulty in developing and synthesizing new drugs through the standard approach of drug discovery, which is a slow and tedious process.[68] The standard approaches consists of 1) optimizing potential drug candidates through derivatisation of current drug molecules, 2) optimizing the current drug therapy methods, including combination therapy and multi-component drugs (single tablet) and 3) the screening and evaluation of natural compounds obtained from plant sources such as *Artemisia annua* (artemisinin).[47,68]

As mentioned, the standard approaches pose difficulties, each of which has its own drawback that hamper the drug development process. In the case of natural compound screening and evaluation, the processes are extremely time consuming as compound isolation from plant material must first be carried out.[68] This is followed by an extensive period of screening in assays to identify possible candidates for further study.[68] A good example of this process was the discovery and isolation of

artemisinin, that took many years of research and development of an effective method of isolating the compound from the *Artemisia annua* plant leaves.[69]

The optimization of currently available drugs essentially requires the synthetic modification and derivatisation of known bioactive compounds that have significant downfalls.[68] Most notably, the analogues all share a common pharmacophore from the original active compound, i.e. the quinoline analogues were derived from the original quinine structure.[68] This structural similarity has the disadvantage of possible cross-resistance developing, whereby the original is ineffective because the parasite gained resistance towards it.[68] This resistance mutation within the parasite may also be effective against new compounds or alternatively develop into a new mutation very rapidly, thus giving the compound a very short clinical lifetime as a useful antimalarial drug.[68] The last dilemma faced during the development of new drugs is the issue of using multi-component and combination therapies. These approaches to malaria prophylaxis are prone to adverse drug-drug interactions occurring if the correct combination of drugs, or ratio thereof, are not used during treatment.[68,70]

1.5.2 Introducing Hybrid Compounds

Recently, through an approach of rational drug design, a new class of antiplasmodial compounds has been developed, namely the hybrid class. The hybrid compound is classically defined as a structure that is constructed from two different, but complimentary, bioactive compounds with different modes of action into a single compound by a covalent bond.[65,68,71] Hybrids compounds, in general, are classified into four classes according to their construction, which are briefly discussed below.

Conjugates contain two molecular frameworks (pharmacophores), each with its own target and mode of action, separated by a distinct linker that is metabolically stable and not found in either of the two frameworks.[65,68,71]

Cleavage conjugates are similar to the conjugates, but the linker is not metabolically stable and, once metabolized, releases the two frameworks (drugs) which then work independently from one another.[65,68,71] Generally ester-based linkers are incorporated which can be cleaved *in vivo* by plasma esterases that subsequently release the frameworks.[71]

Merged hybrids take advantage of structural similarities in the two frameworks to merge them into a smaller and simpler structure.[65,68,71]

Fused hybrids are structures where the two pharmacophores are connected by a linker that is so short that the two components are virtually touching, making a more rigid structure.[65,68,71]

The structures illustrated in Figure 12 are two current antiplasmodial hybrid compounds **H1** and **H2**,[26,63] that contain the two important substructures (indole [blue] and quinoline [red]) that are the

central theme of this study and the investigations performed and discussed in the ensuing chapters. Taking note of the half maximum inhibitory concentration (IC_{50}) values obtained for the compounds when compared to Chloroquine-Sensitive (3D7) and Chloroquine-Resistant (K1) *P. falciparum*, it can be justified that combining an indole with a quinoline into a hybrid can be beneficial in the development of a new antimalarial drug.

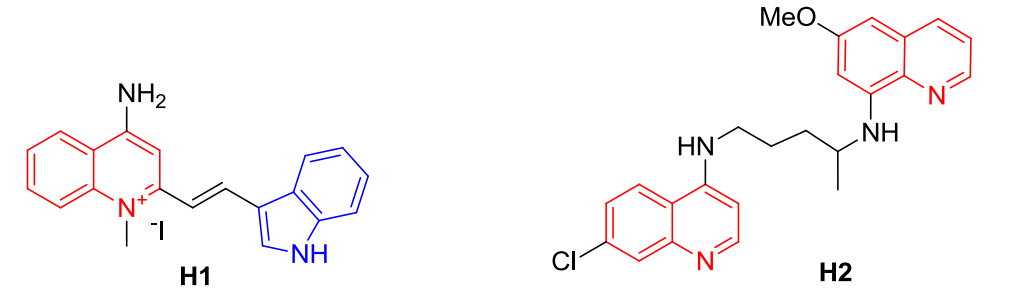

IC_{50} (μM) = 0.17 (3D7), 0.23 (K1)

IC_{50} (nM) = 640 (3D7), 80 (K1)

Figure 12 – Examples of quinoline-indole hybrids that show some success as antiplasmodial compounds with regards to Chloroquine-Sensitive (3D7) and Chloroquine-Resistant (K1) *P. falciparum*.[26,63]

For this project, we focused our attention on indole and quinoline structures similar to those of **H1** and **H2**, which will be discussed in the coming Chapters 2 and 3, with the aim of coupling them together with an amide-amine linker into a conjugate hybrid molecule similar to **H1** reported above. As previously mentioned, conjugate hybrids contain two pharmacophores, each with its own mechanism of action, that are linked by a metabolically stable linker i.e. the alkyl amine chain in **H2**.[68] Typically, when hybrid molecules are formed from two pharmacophores, the resulting molecule is much larger than the two independent substructures. As a direct result of the size increase, the lipophilicity of the compound decreases, reducing the molecule's solubility and ability to pass through the parasite membrane.[63,65,67,68] The addition of a shorter linker keeps the overall size of the molecule down and by adding the amine moieties **H2**, the lipophilicity can be increased to aid in the passage of the molecule through the parasite membrane.[63,67,68]

The rationale behind the design and development of hybrid compounds is as a result of the previously discussed difficulties faced in the standard drug development approach. The advantages of employing hybrids include a lower risk of adverse drug-drug interactions as a result of the coupling linker restricting interaction between frameworks.[64] In principle, they may be less expensive as the cost of synthesis may not be significantly different to the synthesis of a single entity.[64] They have the ability to increase efficacy as a single compound has a potential dual activity and furthermore, can also assist in preventing the rapid onset of drug resistance.[64] Customization to suit specific resistance mutations faced in different malaria regions can be achieved and lastly, fast-acting drugs can be combined with

slow-acting drugs to improve the latter's uptake by sharing favorable properties to assist in interactions with parasite targets.[65,68]

There are, however, a few disadvantages with hybrid compounds. There is no possibility of adjusting the ratio of the two frameworks to optimize pathway targeting. The selection of the linker to be used, the type of functionality within the linker and the length all play a role and can have adverse effects on the activity of the compound if not selected properly.[64,65] Studies report that the linker chain should not contain cyclic structures but rather be limited to two or three carbon atoms which can have methyl substituents if desired.[72] It is also difficult to rationally apply the concept of hybrid drugs to malaria as the life cycle of the parasite is so complex. There are also only a few confirmed targets available in the life cycle.[67]

Nevertheless, the advantages seem to outweigh the disadvantages and several hybrid compounds are currently in research and development and showing excellent results with regards to efficacy towards the inhibition of the *Plasmodium* parasite and drug resistant species.[26,63-67] In spite of the promising results currently shown by a number of hybrid compounds towards the Plasmodium parasite, the development of effective compounds is not the only criteria to satisfy.[26,63-67] Safety with regards to toxicity towards the human-host is a problem that may arise during clinical trials or clinical use, where the compound may be effective towards the parasite but has negative side-effects for the host.[26,63-67] However, further research and development may prove successful in identifying suitable structures and compounds that will, at least in part, overcome the negatives to ultimately enable the design and synthesis of suitable, effective, safe and cheap antiplasmodial compounds.[26,63-67]

1.6 INTRODUCING OUR STRATEGY

The overall objective of this project was to design and synthesize a novel conjugate hybrid compound as a possible dual-active inhibitor for *Plasmodium vivax* NMT and *β*-hematin formation. However, the whole project was not a solo effort as a second student (Leon Jacobs) was also working on synthesizing a larger group of similar compounds. Modeling studies carried out by a member of the group indicated that it would be of benefit to have a large bicyclic moiety as a pendant to the indole. As a result of, we decided that it would be interesting to insert the quinoline as a second bicyclic moiety. This had an added benefit in that the quinolines synthesized could be used by a student (Sharné Fitzroy) who was studying the quinolines and the mechanism of *β*-hematin inhibition.

As the project got underway, it was clear that the optimization of these reactions would pose a significant synthetic challenge. To this end, again a decision was made to maximize productivity, in that the major focus of this part of the project would be on developing good methodology. This led to the main objective of a full investigation into the synthetic procedure used to synthesize starting

materials, precursors and scaffolds and would lead to the main aim of the project which was the synthesis of an indole-quinoline hybrid. Figure 13 illustrates the intended major target compounds (indole **8**, **9** and **11**, and quinoline scaffolds **12a-i** and **13a-i**) and the intended conjugate hybrid compound scaffold (**H3g-h**) to be synthesized and investigated.

To maximize the synthetic success, the project had three clear avenues: a) the optimization of the synthesis of indole ring system, this included various protection and deprotection steps and condensation or addition reactions to attain the correctly substituted indole (Figure 13 – **8**, **9** and **11**); b) The optimization of the quinoline synthesis allowing for variation in the substitution on the 4- and 7-position (Figure13 – **12** and **13**), and finally c) the linking the two heterocycles (Figure 13 – **11** and **12**) to form the novel hybrid molecules (Figure 13 – **H3g-h**).

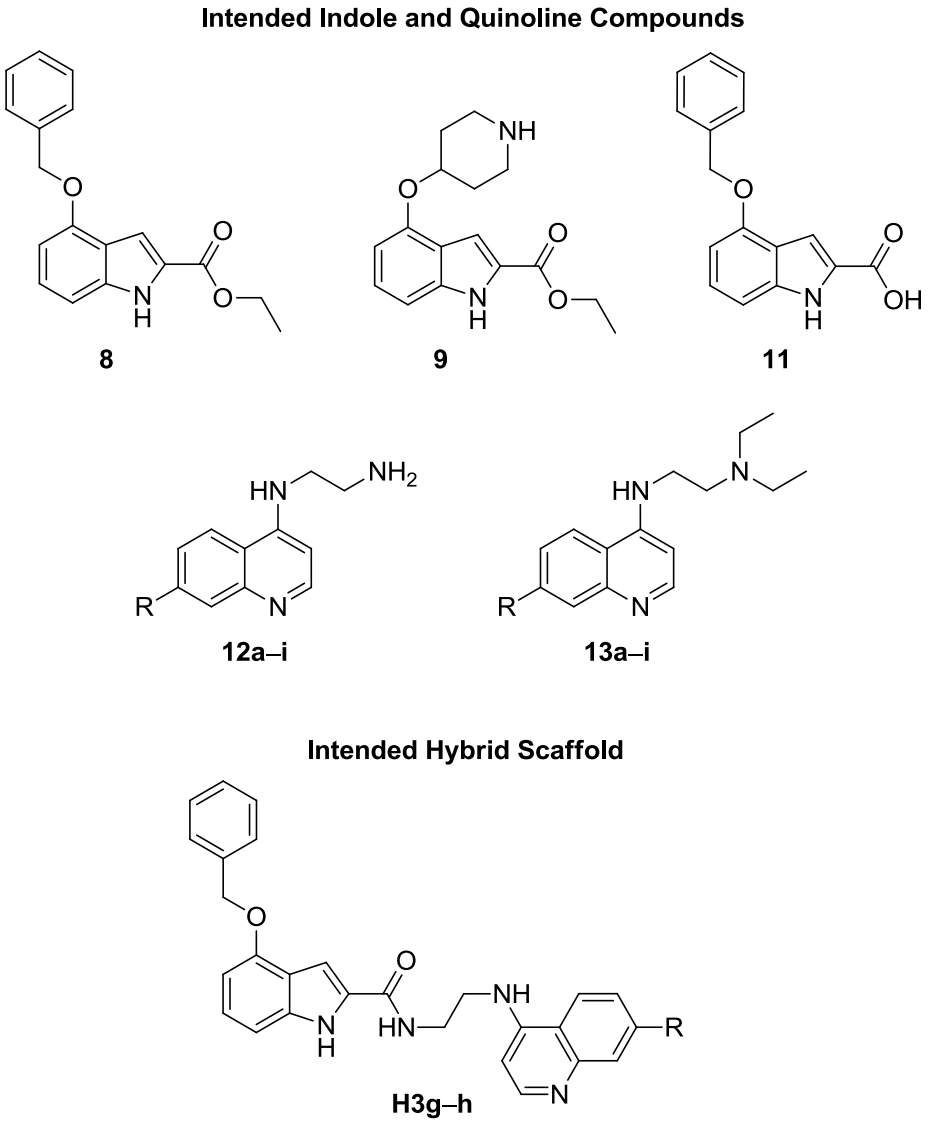

Figure 13 – Illustration of the intended compounds to be synthesized in this project

To this end, significant effort was made to research the synthesis of both indoles and quinolines. This project then focused on developing synthetic methodologies which would be robust and efficient given the available starting materials and the time frame.

1.6.1 Aims and Objectives

The main aim of this project was the investigation into the synthesis of a hybrid compound and also to optimize methods of synthesizing indole and quinoline substructures for use as hybrid pharmacophores. The synthesis of a hybrid compound however, would be carried out once the methodologies for the synthesis of the indole and quinoline moieties was established.

The following objectives were devised to achieve the aim of hybrid synthesis:

1. Literature study was undertaken to understand the mechanistic workings of the reactions and the knowledge gained from the literature study was applied to the synthetic procedures.
2. The synthesis of starting materials and precursors for indole scaffold and also the utilization of the precursor material to synthesize the desired indole scaffold via the Knoevenagel condensation reaction followed by synthesis of the novel indole compound using the Mitsunobu reaction.
3. Investigation into the Horner-Wadsworth-Emmons and cerium(IV) ammonium nitrate (CAN) reactions as possible alternative methods for achieving objective 2 more efficiently.
4. The synthesis of quinoline scaffolds by various methods including the Gould-Jacobs, Skraup and Doebner-Miller reactions to identify the most efficient and cost effective approach for future synthetic research purposes.
5. The synthesis of known quinoline antiplasmodial compounds.
6. The utilization of the synthetic procedures that were employed for the synthesis of the known quinoline compounds to synthesize other quinoline derivatives for use as a moiety in a hybrid compound.
7. Carry out optimizations of all the above mentioned reactions to increase their efficiency, decrease chemical waste and lower synthesis costs.
8. Time allowing and objectives 1–7 completed successfully, attempt the synthesis of an indole-quinoline hybrid using the above mentioned indole scaffold and quinoline derivatives and optimize the reaction as a starting point for future hybrid research purposes.

CHAPTER 2: INDOLES

2.1 INTRODUCTION TO INDOLES AND OUR CONCEPT OF NOVEL INDOLE COMPOUNDS

The indole ring system, first isolated by Baeyer,[73] has intrigued organic and medicinal chemists for decades and remains an important structure in the medicinal chemistry community for its biological activities.[74-77] The indole moiety (Figure 14) is one of the most abundant heterocycles in nature and is found as a substructure in a wide range of naturally occurring and synthetically made compounds with diverse biological activities.[74,78] These compounds range from simple derivatives such as serotonin (found in the body) to more complex naturally and synthetically made structures such as reserpine (an antihypertensive alkaloid).[74,78]

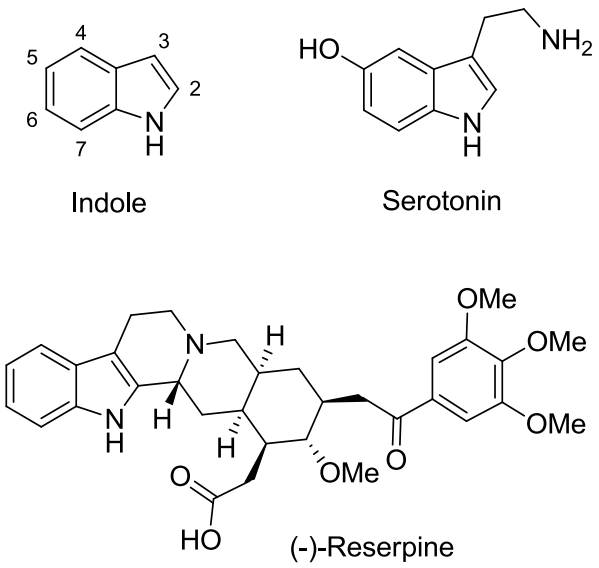

Figure 14 – Indole and selected examples of indole derivatives.[74,78]

As the indole moiety is such a prominent structure in nature, it stands to reason that the use thereof in the design and synthesis of novel medicinal compounds could be advantageous. In this chapter, we focused on investigating the available methods of synthesizing the indole structure to identify the most reliable and efficient method by which to synthesize structures with substitutions at very specific positions. A study by Yu *et al.*[58] demonstrated that derivitising a benzofuran scaffold **1** (Figure 15) showed favorable results as inhibitors for *Plasmodium vivax* NMT.[58] This led to the decision to investigate the synthesis of a novel indole-based compound **2** (Figure 15) by substituting the

benzofuran (red) for an indole (blue) that would possibly show improved inhibitory effects when compared to **1**.

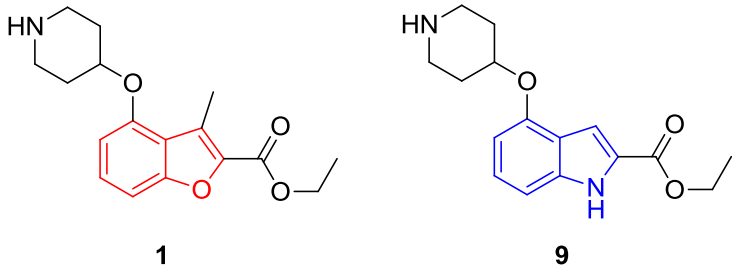

Figure 15 – Illustration of benzofuran compound **1** by Yu *et al*.[58] and our intended novel indole compound **9**.

The structures of **1** and **9** are similar with the exception of the heteroatom in the heterocycle. The presence of the proton on the nitrogen could provide another site for hydrogen bonding to occur within the parasite enzymatic structure. This could be advantageous and possibly provide greater efficacy for an inhibitor of *Pv*NMT.[62]

Having mentioned earlier that this chapter focuses on the synthetic methodologies of the indole **2** substructure to obtain **9,** a literature study was undertaken to identify suitable methods. The most obvious process would involve using indole as the starting material and doing substitution reactions on positions 2 and 4 to obtain **9**. However, this would be problematic because of the inherent regio-selectivity in substitution reactions on the indole scaffold.[79] Indoles are benzo derivatives of the parent molecule pyrrole and thus exhibit similar properties to that of pyrrole.[79] The 3-position is thus favored for substitution in the pyrrole, where we required the 2- and 4-position substituted products. This can be explained by the resonance possibilities of pyrrole during attack on the ring.[79] Illustrated in Scheme 2 are the resonance possibilities of the pi-excessive (indole) structure during an electrophilic attack at positions 2 and 3.

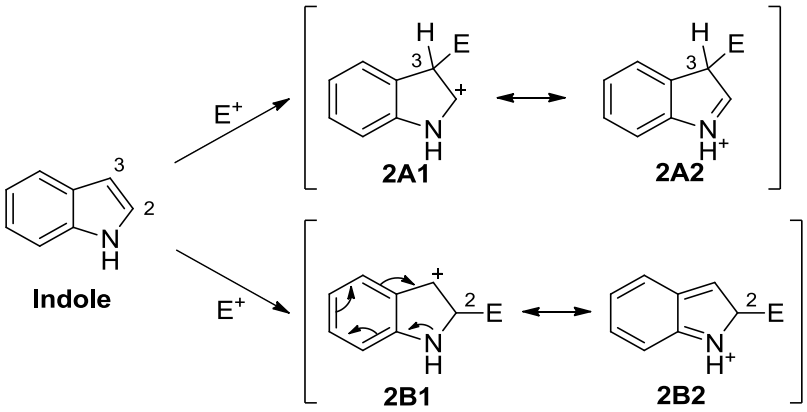

Scheme 2 – Electrophilic attack on indole pyrrole ring at position 2 and 3.[79]

With an attack at the 3-position it is clear that the carbocation intermediate 2**A2** is stabilized more effectively by electron release from the nitrogen than the intermediate 2**B2** from attack at the 2-position. This is because of the less stable arrangement of the pi-electrons that is caused by the electron release from the nitrogen 2**B1**, by having to proceed through the benzene ring to stabilize the carbocation and in-turn disrupting the aromatic system of the benzene ring.[79] Furthermore, once the 3-position substituent is in place, the next favored position becomes the 2-position of the pyrrole ring and not the benzene ring positions. To be able to substitute the 4-position, the 2- and 3-position (that are favored) have to be substituted first. Only once the 3-position is substituted, is the 2-position favored for substitution followed by the benzene 4-position. By proceeding through these steps the desired product of a 2,4-substituted indole would require the removal of the 3-position substituent without causing any alterations to occur to the 2- and 4-position substituents. Thus using indole as a starting point for the synthesis in **9** is unlikely to be a worthwhile endeavor.

There are many methodologies for the synthesis of indoles, from the conventional condensation and cyclization processes,[75,80-83] to the latest transition metal-catalyzed carbon-carbon and carbon-nitrogen bond forming reactions.[74,75,78,84,85] We decided to approach the synthesis **9** by making use of conventional methods. Although the transition metal-catalysis methods have shown significant improvements over the more conventional methods, the catalysts that are required are very expensive. The methods investigated were the Knoevenagel condensation[80] and the CAN-mediated azide addition[86] to a Horner-Wadsworth-Emmons cinnamate, which would afford the desired indole scaffold **9** with both the desired ester and alkoxy substituents being inherited from simpler starting materials. The retro-synthetic routes, A and B depicted in Scheme 3, illustrates two efficient routes for synthesizing the desired indole compound **9** by way of conventional methods, starting with a simple substituted benzenaldehyde **3** and proceeding through an indole scaffold **8** to eventually afford **9**.

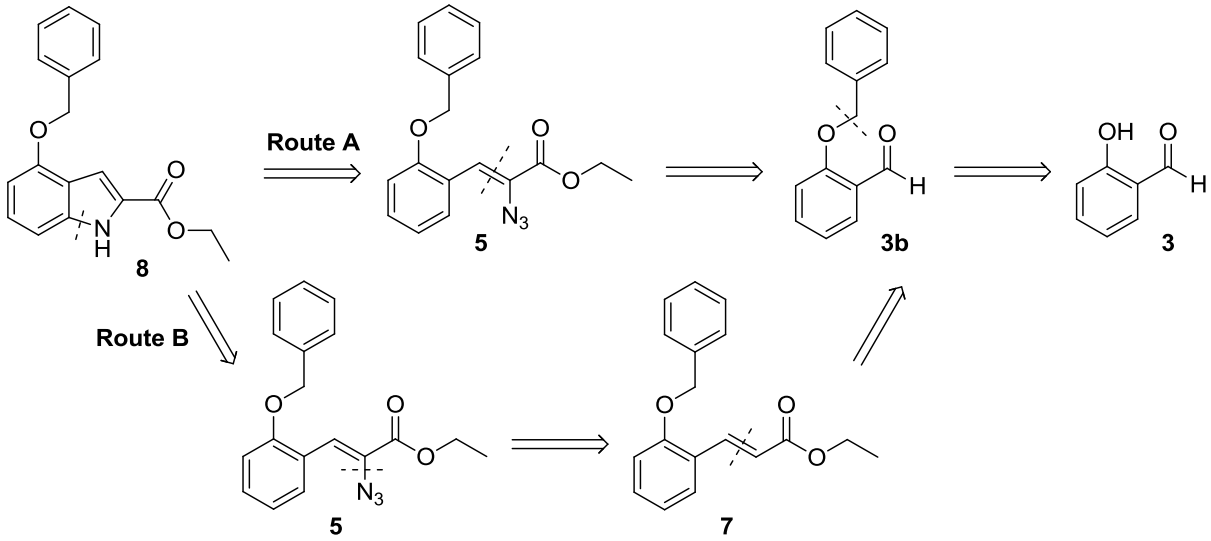

Scheme 3 – Representation of the retro-synthetic routes identified and utilized for the synthesis of **8**.

Our attention was focused on these two conventional methods for the synthesis of **9** because the conditions afforded the inclusion of the desirable moieties (2-acetate and 4-alkoxy) and ultimately gave the required indole **9** with the necessary substitutions in the correct positions. The Hemetsberger cyclization method was selected to be an appropriate method for the synthesis of our desired indole **9**. However, a method for the synthesis of the required stereospecific azido-cinnamate precursor **5** had to be identified. The first method (Route A) utilizes the Knoevenagel-condensation reaction between an aromatic aldehyde **3b** and an alkyl azide to form **5** that when subjected to thermal cyclization would form **9**.[80,81] Although the first method (Route A) had shown some success, it was inconsistent at providing precursor **5,** giving poor yields ranging between 10 and 43%, much lower than reported in literature (50-90%).[80,81]

The alternative method (Route B) employs the Horner-Wadsworth-Emmons reaction to form cinnamate **7** from **3b**, which can be used to synthesize **5** in a cerium(IV) ammonium nitrate (CAN)-mediated azide addition reaction.[86,87] The azido cinnamate precursor was subjected to the same thermal cyclization reaction as the condensation method to afford the indole scaffold **8** and ultimately the intended indole compound **9**.

2.2 SYNTHESIS OF STARTING MATERIALS & PRECURSORS TO INDOLES

With the indole scaffold **8** being a major initial goal in this work, the synthesis thereof required optimized reactions of starting materials and precursors to achieve successful formation of **8** in large quantities. In this section we will discuss the investigation and synthesis of the starting materials and precursors required for the synthesis of the indole scaffold **8** and also derivatisation of **8** to obtain starting materials for the synthesis of hybrid compounds.

2.2.1 Synthesis of 2-Benzyloxy Benzaldehyde 4

Having determined from the retro-synthetic analysis that salicylaldehyde **3** (Figure 16) would be a suitable starting material for the synthesis of the desired indole scaffold **8,** the process of synthesizing **3b** could begin. Salicylaldehyde **3** contains a hydroxyl moiety in the *ortho*-position, as well as an aromatic aldehyde without an *alpha* proton that makes it more stable and less susceptible to self-condensation during the ensuing Knoevenagel condensation reaction.[88] While the aldehyde may be stable, it was important to protect the hydroxyl group, as subsequent reaction steps could cause unwanted by-product formation. Salicylaldehyde is a relatively inexpensive material to use as a starting material for the synthesis of indole compounds and was available in large quantities from our chemical store.

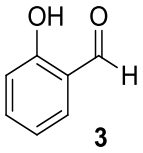

Figure 16 - Salicylaldehyde

Scheme 4 below illustrates the reaction mechanism for the transformation of **3** into the desired product **3b**. Firstly the carbonate base initiates the reaction by deprotonating the hydroxyl group forming the phenolate **3a**. Following the formation of phenolate, **3a** then attacks the electrophilic carbon of the benzyl bromide and displaces the bromide ion in an S_N2-type substitution reaction to finally form **3b**.[88,89]

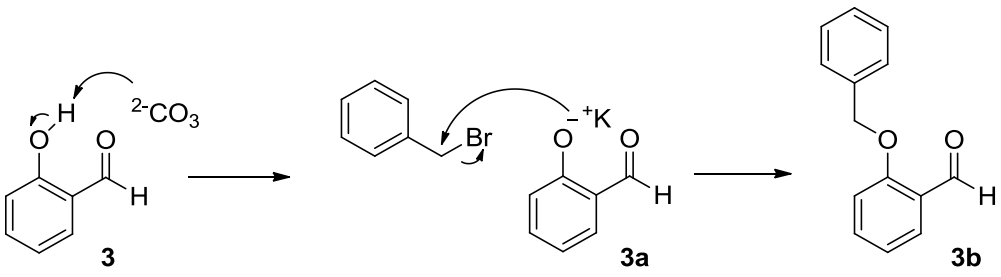

Scheme 4 – Reaction mechanism for the protection of aromatic alcohol.[88,89]

The synthesis of **3b** (Scheme 5) began by adding granular anhydrous potassium carbonate to dry acetone after which the mixture was vigorously stirred to prevent the granules from clumping and

sticking to the side of the reaction vessel. The mixture was heated under reflux and **3** was added dropwise to the solution over 15 minutes. Once the addition of **3** was completed, the mixture was observed to have a yellow color with a white precipitate (**3a**) in suspension. To the vigorously stirring mixture, benzyl bromide was added dropwise, causing the color of the reaction mixture to change from yellow to a reddish-brown. The change in color indicated that the substitution of bromide by intermediate **3a** was occurring well with **3b** being formed. Once the benzyl bromide had been added, the reaction temperature was increased to 75 ºC and left to reflux for 18 hours during which time the precipitate disappeared.

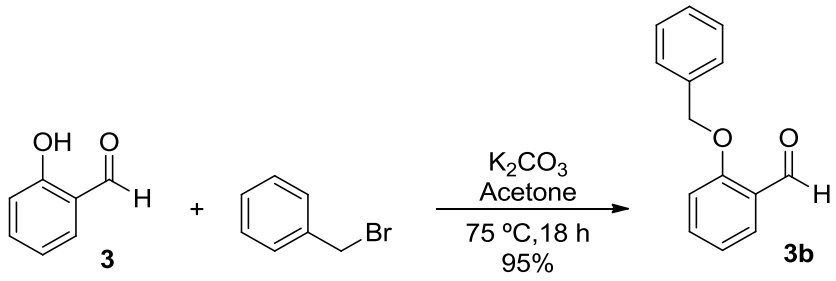

Scheme 5 – Optimized reaction for the synthesis of **3b**.

On completion, the reaction was cooled to room temperature, the acetone removed under reduced pressure, the residue diluted with water and the product extracted using DCM. The solvent was removed under reduced pressure to give the crude product as a yellow oil. The crude product was purified by column chromatography to afford the pure product as a clear oil that crystallized on standing and in excellent yield (95%).

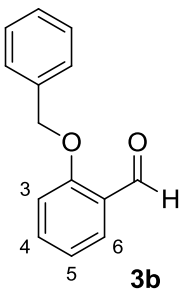

^{1}H NMR spectroscopic analysis confirmed the successful formation of **3b** from the reaction. The benzylic and methylene protons of the benzyl-group are all accounted for. The aldehyde proton was observed as a singlet at 10.57 ppm integrated for 1H. The proton of position 3 was observed as a doublet at 7.86 ppm integrated for 1H, proton 6 was observed at 7.05 ppm as a doublet but overlapped with a triplet from the proton at position 5 and integrated together for 2H. Lastly proton 4 was observed as a multiplet between 7.52–7.56ppm and integrated for 1H. The calculated MS value of 213.0916 *m/z* coincided well with the observed value of 213.0920 *m/z* and the characteristic IR peaks for the aldehyde was observed at 2873 cm^{-1} (ald C-H str.), 1681 cm^{-1} (ald, C=O, str.), 1237 cm^{-1} and 1160 cm^{-1} (C-O-C, str.). All the characterization results correlated well with the literature and all results and spectral data can be found in chapter 6 for all compounds reported in this chapter.[90,91]

In conclusion, the combination of selected literature procedures and repeated attempts, the reaction conditions afforded yields of **3b** in excess of 90%. The results obtained from ^{1}H and ^{13}C NMR, MS as well as IR spectroscopy coincided with reported values from literature confirming the success of the reaction.[62]

2.2.2 Synthesis of Ethyl 2-azidoacetate

For the synthesis of our desired alkyl azide, ethyl 2-azidoacetate **4**, a simple yet effective method was identified that made use of nucleophilic substitution on an alkyl halide with a metal salt and optimized it for our desired alkyl azide **4a** (Scheme 6).[92,93] The described literature reaction was carried out in a heterogeneous bi-phasic system as no single solvent could be identified in which all the reagents were soluble. The alkyl halide was found to be miscible in the organic phase and the metal salt, containing the reacting anion, was soluble in the aqueous phase.

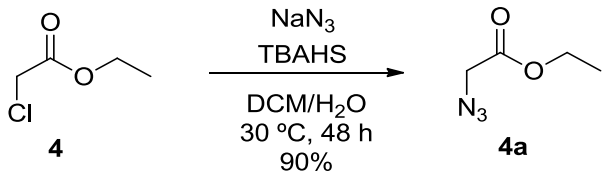

Scheme 6 – Optimized synthetic route for the synthesis of ethyl 2-azidoacetate **4a**.

The reaction was mediated by liquid-liquid phase transfer catalysis (LL-PTC)[94-96] and the introduction of a phase transfer agent to the system facilitated the transfer of the reacting species between the two immiscible solvents.[94] Scheme 7 illustrates the mechanism for the phase transfer of the active anion (N_3^-) from the aqueous to the organic phase by the phase transfer agent.[94] The subsequent nucleophilic substitution mechanism that occurs once the active anion species reaches the alkyl halide in the organic phase is also illustrated by Scheme 7.

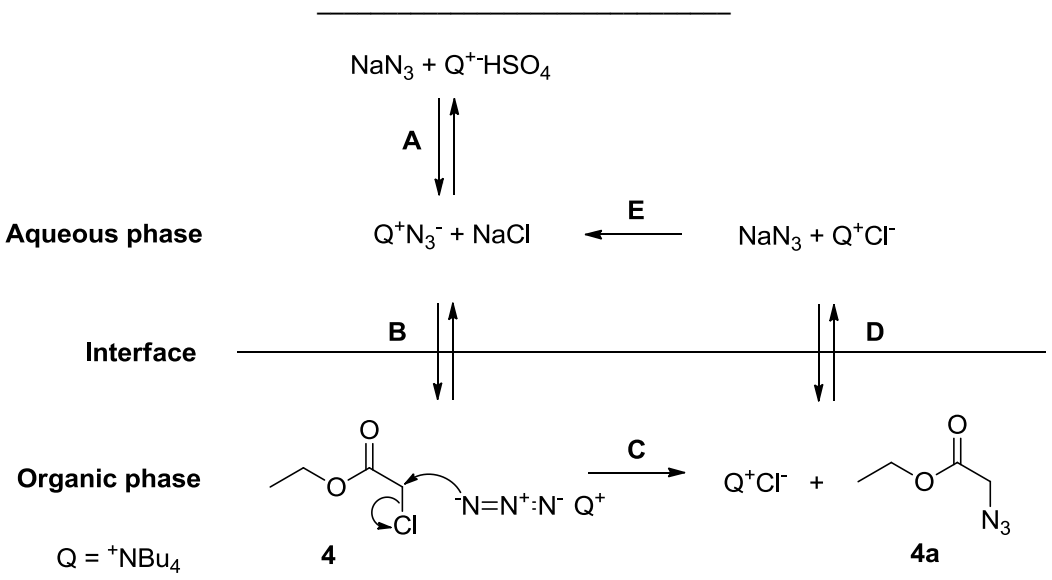

Scheme 7 – Mechanism illustrating the function of the phase-transfer catalyst to assist in the formation of ethyl 2-azidoacetate **4a**.[94-96]

As depicted in Scheme 7, step **A**, an excess of sodium azide and a catalytic amount of tetrabutylammonium hydrogensulfate (TBAHS) were dissolved in water (30 ºC) to facilitate the formation of new ion pairs.[94] DCM was then added to the system, followed by the reactant (**4**) and the reaction mixture stirred vigorously to create a semi-singular phase of solvents. The newly formed quaternary ammonium ion pair ($Q^+N_3^-$) transfers from the aqueous phase to the organic phase (Step **B**) where it exists as a highly reactive species.[94] The azide anion (N_3^-) attacks the alkyl halide in an S_N2 nucleophilic substitution reaction (Step **C**) that displaces the chloride ion to form the desired alkyl azide **4a**. The quaternary ammonium ion (Q^+) is now in the organic phase and for the process to be efficient it must reform a reactive ion pair ($Q^+N_3^-$) in the aqueous phase.[94] The chloride ion provides a means of transferring the quaternary ammonium ion back to the aqueous phase by forming a weaker ion pair with the Q^+ that favors the aqueous phase (Step **D**).[94] Once the weaker ion pair (Q^+Cl^-) has transferred to the aqueous phase, it dissociates, and a new reactive ion pair can be formed between an azide ion (in excess) and the liberated Q^+ (Step **E**) allowing Step **B** to repeat resulting in an increase in formation of **4a**.[94]

As mentioned at the start of this section, the reaction that we had identified from literature was optimized for our desired alkyl azide. The reaction conditions for comparative alkyl azides called for the reaction to be carried out at room temperature, in a water/chloroform solvent system and reaction times of 25 hours.[92] As seen in Scheme 6 the conditions for our method are slightly different with regards to an alternative solvent system (water/DCM), reaction temperatures of 30 ºC and longer reaction time (48 hours). The alteration to the temperature and time proved to be successful for the cooler laboratory conditions with the reaction reaching completion with 95% yield.

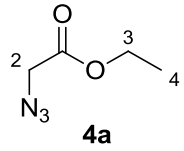

4a

^{1}H NMR spectroscopic analysis confirmed the formation of **4a** was successful with the protons at position 2 was observed as a singlet at 3.80 ppm and integrated for 2H, the protons at position 3 was observed as a quartet at 4.19 ppm and integrated for 2H and finally the protons of position 4 was observed at 1.24 ppm as a triplet and integrate for 3H. The MS observed value of 130.0512 *m/z* coincided with the calculated value of 130.0572 *m/z*. IR spectrum analysis indicated that the azide was present by the appearance of a sharp absorbance peak at 2104 cm^{-1}, indicative of the azide stretching and all of the characterization results correlated with the literature.[80,92,97,98]

Having tested reaction conditions (DCM/H_2O and Acetone/ H_2O) without using the phase-transfer catalyst to synthesize compound **4a**,[80,97] it was clear that the optimized reaction, utilizing a phase transfer catalyst, provided the best yields (90–95%) for **4a**.[92] The insight gained from the use of a phase-transfer catalyst and the mechanism by which it functions to improve substrate-reagent interaction in a bi-phasic system, will prove to be beneficial in future experiments where similar conditions might be required to improve the yields of a reaction.

2.2.3 Knoevenagel Condensation – Method 1

Among the various methods for C-C bond formation, the Knoevenagel condensation reaction has been extensively studied and applied in industrial processes.[80,99,100] The Knoevenagel condensation is a reaction where a dehydration step occurs and an unsaturated C-C bond is formed. As a result, it is useful in the synthesis of α-β-unsaturated esters. The general reaction mechanism for the Knoevenagel condensation, illustrated by Scheme 8, involves a deprotonation of **4a** by the ethoxide base, followed by attack of the enolate **4b** on the aldehyde **3b,** forming intermediate **5a** in an aldol reaction. A proton transfer then occurs from the protonated base to **5a** forming intermediate **5b**, which is then finally deprotonated by the re-formed ethoxide, and yields product **5** in a condensation reaction.[99]

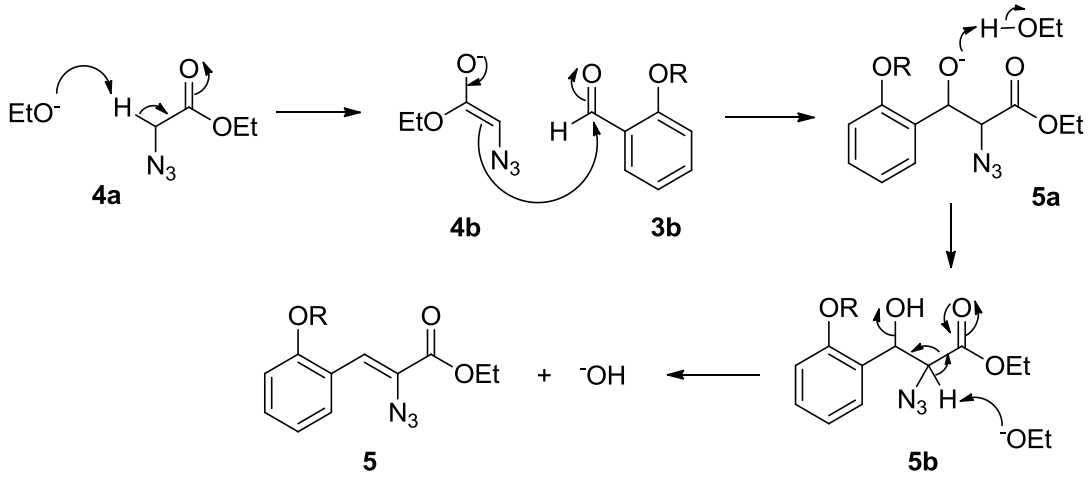

Scheme 8 – General mechanism for the Knoevenagel reaction for the synthesis of *α*-azido-*β*-unsaturated-ester **5**.

In recent years, the Knoevenagel condensation has been well-documented and proven to be a versatile reaction with different procedural conditions including solvent-free reactions, microwave-promoted, and ultrasound-catalyzed reactions that form C–C double bonds.[99] We decided to forgo the complexities of the newer methods and utilized a more traditional method described by Heaner *et al*.[80] The authors investigated a solvent-based method and the common limitations that the Knoevenagel condensation has with regards to low yields and the formation of undesired by-products. The optimized reaction described by Heaner *et al*.[80] utilized a sacrificial electrophile that reacts with the hydroxide ions that are formed in the dehydration step and results in increased yields and decreased by-products formation.[80]

Another limitation of the Knoevenagel condensation is the instability of the alkyl azide in strongly basic conditions due to hydrolysis of the ester moiety by the hydroxide ions, that competes with the formation of the intermediate **5a**. By introducing the sacrificial electrophile, ethyl trifluoroacetate (ETFA), the ester hydrolysis of the alkyl azide, as well as the product **5**, was circumvented as the hydroxide ions were reacting with the more reactive ETFA (Scheme 9).[80] Furthermore, upon interception of the hydroxide by the ETFA, the weaker nucleophilic trifluoroacetate forms **N1**, which is less prone to take part in side reactions and form unwanted by-products.[80]

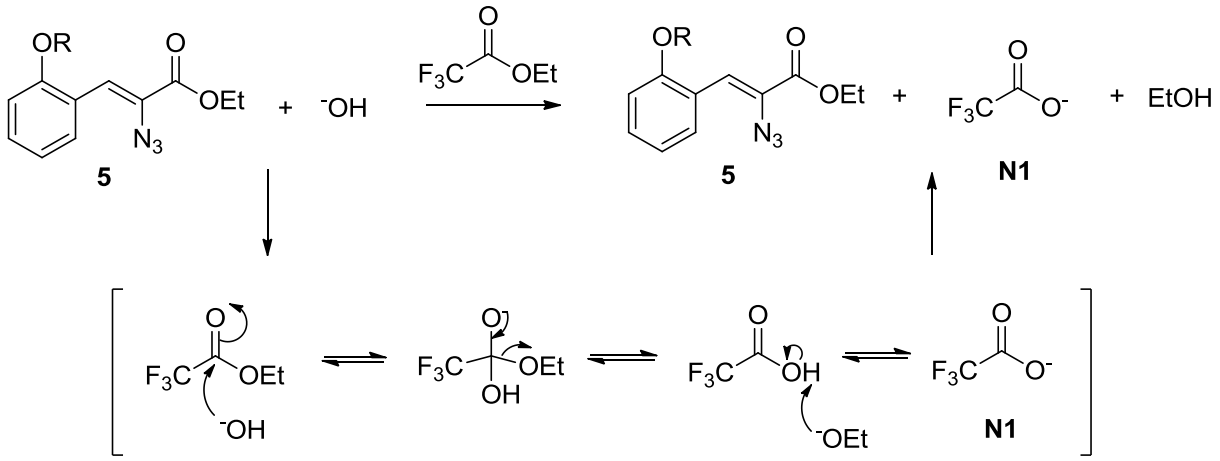

Scheme 9 – Illustration of sacrificial nucleophile, ETFA, intercepting a hydroxyl ion to form a less reactive base **N1**.[80]

Following the literature procedure described by Heaner *et al.*,[80] we formulated a reaction for the synthesis of our desired *α*-azido-*β*-unsaturated ester **5** (Scheme 10). A solution of sodium ethoxide was prepared under an inert atmosphere by dissolving solid sodium in dry ethanol. The solution was cooled to 0 ºC and held at this temperature for the remainder of the procedure. The required benzaldehyde **3b** was added to the stirring viscous reaction mixture in a single portion.

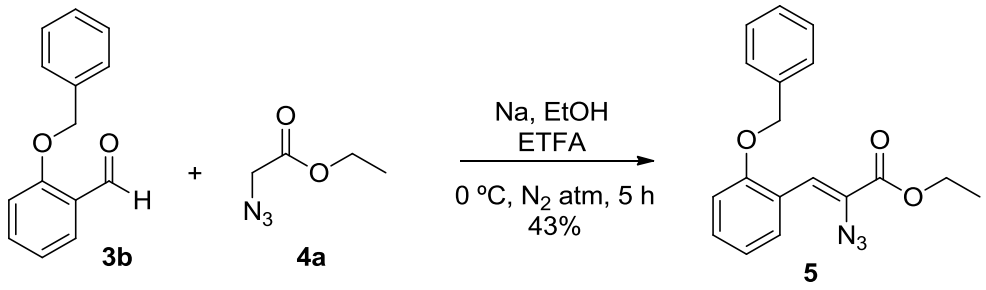

Scheme 10 – Reaction scheme for the Knoevenagel reaction employed for the synthesis of compound **5**.[80]

Once **3b** was added to the reaction mixture the solution was vigorously stirred and a solution of **4a** and ETFA was added dropwise to the mixture. During the addition of the acetate solution the transparent reaction mixture began to turn translucent with the product **5** forming as a yellow precipitate that noticeably thickened the mixture. As more of the acetate solution was added, more precipitate formed and the yellow solution became thick and would barely stir. Once all of the acetate solution was added the reaction was left to stir for 4 – 6 hours under a continuous flow of nitrogen. On completion, the reaction mixture was evaporated under reduced pressure, followed by neutralization with saturated ammonium chloride solution. The aqueous solution was extracted to isolate **5** using

EtOAc and purified by column chromatography, ^{1}H NMR spectroscopic analysis confirmed the formation of the product **5** in a moderate yield of 43%.

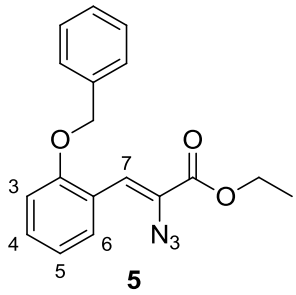

5

^{1}H NMR spectroscopic analysis confirmed the formation of a single product, **5**. The both the benzylic and ethyl ester protons are all observed and accounted for integrating for 12H. The key signal corresponding to proton 7 was observed at 7.53 ppm as a singlet and integrated for 1H. Proton 6 was observed as a doublet at 8.24 ppm and integrated for 1H. Proton 3 was observed as a doublet at 6.95 ppm and integrated for 1H. Proton 4 was observed as a multiplet between 7.23-7.27 ppm integrating for 1H and finally proton 5 was observed between 7.00-7.04 ppm as a multiplet and integrating for 1H. The MS analysis returned an observed value of 324.1348 *m/z* which correlated with the calculated value of 324.1303 *m/z*. Analysis by IR confirmed the presence of the azide group with the characteristic azide stretching frequency observed at 2113 cm^{-1}. All the results coincided with the literature and confirmed the successful formation of **5**.[101]

It was interesting to note that the only product isolated from the above reaction was the *Z*-isomer and not the *E*-isomer. The *Z*-configuration is theoretically the more favorable because it is thermodynamically more stable than the *E*-configuration.[80] Confirmation of the result was accomplished by comparing the ^{1}H and ^{13}C NMR spectroscopic results to the peak results reported in the literature for the position 7 proton and carbon, which coincided well with reported values.[101]

In conclusion, the results obtained from MS, NMR and IR all confirmed the formation of the desired product, but more importantly, that the *Z*-isomer was the only product that had formed. If the *E*-isomer had formed, the cyclization reaction to form **8** would not take place as the *E*-isomer is unable to undergo the necessary ring-closure to form **8**. The reaction methodology we employed for the synthesis of **5** had proven to be successful but the yield was below average and we could not completely inhibit the formation of unwanted by-products. As a result, we returned to the literature to find an alternative method for the synthesis of **5**. Sections 2.3 that follows will discuss the methods that we identified with the hope that they would give greater success in the formation of **5**.

2.3 SYNTHESIS OF INDOLE PRECURSORS – ALTERNATIVE METHODS

With the Knoevenagel condensation discussed in the previous section not consistently providing good to high yields of the azide precursor **5**, the decision was made to find an alternative method that would use **3b** as starting material. A procedure was found that was one step longer than the previous method

but was hoped would ultimately provide the desired azido-ester **5** more consistently, and in higher yields. This would be accomplished through the use of an ylide to form an *α*-*β*-unsaturated ester **7** in a Wittig-type reaction, followed by an azide addition to the unsaturated ester **7**. An advantage of this method was that the precursor **5** synthesis resulted in the formation of fewer by-products. The process of obtaining compound **5** via this alternative method will be discussed in the section below.

2.3.1 Synthesis of Stabilized Phosphorous Ylide

Phosphorous ylides are commonly associated with the Wittig reaction for the synthesis of unsaturated C–C bonds. However, the stabilized ylide **6b** (Scheme 11) that we synthesized was for a modification of the Wittig reaction.[102] The Horner-Wadsworth-Emmons modification (HWE) is a characteristically stereospecific reaction used for the synthesis of α-β-unsaturated esters predominantly in the *trans*-configuration.[102-104]

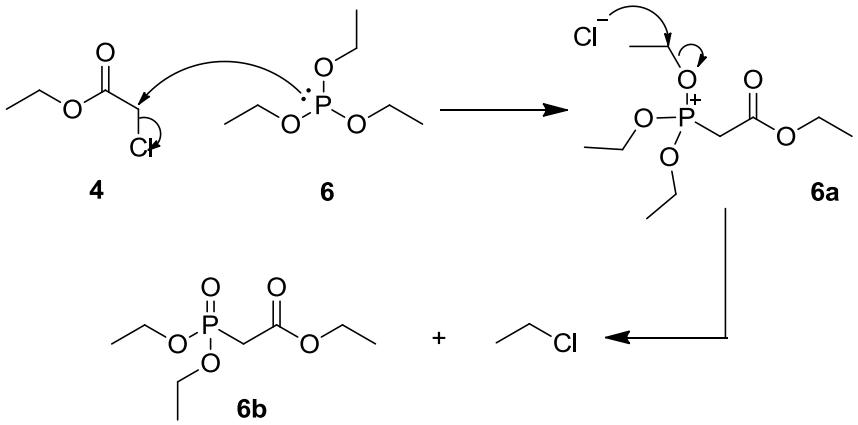

Scheme 11 – Reaction mechanism for the Arbuzov reaction illustrating the formation of ylide **6b**.[105-107]

Earlier in this chapter it was mentioned that two methods were devised for the synthesis of the azido-cinnamate precursor from which **8** will be formed by thermolysis. The procedure for the formation of a *trans*-stereospecific cinnamate can be achieved by the Horner-Wadsworth-Emmons (HWE) reaction and requires the use of a stabilized ylide such as **6b**.[102-104] The mechanism for the formation of the phosphoryl-acetate is illustrated in Scheme 11 and is known as the Arbuzov reaction.[105-107] In the reaction the triethyl phosphite, at high temperatures, functions as a nucleophile and attacks the methylene carbon of **4,** forcing the chloride to leave in an S_N2-type nucleophilic substitution to give **6a**.[105-107] The central phosphorous atom becomes positively charged during the substitution. This causes a reaction whereby the chloride anion attacks and removes an ethyl-group **6a** from an ethoxy-group attached to the phosphorous and results in **6b** being formed.[105-107]

The reaction was carried out as described in the literature, and merely required that **6** and triethyl phosphite **4a** be combined, without solvent or other reagents, and heated under reflux for 8 hours to achieve the formation of **6b** in 95% yield (Scheme 12).

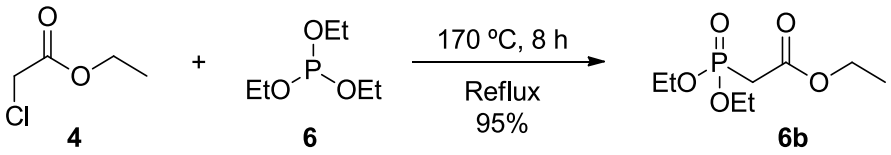

Scheme 12 – Reaction scheme for the optimized reaction employed to synthesize **6b**.

On completion, the reaction mixture was collected and a standard work-up carried out to remove any unreacted **4a**. The organic solvent was removed and the crude yellow oil that remained was distilled to collect the pure product as a pale yellow oil in excellent yield (95%). The confirmation of the product was accomplished by NMR, MS and IR spectroscopic analysis.

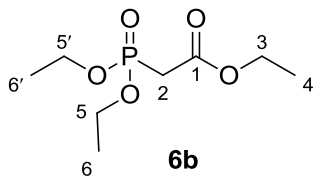

^{1}H, ^{13}C and ^{31}P NMR spectroscopic analyses confirmed the formation of **6b**. In the ^{31}P NMR spectrum a singlet peak was observed at 19.8 ppm that corresponded to the phosphonate. ^{1}H NMR spectrum was observed to have a triple at 1.18 ppm for the protons at position 4 and integrates for 3H. The protons at position 6 and 6′ were observed at 1.24 ppm as a triplet which integrated for 6H. The protons at position 2 were observed as a doublet at 2.85 ppm and integrated for 2H. The doublet observed for the protons at position 2 can be explained by the heteronuclear coupling between the protons and the phosphorous atom, thus giving a doublet and not a singlet. The protons at positions 3, 5 and 5′ were observed as a multiplet between 4.03–4.17 ppm which integrated for 6H. The observed MS value of 225.0883 *m/z* coincided well with the calculated value of 225.0892 *m/z* and together with all the results from characterization coincided with the literature.[108,109]

In conclusion, the Arbuzov reaction that we employed from the literature for the synthesis of **6b** proved to be highly successful and afforded the desired ylide **6b** in excellent yield (95%).

2.3.2 The Horner-Wadsworth-Emmons Reaction

In our search for an alternative method to that of the Knoevenagel condensation for synthesizing *α*-azido-unsaturated ester **5**, we delved into the possibility that the high selectivity of HWE method for the *E*-isomer, *trans*-geometry, may be a more favorable method for the synthesis of an *E*-*α*-*β*-unsaturated ester as precursor to the synthesis of an *Z*-*α*-azido-unsaturated ester **5** in the ensuing

reaction (section 2.3.3).[104] To clarify, the *Z*-isomer product **5** is equivalent to the *E*-isomer precursor **7,** as the structure of **7** constitutes the bulk of structure **5** and the geometrical arrangement of the moieties of **7** are retained and inherited by **5**.

Over the years, many have attempted to explain the observed selectivity for *E* or *Z* alkenes in the Wittig-type reaction using stabilized ylides.[110] The most recent developments and mechanisms that have been proposed by various authors have been summarized by Byrne and Gilheany to shed light on the most recent and plausible mechanisms for product formation.[110] The most plausible was the mechanism proposed by Vedejs and Snoble,[111] of direct irreversible cycloaddition of a stabilized ylide to an aldehyde forming a single oxaphosphatane (OPA) transition state (**TS1** or **TS2**), followed by the irreversible and stereospecific cyclo-reversion of the OPA to form the stereospecific alkene (Scheme 13).[110,112-114]

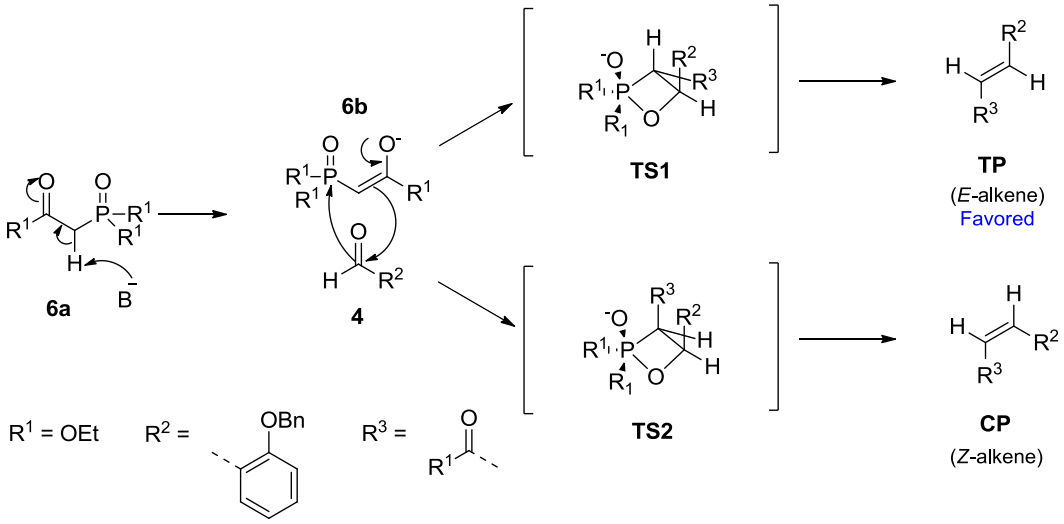

Scheme 13 – Reaction mechanism illustrating the formation of the two possible geometrical isomers *E/Z* of compound **7** via transition states TS1 or TS2, respectively, where the *trans* product is represented by **TP** and the *cis* product by **CP**.[112-115]

Vedejs *et al.*[112,114,115] elaborated on the mechanism proposing that the stereochemistry of the alkene product is decided during the transition state (**TS**) cycloaddition step.[110,112-114] The formation of the favored *trans*-geometrical product **TP** (*E*-alkene) by the use of stabilized ylides, such as **6b**, was explained by Vedejs *et al.*[112,114,115] to be as a result of the **TS** favoring a planar-*trans* geometry that minimizes 1-2 and 1-3 steric interactions (Figure 17, a).[110,112-114] However, this model could not completely account for the formation of *E*-alkenes as Robiette *et al.*[116,117] had pointed out with computational models that there was a dipole-dipole interaction that had to be taken into account with respect to the use of ester-stabilized ylides (**6b**).

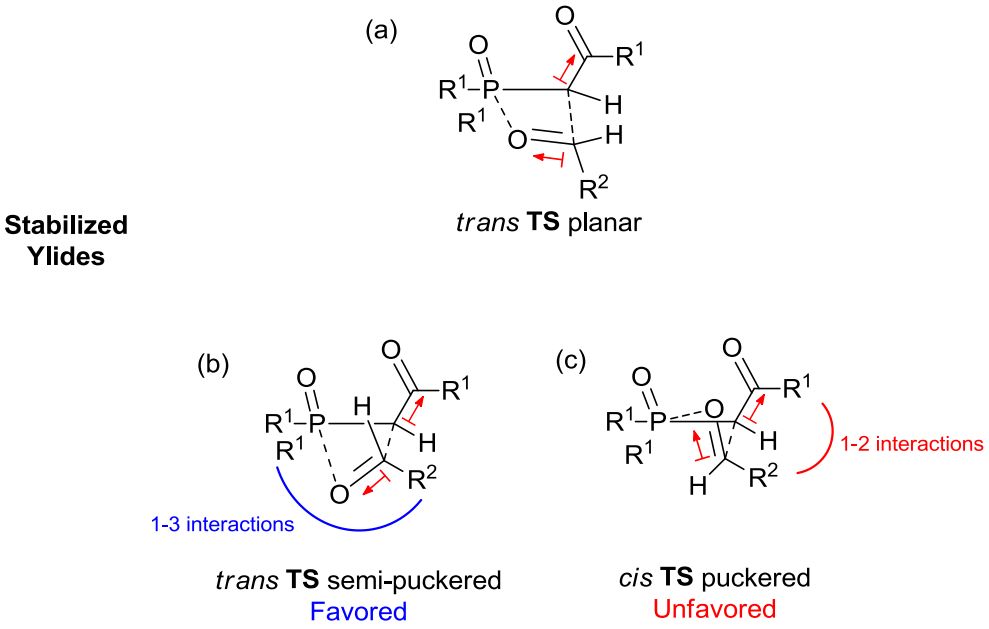

Figure 17 – Illustration of dipole-dipole interactions for a) original planar *trans* TS, b) favoured semi-puckered *trans* **TS** and c) less favoured highly puckered *cis* **TS**.[116,117]

Although, both Vedejs *et al.*[112,114,115] and Rodiette *et al.*[116,117] agreed upon the fact that the *trans*-geometry was favored, the planar nature thereof was brought into question by the dipole-dipole interactions associated with the ester and aldehyde C=O bonds in the **TS**.[110,112-114] As a result the planar geometry therefore becomes slightly puckered in shape which alleviates 1-2 and 1-3 strain resulting in the more favored geometry of a semi-puckered *trans* **TS** (Figure 17, b).[116,117] In contrast, for the *cis*-**TS** to alleviate the 1-2 and 1-3 strain it also becomes puckered due to the dipole-dipole interactions, but destabilizes the geometry as a result of the electrostatic interactions of the two dipoles occurring when they are antiparallel (Figure 17, c).[116,117] Therefore, the stabilized ylides proceed via a slightly puckered, but planar *trans* **TS**, which has a lower steric strain between the 1-2 and 1-3 interactions as well as a lower electrostatic interaction by the two dipoles being in parallel geometry.[116,117] Combing both the mechanism proposed by Vedejs *et al.*[112,114,115] and Rodiette *et al.*[116,117] a new more plausible explanation was obtained for the selectivity of stabilized ylides and the stereoselectivity for the *E*-alkene product.[110]

Recently documented solvent-free HWE reactions have shown some success in synthesizing highly *E*-selective products;[103,104] although for our purposes we decided to make use of more conventional solvent methods for the synthesis of **7** as the starting material **3b** had very low solubility in **6b**.[118,119] A recent paper by Ando and Yamada reported the use of solvent-free HWE reactions with various inorganic bases (NaOH, KOH, K_2CO_3, Cs_2CO_3 and K_3PO_4).[104] While these reaction conditions resulted in average yields for their compounds, selection of the base indicated that the selectivity could be maintained; however, the yields would vary to a large extent. When K_2CO_3 was used as base instead of NaOH, a high selectivity for the *E*-isomer (98:2) was obtained and decomposition of

product and starting material was observed to be minimal.[104] Although, the use of Cs_2CO_3 had shown the best results, 80% and 98:2 *E*-selectivity, the K_2CO_3 was for our purposes the more viable option as it was less expensive than the Cs_2CO_3.[104] Using the described procedure by Ando *et al.*[102] with K_2CO_3 as base,[104] we modified their procedure to include a solvent to dissolve **3b** and which would allow for the reaction to be heated under reflux which we proposed would provide **7** as the *E*-isomer in improved yields (Scheme 14).

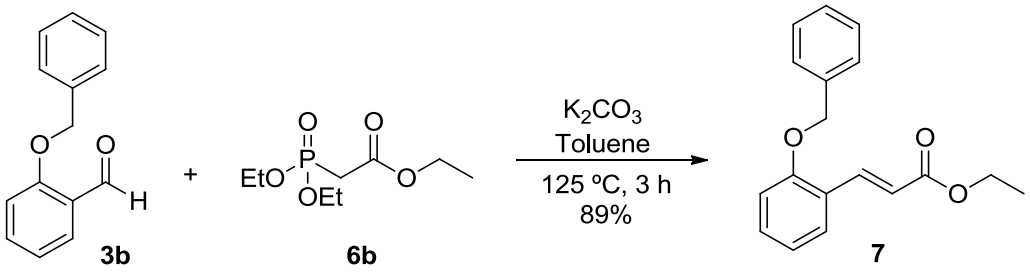

Scheme 14 – Modified reaction scheme for the synthesis of **7** in excellent yield.[104]

The formation of **7** was achieved by dissolving **3b** in warm toluene and adding the K_2CO_3 in granular form to the stirring solution. The solution was stirred vigorously during heating and once the reaction mixture began to reflux the HWE reagent **6b** was slowly injected into the reaction mixture. Once the reaction had been heated under reflux for 3 hours, a standard aqueous workup and purification by silica-gel chromatography afforded the product as a white crystalline material in excellent yield (89%).

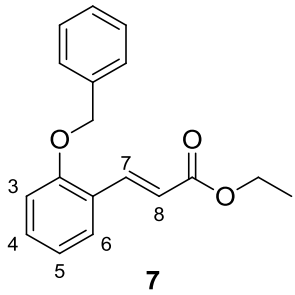

^{1}H NMR spectroscopic analysis confirmed the formation of **7**. The benzylic, methylene and acetate protons were all observed and accounted for and integrated for 12H. Proton 7 was observed at 8.11 ppm as a doublet and integrated for 1H. Proton 8 was observed as a doublet at 6.55 ppm and integrated for 1H. Proton 3 and 5 were observed as a multiplet from 6.94–7.00 ppm and integrated for 2H. Proton 4 and 6 were observed as a multiplet from 7.29–7.36 ppm and integrated for 2H and finally proton 6 was observed at 7.55 ppm as a doublet of doublets and integrated for 1H. The MS analysis returned an observed value of 283.1338 *m/z* which correlated with the calculated value of 283.1334 *m/z*.[120,121]

In conclusion, the modifications made to the Ando and Yamada[104] literature procedure, resulted in great success with excellent yields being obtained for **7** (89%).[104] Proof of the geometrical

configuration was obtained from ^{1}H NMR spectrum by studying the coupling constants for the protons at positions 7 and 8. For a *trans*-configuration a coupling constant (J^{3}_{78} and J^{3}_{87}) should be between 15–18 Hz and for a *cis*-configuration 9–12 Hz.[88,122] The J^{3}-coupling constant from proton 7 to 8 and 8 to 7 was observed to be 16.7 Hz for both and confirmed that the isolated compound **7** was in the expected *trans*-configuration (*E*-isomer).

2.3.3 CAN-mediated Azide Addition

Although we had some success with the synthesis of **5** from the use of the Knoevenagel condensation methodology (Section 2.3.1) we were interested in finding an alternative method that could decrease the possibility of forming by-products as a result of side reactions and improve the yield (Section 2.3.1).

Having returned to the literature, an alternative method for the synthesis of **5** was identified as reported by Nair and George[86] in 2000 and Chang *et al.*[87] in 2005 that utilized similar compounds to that of **7** to afford **5** in average yields.[86,87] These methods showed more promise with regards to less by-product formation and better regio-selectivity for the formation of **5**.[86,87] The methodology that was reported would afford **5** in a two-step cerium(IV) ammonium nitrate (CAN)-mediated azide addition to the HWE product **7**, forming an azido-nitro intermediate that, in the second step, that was expected to undergo a nitrate elimination reaction to form **5** with fewer by-products (Scheme 15).[86,87]

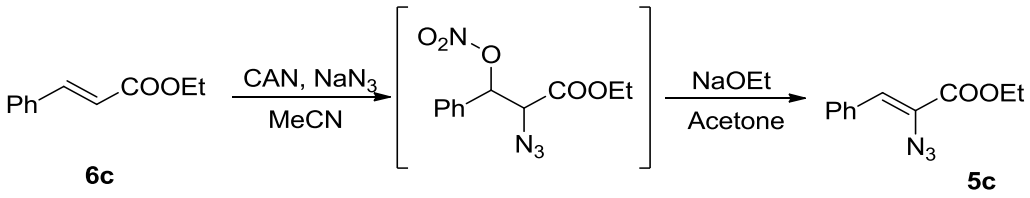

Scheme 15 – General reaction scheme described by Nair and George[86] for the synthesis of an α-azido unsaturated ester **5c**.[86,87]

Cerium(IV) ammonium nitrate (CAN) is a versatile reagent that has lent itself to a wide range of applications in organic chemistry research and industry.[123] It was invented in 1936 by Smith *et al.*[98] and functions as a single electron oxidizing reagent and has been widely used in the formation of carbon-carbon bonds.[86] The uses of CAN have been extensively studied over the years and many examples of its use in organic chemistry have also been reported.[86,87,123-127] Examples of the types of reactions for which CAN is used include oxidation, photooxidation, nitration, oxidative addition, chemical conversion and also as a catalyst in polymerization reactions.[87,123] Because of this versatility, it has become a useful tool in the arsenal of organic chemists in academic and industrial research

environments.[123] We decided to employ the methodology proposed by Nair and George,[86] where it is reported that it is possible to synthesize an *α*-azido-*α*-*β*-unsaturated ester **5** using CAN through the addition of an azide group to **7**.[86] Scheme 16 illustrates a mechanism proposed by Nair and Geroge[126,127] that may possibly explain the formation of the azido-nitro intermediate and finally the formation of a *Z*-azide product **5**.[86,124-128]

The reaction is initiated by CAN (single electron oxidizing agent) which reacts with an azide ion in solution. The interaction between CAN and azide reduces the cerium(IV) to cerium(III) as it gains an electron from the azide ion, resulting in the formation of an azide radical **5d**.[126,127] This radical then proceeds to react with the unsaturated ester, forming a new C-N bond at the alpha carbon position **5e**. A new radical is formed on the *β*-carbon position **5e** and is believed to react with a molecule of CAN (in excess) through a ligand transfer of a nitro group from the CAN complex to the carbon radical to give **5f**.[125-127] The addition of sodium acetate in the second step removes the *alpha* proton in **5f** to give **5g** and the elimination of the nitro group occurs via an E1cB-type elimination reaction that forms the *α*-*β*-unsaturated C–C bond of the product **5c**. [125-127]

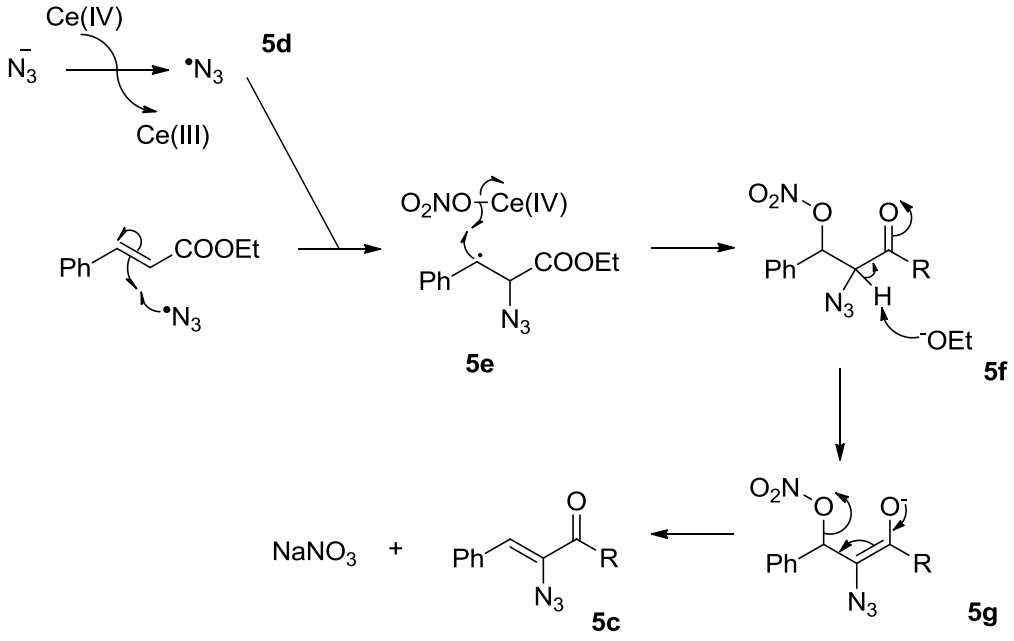

Scheme 16 – Proposed mechanism for the use of cerium(IV) ammonium nitrate to mediate the addition of an azide to an *α*-*β*-unsaturated ester.[126,127]

Having decided that the methodology describe by Nair and George.[86] would be a suitable alternative to the Knoevenagel condensation method described in Section 2.2.3, for the synthesis of **5**, we went ahead and utilized the CAN-process instead for our study (Scheme 17). The procedure described Nair and George.[86] required reacting **7** with sodium azide in the presence of excess CAN and deoxygenated

acetonitrile, followed by subjecting the crude intermediate to sodium acetate in acetone to afford **5** after work-up in 68% yield.[86]

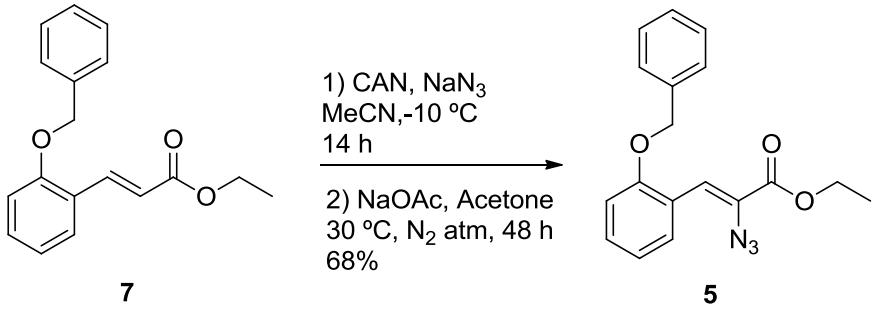

7 **5**

Scheme 17 – Scheme of the reaction employed for the synthesis of **5**.

By making alterations to a literature procedure,[86] the reaction solution was prepared by adding NaN_3 to a Schlenk tube, followed by dry acetonitrile and then dissolving **7** into the solution. It is important to note that NaN_3 has a low solubility in organic solvents, and settling of the NaN_3 would occur if the reaction was not stirred thoroughly during the reaction time period. It was found that the settling of the NaN_3 had an adverse effect on the yield and that the NaN_3 had to be distributed in the solution as much as possible to increase the available surface area and thus increase the possibility of interaction between the NaN_3 and CAN to form the azide radical **5d**. The CAN solution was prepared separately using the same solvent, also in a Schlenk tube, and sealed in preparation for the degassing procedure. Both solutions were deoxygenated by the freeze-pump-thaw method to remove any dissolved oxygen from the solutions. Nair and George.[86] proposed a mechanism for a by-product that can form due to the trapping of oxygen by the carbon radical **5e**, that results if the solutions are not thoroughly degassed (Scheme 18).[126,127]

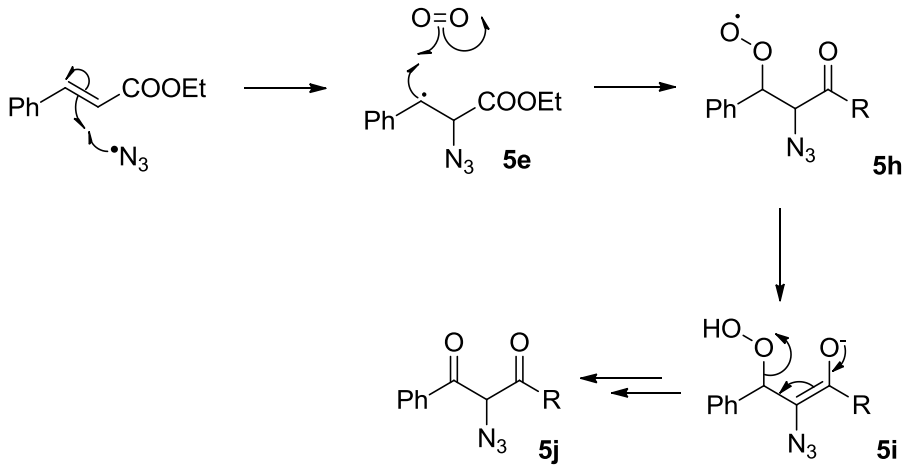

Scheme 18 – Proposed mechanism for the formation of by-product **5j** in the presence of oxygen in the reaction solvent.[126,127]

Once the first reaction between the azide radical and the unsaturated ester had taken place, dissolved oxygen in the solutions could lead to a hydroperoxide **5i** forming from the reaction of the free carbon radical of **5e** with the oxygen. [126,127] The formation of **5i** then ultimately leads to a phenacyl azide **5j** by-product and as **5h** also contains an active oxygen radical other undesired side-products could also form which lowers the yield of desired product **5**.[126,127] Having thoroughly degassed the solutions, the two flasks were filled with an inert atmosphere and cooled. The NaN_3 solution was cooled to -10 ºC using an ice and KCl cooling bath and the temperature maintained below -10 ºC by the periodic addition of KCl/ice slush. The CAN solution was kept cold in an ice bath at 0 ºC and injected dropwise into the NaN_3 solution.

After several attempts at changing the rate of injection and volumes, it was found that slower injection during the start of the addition favored the formation of fewer by-products and resulted in ease of purification. It was observed that injecting the solution too fast in the early stages caused unknown side products to form that were observed on TLC (during and after completion of the reaction). Initially the CAN solution was injected into the reaction flask at a very slow rate (0.5 mL/min) using an automated syringe injection pump to avoid flooding the reaction with CAN reagent. Only after a third of the CAN solution had been added, was the rate of injection increased to finish the addition of the CAN solution. The addition of KCl/ice slush was ceased after the injection was completed and the reaction left to stir under atmosphere for 14 hours.

Once the first step of the reaction was complete, the acetonitrile was removed under reduced pressure and the crude residue was diluted with ethyl acetate and washed with water to remove the excess CAN and unreacted sodium azide. The ethyl acetate solution was dried over magnesium sulfate to remove trace amounts of water that could cause side-reactions in the ensuing step. The ethyl acetate solution was collected by filtration and evaporated under reduced pressure to give the crude azido-

nitro intermediate **5f** (Scheme 16) that was used without further purification in the second step. The crude intermediate was dissolved in dry acetone, followed by the addition of anhydrous sodium acetate to the solution. The flask was closed and the reaction stirred under an inert atmosphere for 48 hours at room temperature. On completion, the acetone was removed under reduced pressure and a standard aqueous worked performed. The crude product was isolated in EtOAc and concentrated to give a brown oil which was purified by column chromatography to afford the product **5** in 68% yield.

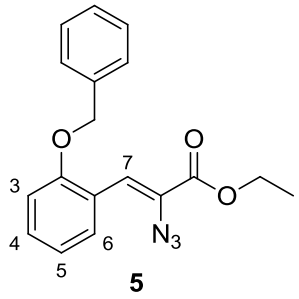

5

^{1}H NMR spectroscopic analysis confirmed the formation of **5**. The benzylic, methylene and acetate protons were all observed and accounted for and integrated for 12H. Proton 7 was observed at 7.54 ppm as a singlet and integrated for 1H. Proton 6 was observed as a doublet at 8.11 ppm and integrated for 1H. Proton 3 was observed as a doublet at 6.95 ppm and integrated for 1H. Proton 5 was observed as a multiplet from 7.00–7.04 ppm and integrating for 1H. Proton 4 was observed as a multiplet from 7.27–7.32 ppm integrated for 1H. The MS analysis returned an observed value of 296.1282 *m/z* which does not correlate to the calculated value of 324.1348 *m/z* as for the Knoevenagel product presented earlier. However, it is not entirely unexpected as the compound is light and air sensitive and once the calculated value is adjusted for the loss of a nitrogen molecule from the unstable azide (calc. value 296.1287 *m/z*), the observed value does confirm the formation of the compound. This was supported by the IR data. The azide stretching peak at 2115 cm^{-1} observed before the MS was carried out, supports the successful formation of **5** and furthermore the observed change in MS value due to the decomposition of the compound.[101]

In conclusion, the CAN-mediated azide addition to the *α-β*-unsaturated ester **7** proved to be a more successful and reproducible method for the synthesis of the desired azide product **5** both in ease of synthesis and purification. Therefore, this method was chosen as the preferred route of synthesizing **5**. The alterations that were made to the reaction procedure; injecting CAN solution at -10 ºC, controlling injection rate and degassing the solutions by the freeze-pump-thaw method, all culminated in higher and more consistent yields. A consistent yield of 60–68% was obtained by the altered procedure, which once compared to the 43% afforded by Knoevenagel condensation method discussed in Section 2.2.3, made the CAN-method the preferred method of obtaining **5**. This method also has the advantage of up-scaling to gram scale with no noticeable changes in the average yield obtained from repeated reactions. Important insight was gained with regards to the rate of addition of reagents and the effects that wet or non-degassed solvents have on a reaction and overall outcome of product formation. Further practical knowledge was gained in light of the fact that compound **5** was inherently unstable and that precautions had to be taken to protect it from exposure to light and air if

the compound was to be transported or stored for extended periods of time. Regardless of the small drawback of decomposition observed for **5** during the storage over an extended period of time, the reaction method proved to be the more efficient route for synthesizing **5**.

2.4 SYNTHESIS OF INDOLE SCAFFOLD AND DERIVATIVES

Having identified a suitable method for the synthesis of compound **5** by way of a CAN-method, and employing the methodology to obtain **5** in substantial amounts, the cyclization could be carried out. In this section we discuss the cyclization procedure, derivatisation of compound **8** and the indole precursor formation for use in the synthesis of a novel indole-quinoline hybrid (discussed in Chapter 4).

2.4.1 Thermolysis of Azido-cinnamate

There are various named reactions associated with the synthesis of an indole scaffold such as **8**, including the Hemetsberger, Fischer, Madelung, van Leusen, Buchwald and Julia reactions.[74] The Hemetsberger indolization is one of the simplest methods for the formation of an indole structure.[74,80] The Hemetsberger methodology converts **5** into the corresponding indole **8** by thermolysis using an appropriate solvent (Scheme 19). The simplicity of the procedure makes it an attractive alternative to the other methodologies as the only requirement is a high boiling point solvent in which the thermal cyclization can be carried out. Many suitable choices of solvent have been reported, with *p*-xylene, mesitylene and chlorobenzene being the most common.[80] Recent reports have described more modern modifications of the Hemetsberger reaction by microwave-assisted thermolysis to form indoles from α-azido-β-unsaturated esters synthesized by methods described in the previous sections.[82,83]

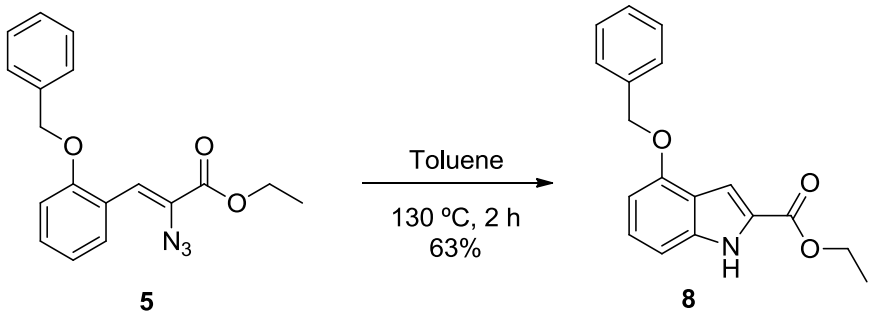

5 **8**

Scheme 19 – Optimized reaction for the thermal cyclization of **5** to afford **8** in good yield.

Having decided that the Hemetsberger methodology was the most suitable method for our purposes of indole formation, we proceeded to carry out the synthesis of our desired indole **7** from **5**. A

modification reported by Sheng *et al*.[62] of the conventional procedure described by Heaner *et al*.,[80] for the formation of **8**, was followed in which toluene was used as a reaction solvent instead of any of the other reported alternatives.[80-83] The mixture was heated under reflux after which **5** (dissolved in a minimum amount of solvent) was injected slowly into the refluxing toluene and left to reflux for 2 hours. On completion the crude product was purified by column chromatography that afforded **8** as a solid white material in good yield (63%); however, the product was light sensitive and was observed to discolor over time to a pale green if it was not covered and kept cold.

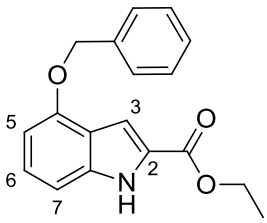

8

^{1}H-NMR spectroscopic analysis confirmed the successful formation of **8** with the benzylic, methylene and ethoxy protons all clearly accounted for. The indole nitrogen proton was observed at 8.96 ppm by a broad singlet (common to amine-protons) and integrated for 1H. The proton at position 3 appeared as a multiplet from 7.39–7.44 ppm and integrated for 3H due to overlap from benzylic protons. The proton of position 6 was observed as a multiplet from 7.20–7.24 ppm integrating for 1H and the proton at position 7 appeared as a doublet at 7.03 ppm integrating for 1H. The proton at position 5 was observed as a doublet at 6.58 ppm and also integrating for 1H. Final confirmation of **8** was achieved by MS and IR spectroscopic analysis with an observed value of 296.1283 *m/z* that correlated well with the calculated value of 296.1287 *m/z*, and the disappearance of the characteristic azide peak at 2114 cm^{-1} and appearance of two peaks corresponding to the 2° amine of the indole at 3321 and 1682 cm^{-1}. All the values from characterization coincided well with the literature.[62,81,101]

Although the reaction conditions for the Hemetsberger procedure are very simple, the mechanism is not as straight forward. The general belief is that the cyclization occurs through a stepwise azirene intermediate formation followed by cyclization.[74,80,101] Scheme 20 below illustrates a proposed mechanism for the thermally induced formation of an azirene intermediate **8a** through the loss of molecular nitrogen (N_2) from **5**.[80] **8a** then undergoes an electrocyclization onto the aromatic ring to form **8b**, followed by a [1,5] proton-transfer to the nitrogen and tautomerization to form the indole **8**.[80]

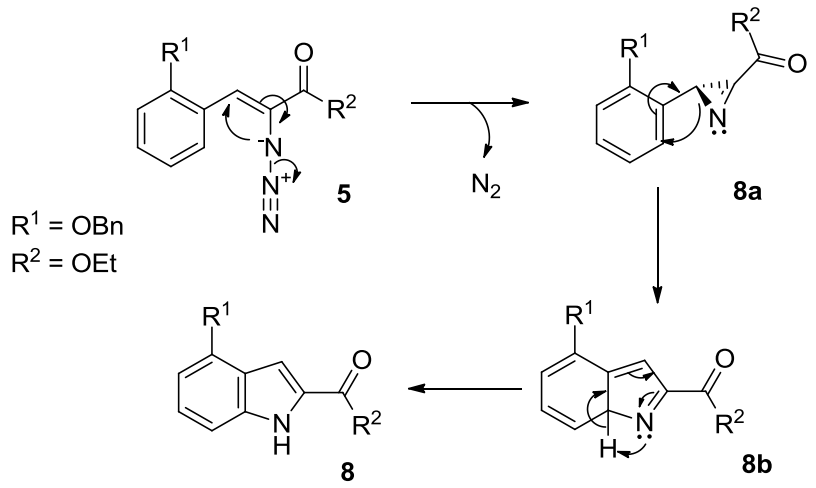

Scheme 20 – Proposed azirene reaction mechanism for the thermal cyclization of **5**.[80]

Studies carried out by Heaner *et al.*[80] on the use of purified versus unpurified starting materials indicated that there was no significant effect on the formation of indole by the presence of the impurities.[80] This was confirmed by our research that the only change observed on TLC was the disappearance of **5** and the appearance of **8** and after purification obtained compound **8** in 63% yield. Using unpurified **5** simplified the synthetic process as the purification of **5** proved difficult primarily due to its instability described above.[80] However, once the product had been formed, the separation of **7** from the by-products was relatively simple and afforded the pure product.

In conclusion, the use of the Hemetsberger thermolysis methodology proved successful for the formation of the desired indole structure **8** from **5**. Although, the modification to the injection procedure was done, the procedure can still further be optimized to afford higher yields of the product by further investigating the effect of temperature (increasing or decreasing reaction temperature) and possibly look at the effect solvent alterations may have on the dissolution of the sodium azide to increase free azide ions.

2.4.2 Mild and Efficient Debenzylation of 8

Following on the formation of **8**, a deprotection had to be carried out to unveil the hydroxyl group on which the ensuing Mitsunobu reaction (section 2.4.3) was to be performed that would afford the intended compound **2**.

Although various methods and conditions for the debenzylation of a phenol group are available, i.e. H_2 Pd/C, Lewis acids ($SnCl_4$, $FeCl_3$), K^+ in NH_3 and $NaBrO_3/Na_2S_2O_4$[129,130] there are limitations imposed by some of these reagents, substrates and procedures.[129,130] For our initial attempt at the debenzylation of **8** using H_2 and Pd/C, difficulties were encountered whereby **8** would either

decompose into unknown products or in some cases the reaction did not proceed at all. We therefore set out to investigate different methods that also had similarly mild conditions to that of the Pd/C method for debenzylation. Research led to an alternative methodology developed by Chouhan *et al.*[130] that makes use of $NiCl_2 \cdot 6H_2O$ and $NaBH_4$ to chemoselectively deprotect ethers.[130] These methods are reported to be as mild and efficient as the commonly used Pd/C method.[130] This procedure is described to be simple and has many advantages over the generally accepted methods for debenzylation.[130] Air and moisture need not be excluded by the use of an inert atmosphere, no strongly basic or acidic conditions are required, the reagents need not be prepared in advance, are inexpensive and lastly, yields are excellent and obtained from very short reaction times (5-20 min).[130] The debenzylation procedure by Chouhan *et al.*[130] was followed without modification to afford **9** in 70% yield (Scheme 21).

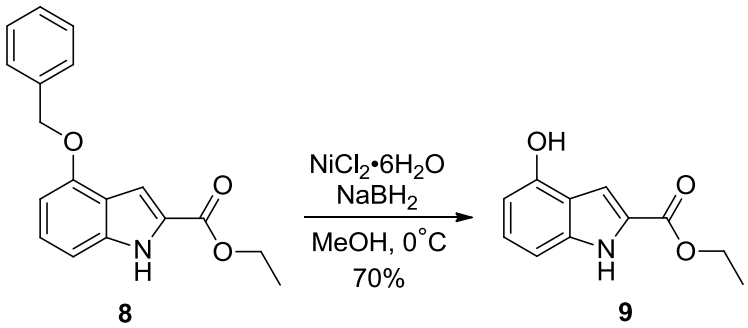

Scheme 21 – Reaction procedure for the debenzylation via the described method by Chouhan *et al.*[130]

The simplicity of the procedure was marked by combining the reactant **8** and the reagents ($NiCl_2 \cdot 6H_2O$, $NaBH_4$) in cold methanol (0 ºC). The reaction was left to stir at room temperature for 10 minutes and monitored for completion by TLC. On completion the reaction was quenched with a small amount of methanol and stirred at room temperature for a further 20 minutes, after which the reaction mixture was filtered through Celite and the methanol removed under reduced pressure. The collected crude residue was purified by automated column chromatography that isolated the product **9** from an unknown fine black residue that could not be trapped in the Celite during filtration. TLCs carried out during the reaction indicated no by-product formation, but that spot-to-spot conversion had occurred. This was confirmed by the onboard UV spectrometer of the automated column chromatography instrument that was available. The UV spectrum obtained for the purification indicated the presence of only one compound **9**, by the appearance of a single absorbance peak at the 256 nm wavelength generally used to visualize TLC plates. The spectrum was merely used to identify the formation of product and if there were any other products formed by the reaction as was indicated by TLC. The appropriate characterization of the isolated compound was done by NMR, MS and IR spectroscopic analysis techniques to confirm the isolated compound was indeed **9**.

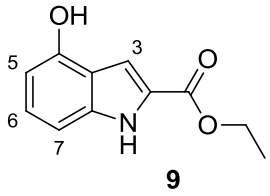

9

^{1}H NMR analysis confirmed the formation of **9**. The ethoxy protons were all accounted for, so too was the indole nitrogen proton. The phenolic proton was observed at 5.31 ppm as a broad singlet integrating for 1H, the proton at position 3 was observed as a singlet at 7.34 ppm integrating for 1H, and proton 5 was observed as a multiplet from 6.54–7.50 and integrated for 1H, the proton at position 7 was observed as a doublet that integrated for 1H at 7.01 ppm. Finally, the proton at position 6 was observed as a multiplet from 7.15–7.19 ppm that integrated for 1H. The observed result from MS of 206.0848 *m/z* coincided with the calculated value of 206.0818 *m/z*, from IR, the characteristic peaks of the hydroxyl group that formed were observed at 3420 cm^{-1} (O–H str.) and 1235 cm^{-1} (C–O str.). The results all coincided with what has been reported in the literature confirming the successful formation of **9**.[62]

In conclusion, the alternative method developed by Chouhan *et al.*[130] had proven to be more successful in debenzylating **8** and affording **9** in higher yield with no by-products forming. The simplicity of the procedure, short reaction time and no by-product formation all contributed to the decision to use this method over that of the previously used H_2 and Pd/C.

2.4.3 Mitsunobu Reaction of Indole 2

Having obtained the debenzylated indole **9**, the final step in the synthetic process was to derivatise **9** by substituting the 4-position alcohol in the structure for the piperidine group so that the final compound **2** could be obtained. However, the displacement of the OH-group in **8** is not possible, and the substitution of the OH-group of **10** (4-hydroxypiperidine) would not be as simple as it would seem. The reason for this is that under basic conditions OH-groups are never leaving groups in nucleophilic substitution reactions.[88] Hydroxide ions are highly basic and strong nucleophiles, and if another nucleophile were strong enough to displace the OH-group, it would be strong enough to deprotonate the OH and thus the desired substitution reaction would not occur.[88] However, the Mitsunobu reaction overcomes the potential difficulties by converting the OH-group of **10** into an electrophile and a weaker nucleophile, alcohol of **9,** can then facilitate the substitution. Scheme 22 illustrates the mechanism for the Mitsunobu reaction for the intended reaction of indole **9** with reagent **10**.[88]

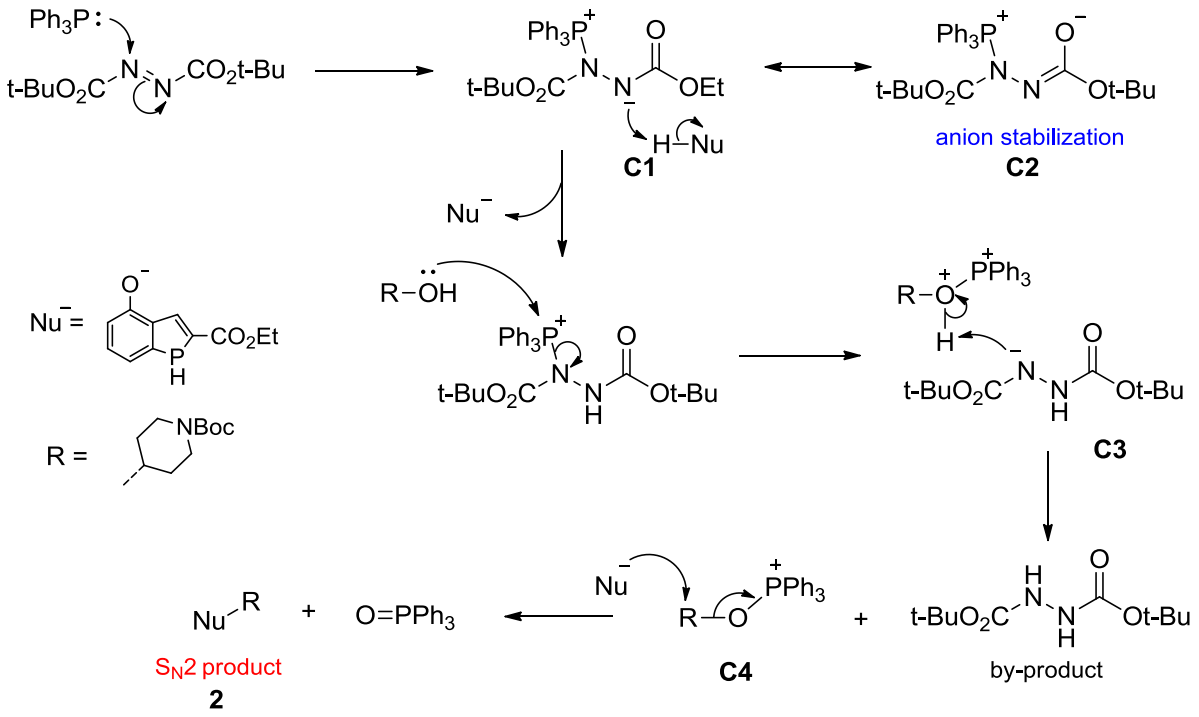

Scheme 22 – Reaction mechanism of the Mitsunobu reaction employed for the synthesis of compound **9**.[88]

The first step of reaction involves the triphenyl phosphine (nucleophilic but not basic) and di-*tert*-butyl azidodicarboxylate, where the phosphine adds to the weak N=N π bond to form an anion **C1** which is stabilized by a neighboring ester group **C2**.[88] This newly formed anion **C1** is basic enough to deprotonate a nearby protonated nucleophile (conjugate acid), in this case indole **9**, to generate the nucleophile (**Nu**$^-$) ready for the nucleophilic substitution in a later step.[88] Next the step, the positively charged phosphorous is attacked by the alcohol (**10**) thus forming another nitrogen anion, stabilized by the neighboring ester, which rapidly removes a proton from the alcohol to form an electrophilic R-O-PPh_3^+ species **C4**.[88] Along with the electrophilic species **C4**, the reduced di-*tert*-butyl azidodicarboxylate by-product is formed.[88] The final step involves the attack of the nucleophile **Nu**$^-$, generated earlier, on the carbon of the electrophilic species **C4** in an S_N2 reaction generating a phosphine oxide as a leaving group and the final desired product **2**.[88]

Following the literature procedure described by Yu *et al.*,[58] we attempted to synthesize compound **2** using **9** (Scheme 23). The reaction was carried out by combining **9**, triphenyl phosphine and **10** in anhydrous THF and stirring under inert atmosphere at room temperature. To this mixture, the di-*tert*-butyl azidocarboxylate (DBAD) was added dropwise after having dissolved it in a small amount of the same anhydrous solvent. The reaction was left to stir at room temperature for 4 hours during which time the reaction was monitored by TLC.

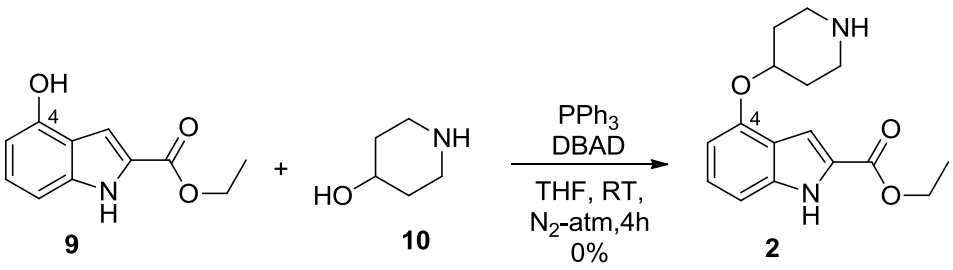

Scheme 23 – General reaction scheme illustrating the Mitsunobu reaction for the substitution of the piperidine OH-group of **10** by **9** forming **2**.

A change was observed during the reaction time and the starting material was being consumed. On completion the mixture was concentrated and gave an oily residue. This residue was purified by column chromatography as described by the literature procedure,[58] unfortunately none of the isolated compounds were the desired product (only side-products of unknown identity). The reaction was repeated a number of times; however, none of the desired product was obtained. This led us to investigate the starting material **9** and reagents being used in an attempt to ascertain if any of them where causing the failure. The investigation proved that the reagents were in good form and still active. The starting material was re-analyzed to ascertain if the compound that was being used was indeed the correct product and not, as a result of false interpretation of the characterization results, a different compound. This too was not the case as all the results from IR, MS and NMR spectroscopic analyses of the starting material returned positive for the synthesized compound **9** and confirmed that **9** was present and not degraded in any way.

The solvent (THF) was re-dried using standard laboratory techniques for drying solvents, which made no difference to the results of the reaction. Having investigated the starting material, all the reagents, solvent and thoroughly cleaning of the glassware no definite answer to the problem could be identified or given. At this point further exploration was halted as there was no clear way forward and increasing time pressure for the completion of the project.

Although the reaction was left unfinished and the problem of failure not resolved, the investigation into the failure will be continued in future work as the synthesis of compound **2** remains an important aspect and target of similar work in future study.

2.4.5 Hydrolysis of Indole to Form Hybrid Precursor

Having obtained compound **8**, it was of interest to utilize the compound in the synthesis of an indole-quinoline hybrid by coupling the indole at its 2-position to a quinoline via a short alkyl amine linker.

This would afford a hybrid compound of two different heterocyclic structures in a single compound that may have the ability to function as a dual-activity inhibitor in the *Plasmodium* parasite (Malaria).

Hydrolysis, or saponification, is a reaction where an ester is transformed into a carboxylic acid by a strong base. For the conversion of **8** to **11** (Scheme 24), a base-promoted methodology described in the literature was employed.[54,58,62] The reason for the synthesis of **11** was to function as a precursor for the synthesis of a novel indole-quinoline hybrid compound, however this will be discussed in detail in Chapter 4. Here we will focus on the synthesis of compound **11** in preparation for use in the synthesis of hybrid structures.

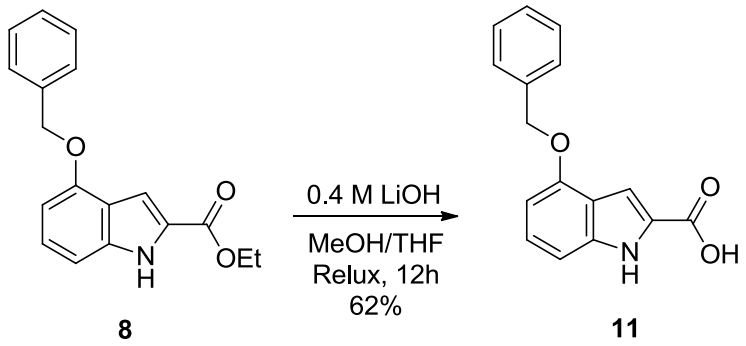

Scheme 24 – Reaction scheme for the hydrolysis of compound **8** to give **11**.[59]

Scheme 25 illustrates a simplified mechanism for the synthesis of **11** by using lithium hydroxide as base. The process is initiated by the hydroxide ion that attacks the electrophilic carbonyl carbon to form the orthoester intermediate **8c**, that undergoes resonance to release the ethoxy group forming **8d** and an ethoxide. The ethoxide is a relatively strong base and is able to deprotonate the carboxylic acid to give **8e** and ethanol. Finally, a strong acid (HCl) is used to neutralize any remaining base and protonate the acid, reforming **11** that precipitates out of the aqueous solution.

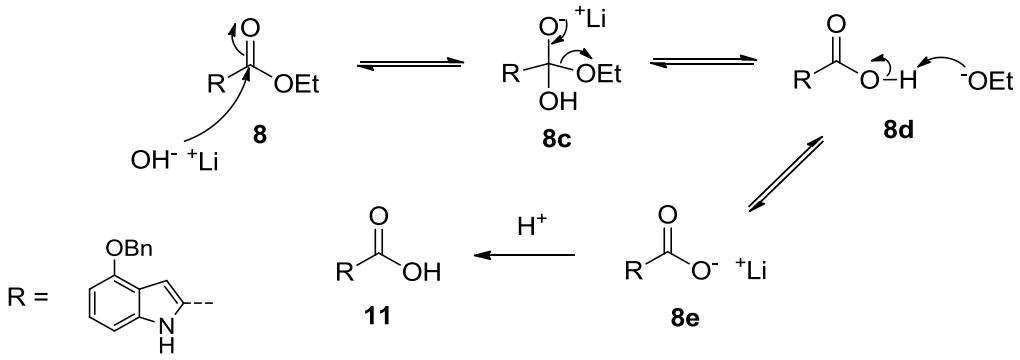

Scheme 25 – Reaction mechanism for the base promoted hydrolysis of an ester to form a carboxylic acid.[59]

Utilizing a reaction procedure described by Sheng *et al*.,[59] we proceeded to synthesize compound **11**. Compound **8** was combined with methanol and THF in a round-bottom flask and stirred until **8** was completely dissolved. In a separate glass vial, LiOH was dissolved in a minimal amount of water and drawn up into a syringe in preparation for the injection into the stirring reaction mixture. The flask was equipped with a condenser. The LiOH solution was then added dropwise to the stirring mixture and once completed the flask was sealed. The reaction mixture was then lowered into an oil bath pre-heated to 60°C and left to stir for 12 hours. On completion the reaction was cooled to room temperature and the mixture acidified with 2M HCl to a pH of approximately 2. The product precipitated out of the solution as a white precipitate and was collected by filtration followed by washing the product with water. The semi-wet product was transferred to an open vial and placed in a vacuum desiccator for 24 hours which afforded the product **11** as a pale-brown solid in 62% yield.

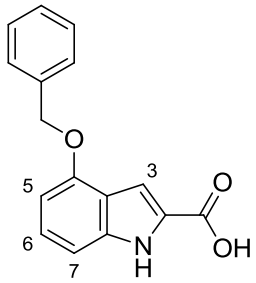

11

Analysis by ^{1}H-NMR spectrum revealed the successful formation of **11** via the hydrolysis of **8**. The spectrum revealed that all the benzylic and methylene protons were accounted for. The carboxylic proton was observed at 11.77 ppm as a broad singlet integrating for 1H. The proton at position 3 was observed as a multiplet from 7.07–7.10 ppm integrating for 1H and the proton at position 7 was observed at 7.02 ppm as a doublet integrating to 1H. The proton at position 6 was observed as a multiplet from 7.11–7.17 ppm integrating for 1H. The proton at position 5 was observed as a doublet at 6.62 ppm and integrated for 1H. The amine proton of the indole was not observed as it is characteristic of the nitrogen proton to chemically exchange with the solvent, thus causing the generally weak and broad singlet to disappear.

Mass spectroscopy results were obtained for **11** and the observed value of 268.0966 *m/z* coincided with the calculated value 268.0974 *m/z* and together with ^{1}H, ^{13}C NMR spectroscopic results confirming the formation of **11**.[131]

Having repeated the reaction a number of time we found that the procedure by Sheng *et al*.[59] utilizing organic solvents proved to be a successful method of obtaining the desired carboxylic acid compound **11**. The purification procedure was also easier and more effective in isolating **11**, due in part to the organic solvents dissolving any unreacted starting material and flushing it out during filtration.

2.5 CONCLUDING REMARKS

To conclude, we had set out to study available reaction methodologies for the synthesis of an indole scaffold, identify a suitable method to employ by which we could synthesize novel compound **2**. Compound **2** had specific substituents that had to be on the indole substructure as we intended to test

the compound for its inhibitory effect against *Pv*NMT and possibly *Pf*NMT. Having identified two method for obtaining compound **5**, the investigation of the reactions had proven that the HWE, CAN method was the more suitable and reliable method for the synthesis of our desired compounds. We tested the methods and optimized them where possible and finally gained valuable knowledge and experience in the study of reactions, procedural application in the laboratory and lastly successfully apply the knowledge and skills developed during the course of this work to successfully obtain the desired indole compounds **8** and **9,** as well as prepare an indole structure **11** in preparation for hybridization with a suitable quinoline pendant group.

CHAPTER 3: QUINOLINES

3.1 INTRODUCTION

Quinolines play an essential role in modern pharmacological research and drug developmentent.[132-134] The quinoline chromophore has shown excellent biological activity as anticancer, anti-inflammatory, analgesic, antiallergenic and antiplasmodial agents. It is therefore not surprising that the development of methodologies for their synthesis has been widely studied and reported.[134,135] Some of the more well-established reactions include the Skraup, Gould-Jacobs, Combes, Conrad-Limpach, Friedlander, Pfizinger and Doebner-Miller, which all provide quinoline and its derivatives via a variety of mechanisms.[134,136] Of all the methods available, the Gould-Jacobs (Section 3.2) and Skraup (Section 3.3) reactions were the most attractive methods of synthesis for the 4,7-disubstituted quinoline compounds that we desired. These methods are simple, relatively inexpensive in terms of starting materials and reagents readily available.[134] For this study, we focused on the synthesis of known quinoline compounds (Figure 18) that are reported to have inhibitory activity against the *Plasmodium* parasite, and the formation of synthetic hemozoin *β*-hematin.[15,38,41,44,137-139] Initially, the purpose of these compounds was to be utilized by a fellow student for further study and that we would synthesize compounds **13a–i** for them to use in their research. We decided that we could make use of the synthetic procedures of obtaining **13a–i**, to synthesize similar compounds **12a–i** and extend our study into hybrid compounds that will be discussed in more detail in Chapter 4.

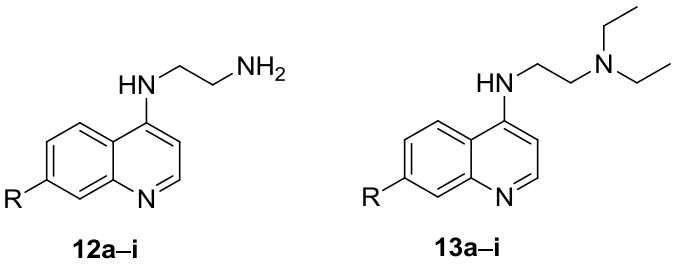

12a–i **13a–i**

R = a) F, b) Br, c) NO_2, d) CH_3, e) OCH_3, f) I, g) CF_3, h) Cl and i) H

Figure 18 – The quinoline structures known to be active *Plasmodium β*-hematin inhibitors and the intended target compounds to be synthesized in this chapter.[38,138]

Initially we employed the Gould-Jacobs reaction for the synthesis of these compounds; however, we later broadened the synthesis by investigating alternative methods in an attempt to circumvent some of the technical difficulties faced when using the Gould-Jacobs reaction. These compounds were to be used as pendant groups for an indole-quinoline hybrid that will be discussed in Chapter 4. In Chapter

3 we focus on two methodologies for the synthesis of these known quinoline compounds (**12a–i** and **13a–i**) and the results obtained during the investigation of their methods.

3.2 GOULD-JACOBS METHODOLOGY OF QUINOLINE SYNTHESIS

The Gould-Jacobs (G-J) reaction, first employed by Gould and Jacobs in 1939, is a sequence of reactions for the formation of a quinoline ring system (Scheme 26).[140,141] The first step involves the condensation of *meta*-substituted anilines **14a–e** with diethyl ethoxymethylenemalonate, via a fast Michael addition and elimination of ethanol, giving the *N*-substituted acrylates **15a–e**.[140-144] Subjecting **15a–e** to a thermal cyclization (Step 2) at high temperatures results in the quinoline intermediate **16a–e**.[140-144] Following the cyclization, hydrolysis (Step 3) converts the ester group of **16a–e** into a carboxylic acid **17a–e** and a subsequent thermal decarboxylation (Step 4) gives 4-hydroxy-7-substituted quinolines **18a–e**.[140-144] Finally, a chlorination reaction converts the 4-hydroxy moiety into a chloride via a nucleophilic substitution reaction (Step 5) that affords the desired 4-chloro-7-substituted quinoline **19a–e**.[137-139,142]

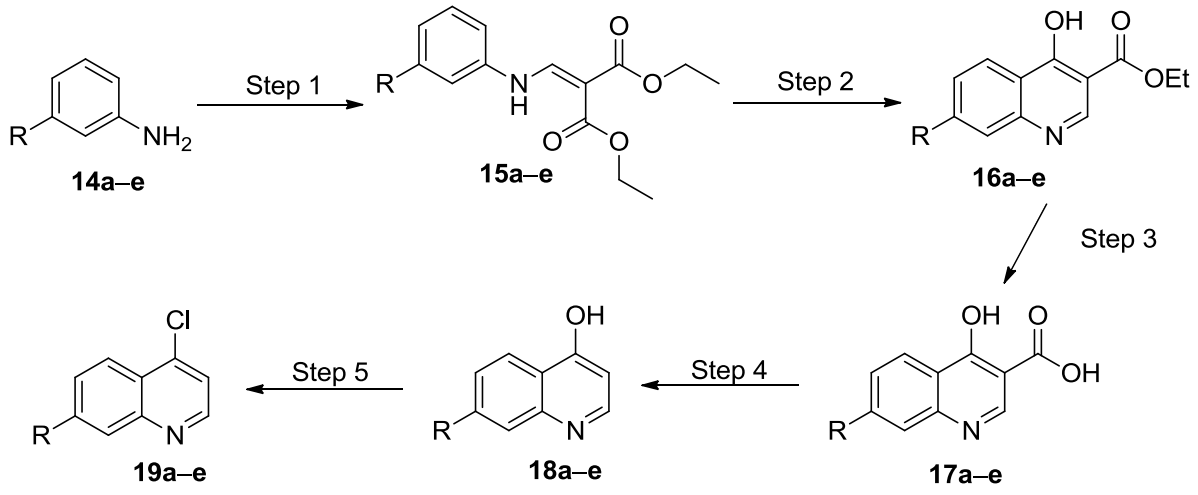

Scheme 26 – Gould-Jacobs reaction scheme for the synthesis of quinoline **19** from aniline **14**.[137-139,142]

For the synthesis of the desired quinoline of **19,** a combination of literature procedures was employed to obtain the highest yields using the simplest procedure.[137-139,142] In an attempt to simplify the synthesis, the procedure described in Scheme 26 was divided into two parts, rather than isolating and purifying the product after each step. In the first part the desired acrylate **15a-e** was synthesized Scheme 27, which could easily be isolated and purified by conventional chromatographic methods. In the second part this acrylate **15a-e** was used to form the desired quinoline product without extraction

and purification at each step (Scheme 26). Only once the final desired 4-chloro-7-substituted quinoline products (**19a–e)** were obtained from the total synthetic process illustrated in Scheme 25, could extraction and purification steps be undertaken to obtain pure products.

3.2.1 Synthesis of Acrylates 14a-e

The reaction, according to literature procedures,[140,141,145] merely requires combining the chosen *meta*-substituted aniline **14** and diethyl ethoxymethylenemalonate **20** and heating to 110 ºC for 45 minutes. However, it was found that the reaction gave lower than expected yields and we suspected the reaction was occurring too fast forming a number of side-products that were identified on TLC. I proceeded to optimize the reaction by studying the mechanism and noting that ethanol (EtOH) is formed as a result of the substitution that occurs. It was decided to make an alteration to the procedure by adding a small amount of ethanol which, 1) would assist in dissolving **14** and **20** and, 2) based on Le Chateliers principle would possibly control the rate of the reaction by shifting the equilibrium to favor the starting materials.[146,147] It was hypothesized that during heating of the reaction the additional ethanol, which was impeding the reaction, would slowly evaporate and shift the equilibrium to the products, **15** and EtOH, thus controlling the rate at which the reaction takes place. Although, the addition of ethanol may have merely overcome a solubility issue with regards to the aniline not being soluble enough in the malonate **20**. Nevertheless, this alteration showed excellent results with the reaction producing fewer to no by-products and as a result thereof higher yields for compound **15a–e**. It was noted that increasing or decreasing the reaction temperature of the altered procedure had no significant effect on the reaction with regards to the formation of more or less side-products. Scheme 27 illustrates the optimized reaction for the synthesis of the acrylates **15a–e**.

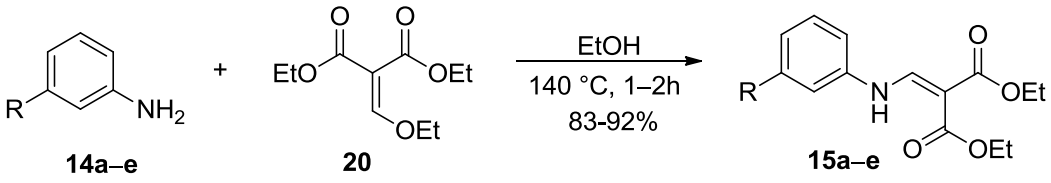

R = a) F, b) Br, c) NO_2, d) CH_3 or e) OCH_3

Scheme 27 – Optimized reaction scheme for the synthesis of acrylates **15** from substituted anilines **14**.

The optimized reaction was as follows: *m*-substituted aniline **14** and diethyl ethoxymethylenemalonate **20** were combined with a small quantity of ethanol. The reaction was stirred for 1 – 2 hours at 140 ºC in an open flask and the flask continuously flushed with nitrogen to expel the ethanol vapor that forms from the reaction vessel. After confirmation by TLC that **14** had

been consumed, the product was isolated and purified by column chromatography to afford the pure acrylate products **15a–e** as crystalline material of varying color in excellent yields (82-92%).

The substrates and results of the synthesis of acrylates from anilines **14a–e** are given in Table 1 and illustrates the excellent yields obtained for the desired acrylates **15a–e** (83-92%).

Table 1 –Yields obtained for acrylate compounds **15a–e** from *m*-substituted anilines **14a–e**.

Compound	Substituent	Isolated yield of 15a–e (%)*
14a	F	84
14b	Br	92
14c	NO_2	83
14d	CH_3	92
14e	OCH_3	91

***Reaction conditions were the same for all five of the reactions.

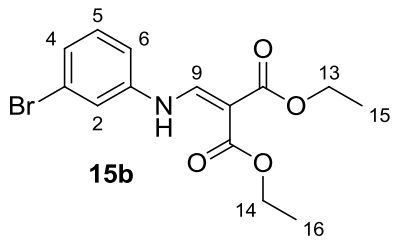

15b

The ^{1}H NMR spectroscopic analysis confirmed the successful synthesis of all the acrylates **15a–e** as all aromatic protons (position 2, 4, 5 and 6) were accounted for. Only the characterization of diethyl 2-{[(3-bromophenyl)amino]methylene}malonate is discussed here. The protons at positions 13 and 14 were observed at 4.27 ppm as a doublet of quartets, each of which integrates for 2H. The proton at positions 15 and 16 were observed at 1.34 ppm as a doublet of triplets also separately integrating for 3H. The amine proton is observed at 10.96 ppm as a broad doublet and integrates for 1H. The observed MS value of 342.0336 *m/z* correlated with the calculated value of 342.0341 *m/z*. Furthermore, infrared spectroscopy confirmed the presence of the secondary amine (3151 cm^{-1}, weak) as well as the ester functionalities (1681 cm^{-1}, strong). All the results obtained from characterization of all the acrylate compounds coincided well with the literature values.[133,139,148]

3.2.2 Synthesis of 4-chloro-7-substituted Quinolines

With the acrylates **15a–e** in hand, the second part of the Gould-Jacobs synthesis of quinolines (Scheme 28) could now be attempted. As previously mentioned, the second part of the Gould-Jacobs

reaction was carried out as a sequence of reactions using the crude product obtained from the previous step.

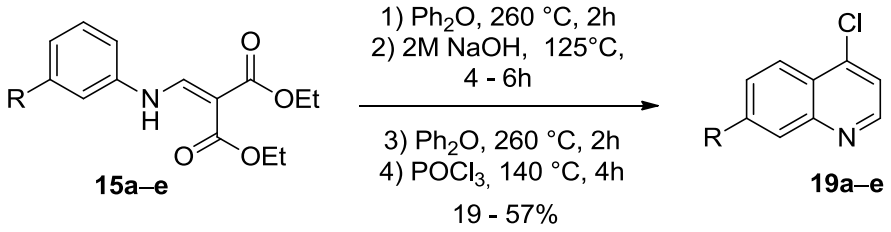

Scheme 28 – General reaction scheme for part two of the Gould-Jacobs sequence of reactions to obtain quinolines **19a–e**.

In the first reaction (Scheme 29), **15** was added to a flask containing diphenyl ether (Ph_2O), pre-heated to 70 ºC, in a single portion and stirred. The reaction mixture was then heated to 260 ºC under reflux and left to stir for a further 2 hours during which time a noticeable darkening in color of the reaction mixture was observed. This change in color indicated that the cyclization of the acrylate was proceeding well. Consumption of the acrylate was monitored by TLC and, on completion, the reaction was cooled to room temperature. The crude product **16** precipitated out of the Ph_2O as a fine powder upon cooling.

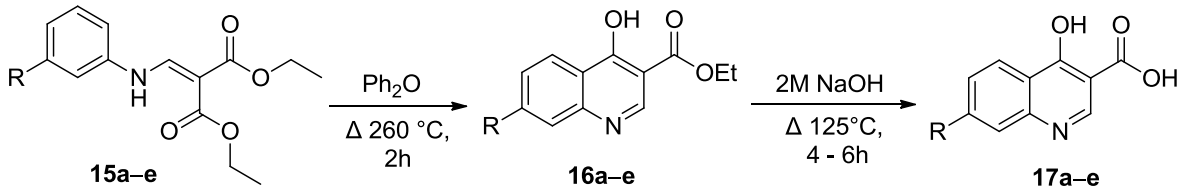

Scheme 29 –Reaction scheme illustrating thermal cyclization of an acrylate **15** followed by saponification of ester **16** to a carboxylic acid **17**.

The addition of hexane to the ether-product mixture prevented the Ph_2O from solidifying (melting point 25–27 ºC) and increased the precipitation of crude product from the solution. The precipitate was collected by vacuum filtration and repeatedly washed with hexane to remove excess Ph_2O. Once collected and dried, the crude product was added to a flask containing 2M sodium hydroxide that was pre-heated to 75 ºC. The solution was thoroughly stirred to assist in the dispersion of the organic product into the aqueous solution. The reaction was stirred under reflux at 125 ºC for 4–6 hours and the progress of the reaction monitored by TLC. On completion, the reaction mixture was cooled to

room temperature and acidified with 2M hydrochloric acid to precipitate the carboxylic acid product **17** from the solution.

It was at this stage that a problem arose with regards to the isolation of the product. Addition of the hydrochloric acid precipitated the product out of solution as expected, but the product formed a gel that was difficult and time consuming to collect. Even under vacuum filtration, the gel retained large quantities of water, but could be dried in an oven at 75 ºC until a dry solid disk was formed. The disk was removed from the paper and broken into small flakes that were able to fall freely down the inside of a condenser.

The flakes were dropped piece-by-piece down the condenser of a flask containing refluxing Ph_2O (Scheme 30). Extreme caution was taken during the addition of the flakes as an extremely violent reaction occurs when the flakes enter the Ph_2O. Once all of the flakes were added to the Ph_2O, the reaction was left to reflux for 2 hours and subsequently cooled to room temperature. Product **18** once again precipitated out of the Ph_2O as a fine powder and was isolated by the same procedure of hexane and filtration as was described above for the cyclization reaction. The isolated crude product **17** was dried in a 75 ºC oven for 30 minutes in preparation for the chlorination step that follows.

It should be mentioned that it was crucial to add the crude product in the described manner and not in a single portion to cold Ph_2O followed by heating of the reaction mixture to boiling point. The reason for this was that once the temperature reached the point at which the decarboxylation occurred, the large quantity of the reaction material rapidly decarboxylates and the reaction boils uncontrollably because of the release of carbon dioxide gas creating an extremely hazardous situation. The alteration to the procedure of adding small flakes of crude product circumvented the dangers faced by the excessive boiling and gave a measure of control over the reaction and thus making the procedure safer.

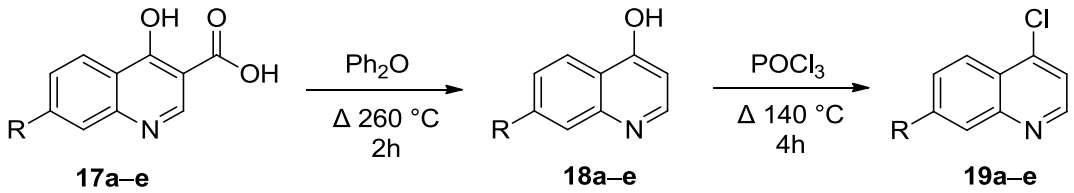

Scheme 30 – General reaction scheme illustrating the decarboxylation of **17** in reaction 3 and chlorination of **18** in reaction 4.

Following the isolation of the crude decarboxylated product, a flask was set up in a -10 ºC ice bath and the dried product **18** from the decarboxylation reaction was added. The flask was equipped with a condenser and a modification made to the setup whereby a small base trap filled with sodium

hydroxide pellets was connected to the top of the flask. To the stirring powder, phosphorous oxychloride ($POCl_3$) was added dropwise. Care was taken to not add the $POCl_3$ too quickly as an extremely violent gas-forming reaction occurs. During the addition of $POCl_3$, HCl gas was formed and moved up the condenser which was neutralized by the base trap.

Once the addition of the $POCl_3$ was complete, the ice bath was replaced with an oil bath, preheated to 140 ºC, and the reaction stirred under reflux for 4 hours. On completion, the reaction was cooled to room temperature and then to -10 ºC. Ice-cold ammonium hydroxide was carefully added to the reaction flask in small portions to neutralize any remaining $POCl_3$. Caution was taken by leaving the base trap attached to the condenser as an extremely exothermic reaction again occurred resulting in the formation of more HCl gas. Cold water was added to the aqueous mixture to dissolve any solids that formed during the neutralization process. The product was extracted using DCM and purified by silica-gel column chromatography to afford the products **19a–e** as crystalline materials in low to average yield (19 – 69%).

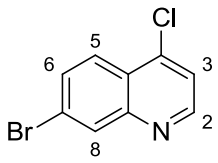

19b

^{1}H NMR spectroscopic analysis confirmed the successful formation of the products **19a–e** as all the relevant aromatic proton peaks (positions 2, 3, 5, 6 and 8) were observed for all the products, but only 7-bromo-4-chloroquinoline is discussed here. The protons at positions 2 and 3 were observed as two doublets at 8.78 and 7.50 ppm, respectively, and each integrating for 1H. Proton 8 was observed as a very narrow doublet at 8.31 ppm and integrates for 1H. The proton at position 5 was observed as a doublet at 8.10 ppm and integrating for 1H. Lastly proton 6 was observed as a doublet of doublets at 7.73 ppm and also integrated for 1H. The observed MS value of 241.9373 *m/z* correlated with the calculated value of 241.9372 *m/z*. In addition, the results from the characterizations of all the compounds coincided with the literature.[137-139,142,144] In Table 2 below is given the final percentage yield obtained for the compounds **19a–e** from the sequence of reactions starting with the acrylates **15a–e**.

Table 2 – Results of the total synthesis procedure of affording compounds **19a**–**e** in low to good yield.

Substrate	Substituent	Isolated yield of 19a–e (%)
15a	F	69
15b	Br	54
15c	NO_2	19
15d	CH_3	30
15e	OCH_3	57

3.2.3 Insights Gained from G-J Methodology and Alterations

Although reactions, in some cases only consist of a substrate and a reagent (Scheme 26), it was important as a chemist to mechanistically understand how reactions take place. During the synthesis of acrylates **15a–e**, studying the reaction mechanism provided a solution to decrease the formation of by-products and improve the yield of the products. By introducing a solvent (ethanol) an aspect of control over the rate of the reaction was possibly taking place and managed to improve the yields.

It was also important to utilize technical skill to understand the procedures by which the reactions had to be performed. By understanding the procedure the appropriate decisions and strategies could be made on how the procedure could be carried out and make the reaction work more effectively, but more importantly, safer for oneself and those working around you. In the cases of synthesizing the compounds of **16**, **18** and **19,** the hazardous situations created by gas formation and conducting reactions at extremely high temperatures all posed some form of risk. By adapting the procedures and reaction setups, the risks were minimized to a large extent making the reactions safer and also giving improved yields such as in the case of the decarboxylation of compounds **17a–e**.

3.3 Alternative Method: Skraup and Doebner-Miller Methodology

Having faced many hazardous situations, technical difficulties and significant losses of intermediate products in the G-J sequence of reactions to obtain the final quinolines **19a–e**, we decided to take on a side-line investigation into alternative methodologies for the synthesis of our desired quinoline structures **19a–e**. The goal was to synthesize the same 4,7-disubstituted quinolines as that obtained from the G-J methodology, but with fewer hazardous conditions, and lower cost, while making use of the same *m*-substituted anilines **14** already in hand.

During further investigation of the literature, two possible methods were identified that satisfied the criteria for an alternative method to synthesize the quinoline structures **19**, namely the Skraup reaction (Scheme 31 – Route A) and a Doebner-Miller (D-M) modification (Scheme 31 – Route B) of the Skraup.[135,136,149-154] Although the same aniline starting material **14** from the G-J is employed by the Skraup and D-M methods, the quinoline structures that are afforded lack the hydroxy or chloro group at the 4-position of the quinoline ring necessary for further derivatisation. The reason for the substitution only being in the 5- or 7-position of the quinoline ring is as a result of the substituted aniline **14** and glycerol (or acrolein) that is used in the reaction.[135,149] However, there are two single step reactions (*N*-oxide formation and chlorination) that can be employed to obtain the final desired 4-chloro-substituted quinolines **19** from the Skraup and D-M products.[155,156]

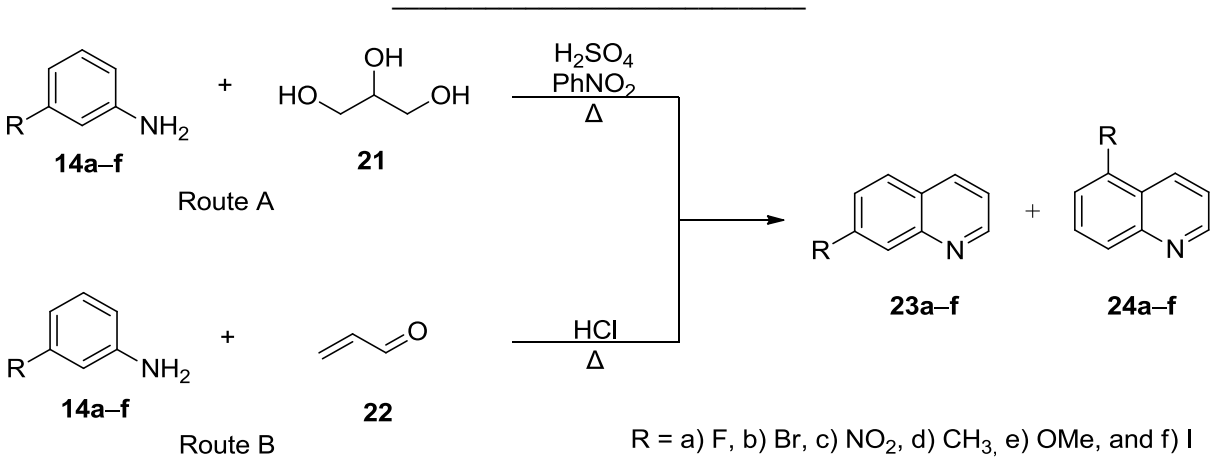

Scheme 31 – General representation of the synthesis of 7-substituted **23** and 5-substituted **24** quinolines via the Skraup reaction (Route A) and Doebner-Miller modification (Route B).[149]

The Skraup (in 1880) and the Doebner-Miller (in 1881) reactions share similarities in their use of anilines as starting material,[149] although the Doebner-Miller reaction utilizes acrolein as a reagent instead of the *in situ* formation thereof by dehydration of glycerol.[149] The Skraup method makes use of glycerol **21**, a by-product of the biodiesel industry, which is inexpensive and readily available.[136,149,157] A strong acid, such as sulfuric acid, facilitates the dehydration of **21** for the *in situ* formation of acrolein **22**.[135,136,149] The acrolein formed from the dehydration is the source of a three carbon chain necessary to form the quinoline ring system **23** and **24**.[135,136,149] Scheme 32 demonstrates the double dehydration of **21** via the elimination of two water molecules that affords acrolein in its protonated form **25**.[135,136,149,157]

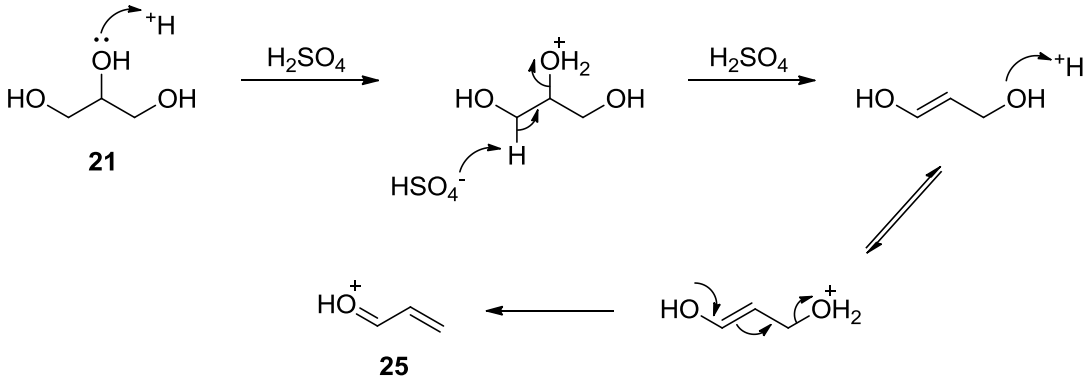

Scheme 32 – Reaction mechanism illustrating the acid-catalyzed dehydration of glycerol forming acrolein **25** in its hydrated form.[135,136,149,158-160]

The protonated acrolein species **25** promotes the nucleophilic attack of the aniline amine **14a–f** and ultimately leads to the formation of the quinoline products **23a–f** and **24a–f**.[135,136,149] An unfortunate side effect of the highly acidic conditions is the formation of side-products from self-condensation

and polymerization of acrolein at elevated temperatures.[157,161-163] Scheme 33 demonstrates the mechanism of the Skraup reaction whereby the substituted aniline **14a–f** attacks the activated acrolein species **25** in a 1,4-addition, forming the Schiff-base intermediate **26a–f**.[135,136,149] Following a protonation and subsequent deprotonation of **26a–f**, an intramolecular ring closure of **27a–f** occurs at the *ortho*-position of the anilines forming **28a–f**.[135,136] A 1,5-proton transfer occurs in **28a–f** followed by a dehydration of **29a–f** that affords 1,2-dihydroquinoline **30a–f**.[135,136,149] Finally **30a–f** undergoes an oxidation reaction to complete the formation of the 7-substituted quinoline **23a–f**.[135,136,149]

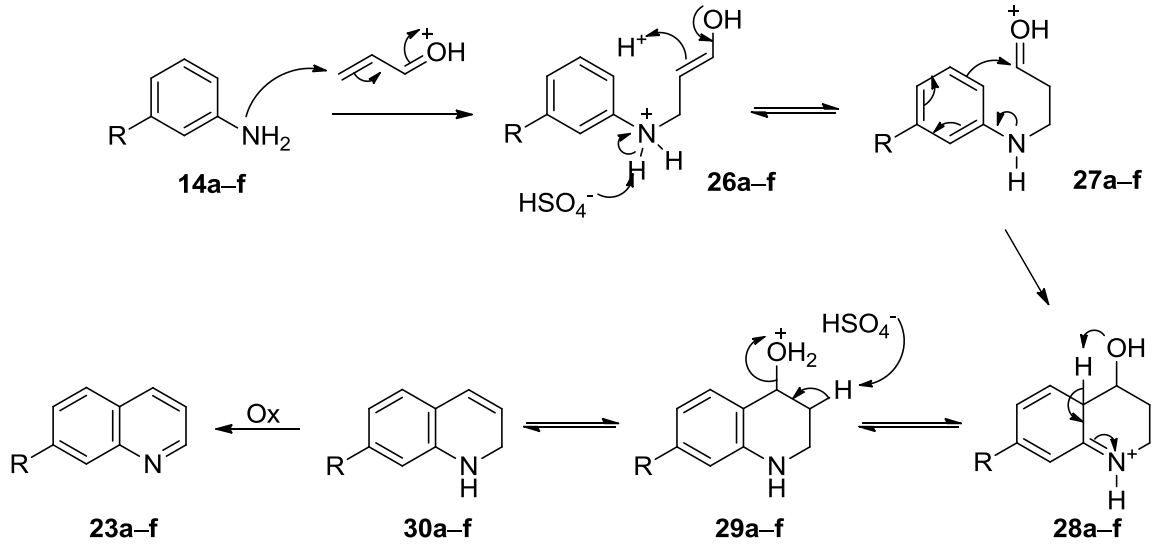

R = a) F, b) Br, c) NO_2, d) CH_3, e) OMe, and f) I

Scheme 33 – Reaction mechanism for the synthesis of 7-substituted quinoline **23a–f** from **14a–f**.[135,136,149]

Although the original Skraup reaction described above comes across as a simplistic method of obtaining quinolines, the reaction does suffer from several drawbacks.[136] The reaction is well-known to be a "dirty" method that gives numerous unknown by-products, regio-isomers and makes for tedious extraction and purification procedures.[134,136,150,164] Nevertheless, the drawbacks did not discourage us from continuing to investigate the method and its modifications as an alternative for the synthesis of the desired quinoline structure **23**. Herein we will discuss the Skraup reaction, our attempts at synthesizing 7-substituted quinolines and some of the drawbacks faced during the investigation.

3.3.1 Synthesis of Quinoline-ring System by Skraup and Doebner-Miller Reactions

Skraup Reaction

As mentioned above, the original Skraup method has some drawbacks that affect the yield of the desired quinoline product **23**. Studying the literature presented alternatives, more accurately, modifications that are reported to decrease the effects that the drawbacks have and improve the yield.[135,136,149,151-154,165] A set of reaction modifications were chosen and attempted to improve the reaction and increase the yields we obtained from the original Skraup method. Table 3 presents a summary of the modifications that were attempted. For the purpose of consistency *m*-anisidine **14e** was chosen as the model starting material for all initial attempts because the methoxy-group is known to be an effective electron-donating group that activates the ortho-positions of the aniline.[135,149] This activation would give the reaction the best chance of undergoing an intramolecular ring closure from the aniline to the electrophilic carbonyl to form the ring system (see Scheme 33: **27**–**28**). In each case, 1.0 g of **14** was used along with 2 equivalents of glycerol and the reaction repeated three times. Yields are given as an average of the three attempts.

Table 3 – Reaction conditions and results obtained for the modifications to the Skraup reaction that were test and compared to the original procedure (Entry 1)

Entry	Conditions	Isolated yield of 23e (%)
	Compound **14e** + Glycerol **21** ⟶ Product **23**	
1[152]	**21**, conc. H_2SO_4, $PhNO_2$, conc. AcOH	26[a]
2[166]	**21**, conc. AcOH, $ZnCl_2$, $FeCl_3$	0
3[167]	**21**, conc. H_2SO_4, I_2	0
4[134,150]	**21**, 6M HCl, $ZnCl_2 \cdot 2H_2O$	0
5[135]	**21**, conc. H_2SO_4, $PhNO_2$, H_2O, $NaNO_3$	0
6[153]	**21**, conc. H_2SO_4, $NaNO_2$, conc. HCl	0
7[155]	**21**, conc. H_2SO_4, $PhNO_2$, $FeSO_4 \cdot 7H_2O$	63[b]

[a] Yield obtained for synthesis of quinoline structure **23e** from original Skraup reaction.

[b] Improved yield of **23e** using $FeSO_4$ modification to original Skraup reaction.

Unfortunately, all but one modification failed to either work or improve the yield from the original method. We chose to continue the efforts using the iron(II) sulfate modification[155] (Entry 7) as it had shown to give improved yield compared to the original Skraup reaction (Entry 1) and the extraction process being slightly less complicated. Scheme 34 illustrates the general reaction scheme for the

iron(II) sulfate ($FeSO_4$) modification that we employed to synthesize the desired quinoline **23**. The addition of the $FeSO_4$ is reported to reduce the exothermic nature of the reaction and thus give some degree of control over the tendency of the reaction to become violent.[149,168] Utilizing procedures described by Castellano *et al.*[165] and Rodriguez *et al.*,[155] for the modification of the Skraup reaction by addition of iron(II) sulfate heptahydrate ($FeSO_4 \cdot 7H_2O$), we were able to synthesize some of the intended quinolines.[155,165]

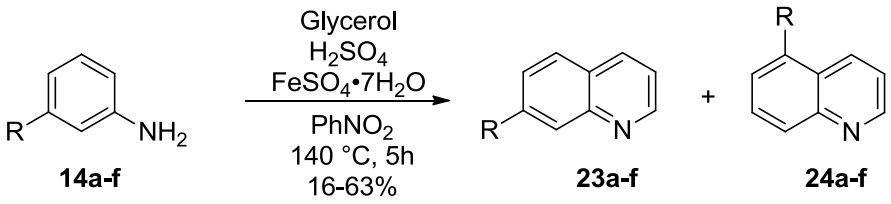

Scheme 34 – Modified Skraup reaction with the addition of $FeSO_4$ to synthesize compound **23**.[155,165]

Glycerol was first added to a flask that was heated in an oven to 75 ºC. The flask was fitted with a condenser and concentrated sulfuric acid added to the glycerol in a single portion. The aniline was then injected into to the stirring reaction mixture, followed by the addition of iron(II) sulfate. Once the iron(II) sulfate was completely dissolved, nitrobenzene was injected dropwise into the mixture resulting in a violent exothermic reaction that turns the reaction mixture completely black. The black color is suspected to be as a result of the sulfuric acid decomposing during the rapid increase in temperature from the rapid exothermic dehydration reactions taking place. Although decomposition of the acid was occurring, the acid was added in concentrated form and in a significant excess and thus the decomposition thereof was negligible when compared to the amount of acid present. Following the addition of the nitrobenzene the reaction flask was then lowered into a pre-heated oil bath (140 ºC) and left to stir for 1-4 hours.

The reaction was monitored by TLC and upon completion, the reaction was cooled to room temperature and the contents transferred to a beaker with a minimal amount of water. The aqueous mixture was then carefully basified with 5M NaOH until the solution was a milky brown color with a pH of approximately 9. The mixture was again cooled to room temperature as it heated up during the neutralization of the acid by the NaOH. The aqueous mixture was then transferred to a separating funnel and extracted with DCM, taking care not to shake too vigorously otherwise the mixture coalesced and emulsified and was extremely difficult to separate. Purification of the crude product by silica column chromatography afforded the products as oils of varying colors in low to moderate yield (16-63%).

^{1}H NMR spectroscopy confirmed the successful formation of products, however after repeated attempts at synthesizing quinolines from a variety of *m*-substituted anilines (H, F, Cl, Br, I, NO_2, CH_3 and OCH_3) we were only able to isolate products for the bromo, methyl and methoxy anilines (Table 4). The 3-anilines of fluoro, chloro, iodo, nitro, and plain aniline could not be successfully isolated or products did not form even after extended reaction times and increased reaction temperatures. In each case for the reactions that worked, the isolated products were the 7-substituted quinolines **23d** and **23e** as the major products with the 5-substituted quinolines **24d** and **24e** obtained in trace amounts. In the case of **14b**, a mixture of 5- and 7-substituted quinolines **23b** and **24b** were obtained with a slight preference for **23b**. It has been reported that a relationship can be seen between the electronegativity of the substituent in the 3-position of the aniline and the probability of the formation of the quinoline products **23** and **24**. Yamashkin *et al.*[149] and Bradford *et al.*[169] reported that the moderate to strong electron-donating groups i.e. methyl and methoxy, respectively, promote ring closure at the 6-position of the aniline giving 7-substituted products such as **23d** and **23e**.[149,169] For the weaker electron-withdrawing groups such as bromide, a mixture of both 5- and 7-substituted products are observed with the latter predominates. [149,169] Another factor contributing to the selectivity of product formation is the steric effects of the 3-position substituents.[149] Larger substituents increase the probability of the 7-substituted quinoline forming through sterically hindering the ring closure at the 2-position of the aniline.[149] Table 4 summarizes the results obtained for the three products (**23b,d** and **e**) with regards to the electronic effect of the substituents, either electron-donating group (EWG) or an electron-withdrawing group (EDG), and the yield obtained for the desired products of **23**.

Table 4 – Yields obtained for the three isolated quinoline compounds from the Skraup reaction Scheme 34.

Substrate	Substituent	Substituent effect	Isolated yield of 23 (%)
14b	Br	Weak EWG	16
14d	CH_3	Moderate to weak EDG	63
14e	OCH_3	Strong EDG	26

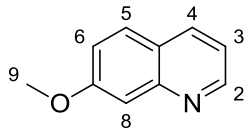

23e

The ^{1}H NMR spectroscopic results confirmed that the intended 7-methoxyquinoline had indeed been isolated. The methyl protons (9) were observed as a singlet at 3.94 ppm and integrated for 3H. The protons at positions 5 and 6 were observed at 7.68 and 7.19 ppm as a doublet and a doublet of doublets respectively, both of which integrate for 1H. The proton at position 8 was observed as a narrow doublet at 7.42 ppm and integrates for 1H. Proton at position 3 was observed as

a multiplet from 7.23–7.27 ppm integrating for 1H and finally the protons at positions 4 and 2 were observed as a doublet of doublets at 8.05 ppm and a doublet of doublets at 8.82 ppm and integrating for 1H each. Mass spectrometry coincided well with the calculated and literature values where an observed value of 160.0756 *m/z* and coincided well with a calculated value of 160.0762 *m/z*.[135,169]

Earlier it was mentioned that the reaction suffered from several disadvantages. This became apparent after multiple attempts of synthesizing quinoline from the various *m*-substituted anilines. The first was the undesired formation of the 5-substituted quinoline isomer **24d** from the aniline **14b**.[135] The dehydration of glycerol also presented another hindrance due to the uncertainty in the formation of acrolein versus other products that were able to be formed such as formaldehyde and acetaldehyde.[158,159]The acrolein **22** was susceptible to self-condensation and polymerization at elevated temperatures which led to multiple short-chain polymer by-products that further decreased the formation of the desired compound **23**.[161-163,170] The exothermic runaway that occurred during the addition of the reagents led to decomposition of the reagents, increased acrolein self-condensations and thus formation of complex reaction mixtures. All of these drawbacks combined to give difficult and tedious isolation and purification processes with dramatic losses in yield.[135,136,149] For these reasons we moved on to a different approach for the synthesis of our quinoline compounds.

Doebner-Miller Reaction

The second alternative we had identified was the Doebner-Miller reaction (Scheme 30 – Route B), which is a modification of the Skraup method but mechanistically works in a similar fashion. The D-M method makes use of milder acidic conditions than that of the Skraup method.[149,164] It utilizes acrolein in a bi-phasic system to circumvent some of the side-product formation that occurs due to the highly exothermic nature of the Skraup reaction during the dehydration of **21**.[134,164] The reaction is also 'cleaner' with regards to the extraction process whereby the solutions are not black and tedious to separate because of excess side-products and decomposition of reagents.[134,164]

A procedure described by Matsugi *et al*.[164] was employed for the synthesis of 7-methoxyquinoline (**23b**) to test the viability of the reaction as an alternative to the two previously used methods. Scheme 35 illustrates the general scheme of the reaction that was utilized.

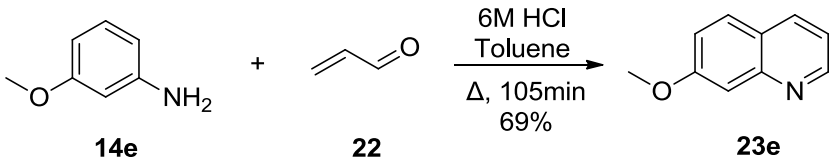

14e **22** **23e**

Scheme 35 – Doebner-Miller reaction for the synthesis of 7-methoxyquinoline **23e** in a biphasic system.[164]

Initially, 6M HCl was warmed to 70 ºC under reflux, followed by the addition of *m*-anisidine **14e**. The reaction was monitored by TLC until all of **14e** was consumed and gas formation in the reaction flask had ceased. A portion of toluene was then added to the stirring mixture and the rate of stirring increased before **22** was added. The reason for the stirring rate increase was to ensure that when the acrolein was injected into the warm mixture that the acrolein was rapidly incorporated, thus reducing the possibility of self-condensation occurring.[164] The acrolein was injected dropwise in a single portion, followed by an increase in the temperature of the reaction to 85 ºC for 15 minutes, and then to 105 ºC for 45 minutes. The temperature was then lowered to 90 ºC and left to reflux for a further 45 minutes. On completion, the reaction was cooled to room temperature and carefully neutralized to a pH of approximately 8 using saturated sodium carbonate solution. Once neutralized, the product was extracted using ethyl acetate and purified by column chromatography to afford the product as a brown oil in a good yield (69%).

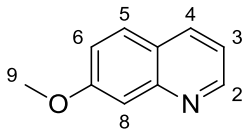

23e

The ^{1}H NMR spectroscopic results confirmed that the intended 7-methoxyquinoline had indeed been formed and was isolated as the product (69%), with 5-methoxyquinoline only being isolated in an insignificant amount. Comparing the results for **23e** from the Doebner-Miller reaction to that of **23e** obtained using the Skraup reaction, it was clear that both reactions afford the same product; however, the Doebner-Miller gave a higher yield from the outset for the desired 7-methoxyquinoline product. The observed MS value of 160.0757 *m/z* coincided with the calculated value of 160.0762. All the results, MS, IR and NMR spectroscopy, obtained from characterization coincided well with the literature.[155,169]

At present, we were only able to test the reaction twice, both using *m*-anisidine **14e**, and it was not clear at this point whether the Doebner-Miller method is a better alternative to both the G-J and Skraup methods. However, the preliminary results from this work do show some promise as the extraction and purification procedures are far simpler. Fewer side-products were formed owing to the milder conditions, which resulted in significantly improved yields (69%) in comparison to the Skraup method (26%) for compound **23b**. It would be interesting and advantageous to continue this investigation to ascertain whether or not the reaction shows similar and/or better results for other aniline substrates. If so, this method would be the obvious choice for the synthesis of similar quinoline derivatives in future endeavors.

Since the 7-substituted quinolines had been synthesized, the next step was to make use of *N*-oxide derivatives to facilitate the substitution of the chloro groups in the 4-position by activating the 2- and 4-positions on the quinoline ring.

3.3.2 N-oxide Facilitated Chlorination of Synthesized Quinolines

Quinoline N-oxides

N-oxides of heterocyclic compounds have found extensive use in pharmacological drugs as active ingredients for anticancer, analgesic and muscle relaxants.[171,172] As the name suggests, these compounds all share a common N–O bond, more accurately, a datively-bonded oxygen to a nitrogen. This type of functionality has been thoroughly studied in recent years for their properties and functional uses as intermediates to facilitate substitution reactions on difficultly substituted *N*-heterocyclic systems.[79,171-173] It is well known that hetero-aromatic systems, such as pyridine and quinoline, have difficulty undergoing regioselective substitutions on the ring and employing harsher conditions are more likely to reduce the regioselectivity for desired products.[171,174] Generally, the *meta*-position of the pyridine ring is the preferred site for substitution.[79,171] However, the formation of *N*-oxides inverts this, making the *ortho*- and *para*-positions more susceptible to substitution, with the *para*-position being favored over the *ortho*.[79,171,174] Fusing a benzene ring to a pyridine has little effect on the characteristics of the parent pyridine ring and the deactivation characteristics are retained.[79] Making a quinoline *N*-oxide has a similar effect on it as that of a pyridine *N*-oxide.[79] The parent pyridine ring of the quinoline *N*-oxide is made more susceptible to nucleophilic substitution at the 2- and 4-positions over the favored benzene ring of normal quinolines.[79,173-175]

Work done by Yokoyama *et al*.,[176] and Heitman *et al*.[156] demonstrates the selectivity of quinoline *N*-oxides for the 4-position during the nucleophilic substitution of a nitrate group, resulting in the formation of the 4-nitroquinoline as the product.[156,176] Rodriquez *et al*.[155] demonstrated similar results by carrying out a chlorination reaction that shows that 2- and 4-position chlorinated products are formed. However, their results also indicate that, depending on substituents on the quinoline prior to chlorination of the *N*-oxide, either the 2- or 4-position chlorinated product would form and in some case a mixture of both.[155] Because of these results obtained by Rodriguez *et al*.[155] we decided to investigate the possibility of forming quinoline N-oxides **31** to function as intermediates and facilitate the synthesis of 4-chloroquinolines **19** from the Skraup and D-M products (Scheme 36).

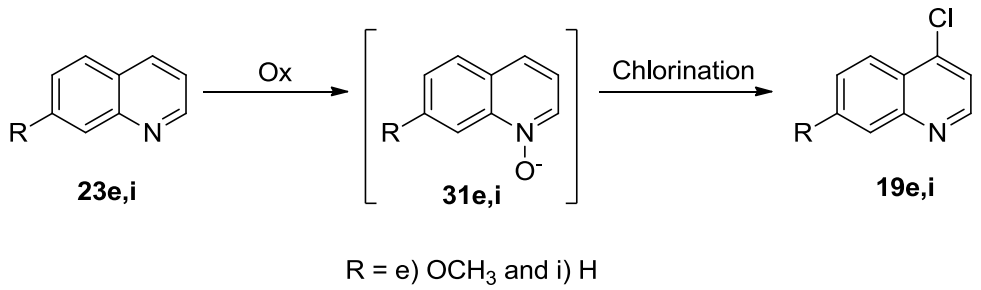

Scheme 36 – Representative reaction scheme for the possible synthesis of 4-chloroquinoline **19** using quinoline *N*-oxides **31** as intermediates.

Employing a literature procedure described by Vörös *et al.*,[171] quinolines can readily be oxidized to their *N*-oxide counterpart under mild conditions using hydrogen peroxide and acetic acid (Scheme 37).[171] Initially, the desired quinoline was added to stirring glacial acetic acid and was then heated to 70 ºC after which 30% hydrogen peroxide was added dropwise and the reaction left to stir for 24 hours.[171]

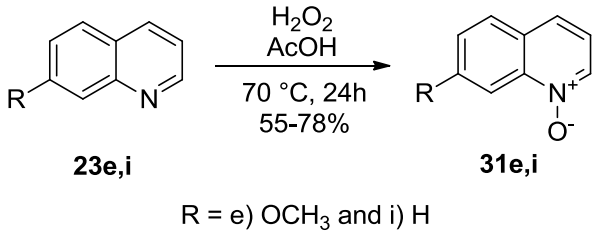

Scheme 37 – General reaction scheme employed for the preparation of quinoline *N*-oxides.

On completion, the mixture was cooled to room temperature and quenched using a 10% sodium metasulfite solution. The product was then extracted with DCM and purified by column chromatography to afford an oil that crystallized under vacuum to give a sticky semi-crystalline material in good yield of 79–87%.

Table 5 gives a summary of the quinoline *N*-oxides that were successfully synthesized and the yield obtained for each of the compounds **31e** and **31i**.

Table 5 – Summary of the results obtained for three of the *N*-oxides that were successfully isolated.

Substrate	Substituent	Isolated yield of 31 (%)
23e	OCH_3	87
23i	H	79

Confirmation of the formation of the *N*-oxides was accomplished by ^{1}H NMR and MS spectroscopy and comparing the characterization data of the starting quinolines to that of the products. In NMR spectroscopy, a characteristic shift, +1 ppm for ^{1}H and +9 to +12 ppm for ^{13}C, of the 2-position proton and carbon atoms should be observed.[173] Below given in brackets, is the ^{1}H NMR chemical shift values for the characteristic protons of the starting quinoline **23i,** to illustrate the dramatic chemical shift that occurs for the protons in the newly formed quinoline *N*-oxide **31i**.

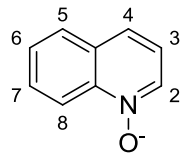

31i

The NMR spectroscopic results of quinoline *N*-oxide confirmed the formation of the product where the 2-position proton was observed at 7.70 ppm (8.88) as a doublet overlapping a triplet and integrated for 1H. The proton at position 8 was observed at 8.69 ppm (8.09) as a doublet integrating for 1H. The proton at position 3 was observed as a multiplet from 7.21–7.28 ppm integrating for 1H. The proton of position 4 was observed as a multiplet from 7.56–7.63 ppm integrating for 1H. The protons at positions 6 and 7 were observed as a multiplet from 7.67–7.75 ppm and integrated for 2H.

With regards to the use of MS, using electrospray-ionization, no loss of the datively bonded oxygen is observed and makes it possible to distinguish between the oxide and the parent amine. The experimental MS result (146.0600 *m/z*) obtained from analysis also correlated with the calculated value (146.0608 *m/z*) and all characterization results coinciding with the literature.[156,172,173]

Chlorination

Having synthesized quinoline *N*-oxides **31e** and **31i**, the final step of chlorinating the oxides was carried out by following the same procedure of chlorination described in section 3.2.2 without alteration. The oxide was subjected to the same reagents and conditions as the 4-hydroxy-7-substituted quinolines **7** of the G-J method (section 3.2.2) and afforded the same 4-position chlorinated product **19i** from **31i**. This was confirmed in the same manner by isolating the products using column chromatography and characterizing them by NMR and MS spectroscopy. This method demonstrates that the *N*-oxide of **23i** can selectively be chlorinated at the 4-position of **31i** affording **19i**. Indicated in brackets next to the chemical shift values of 4-chloro-7-methoxyquinoline are the values for the chemical shifts from the G-J product. The corresponding ^{1}H NMR chemical shift values for the same compound obtained from the G-J method is given in brackets next to each value below to illustrate the correlation between the compounds and confirming that the two compounds are indeed the same and the chlorination was successful.

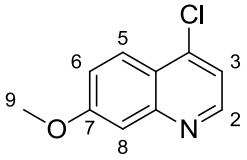

19e

The proton of position 2 was observed as a doublet at 8.68 ppm (8.68) and integrated for 1H, proton 8 was observed at 7.41 ppm (7.42) as a narrow doublet and also integrated for 1H. The proton of 5 and 6 were observed at 7.27 and 8.09 ppm (7.28 and 8.10) as a doublet and a doublet of doublets respectively with each integrating for 1H. The proton of position 3 was observed at 7.33 ppm (7.33) as a doublet and integrates for 1H. Lastly the methoxy protons at position 9 were observed at 3.95 ppm (3.96) as a singlet which integrated for 3H. Both the results obtained coincided well with one another and also to the literature, confirming the formation and success of the process of synthesizing compounds **19** utilizing the alternative method.

3.3.3 Insights from the Study of Alternative Methodologies

With the products coinciding with the results of the Gould-Jacobs procedure, this alternative method has demonstrated that it is a plausible method to obtain the desired quinoline compounds from the same starting material (*m*-substituted anilines). However, the process of obtaining the quinolines **23** via the Skraup reaction are labor intensive and have dirty extraction processes, only to isolate minimal amounts of product. Large quantities of solvent and product go to waste as a result of the generally unsuccessful extractions. The reproducibility of the Skraup method is also not consistent and reliable because of what we believe is as a result of substituent effects on the aniline ring, by-product formation from the dehydration of glycerol, polymerization of the *in situ* acrolein at elevated temperatures and harsh reaction condition leading to decomposition. However, insight was gained with regards to the effects that substituents have on aromatic ring systems, be it a matter of size, electron back-donation or withdrawal from the ring that affect the formation of products and isomers of desired product.

3.4 QUINOLINE DERIVATIVES

Having successfully synthesized a small library of quinoline compounds via both the G-J and Skraup-Doebner-Miller methods, the final step of derivatisation could be carried out to obtain the final compounds (**12g–i** and **13g–i**). These compounds would then be further utilized in the attempt to form hybrid anti-plasmodial agents (Chapter 4). The synthesis of these compounds was accomplished by following well-documented literature procedures that offer an easy and effective method of obtaining amine-derivatives of quinolines **19g–i**.[38,44,137-139,142] Because compounds **19a–e** were obtained during the last stages of this project, we were unable to derivatise them and as a result, only compounds **19g–i** were synthesized (Figure 19).

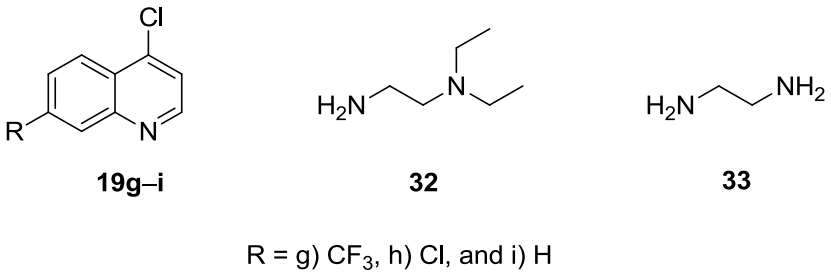

19g–i **32** **33**

R = g) CF_3, h) Cl, and i) H

Figure 19 – Illustration of the quinolines **19** and the two diamino alkyl compounds **32** and **33** that were available.

3.4.1 4-Position Derivatisation of Synthesized Quinolines

Following the literature procedures by Egan *et al.*,[38] and Nsumiwa *et al.*,[138] two small libraries of quinoline derivatives were synthesized using two different diamino alkyl chains (**32** and **33**).[38,138] The libraries consist of compounds containing 7-trifluoromethyl-quinoline, 7-chloro-quinoline and quinoline as the substructures and a 4-position side-chain of either **32** or **33**. The first set of compounds (**12a–i**) were synthesized based on previously reported structures by reacting **19** with **32** to give the respective compounds of **12**. These compounds were synthesized to test the literature procedures and optimize the reactions for each of the substrates **19g–i** and diamino alkyl reagent **33** (Scheme 38). The second diamino alkyl chain **33** was the most important as it consists of a short ethylene chain and two amino groups that would facilitate coupling to the indole scaffold (**11**) synthesized in Chapter 2.

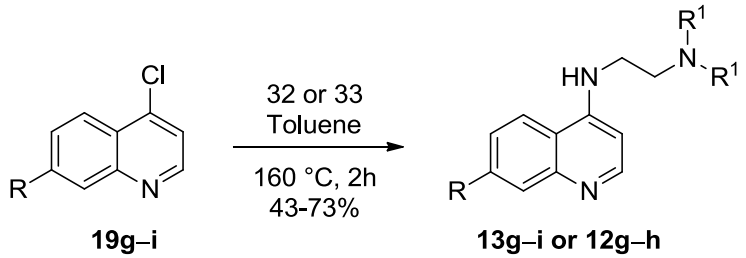

19g–i **13g–i or 12g–h**

R = g) CF_3, h) Cl, and i) H
R^1 = H or Ethyl

Scheme 38 – Optimized reaction scheme employed for the synthesis of derivatised compounds **12** and **13**

Utilizing a procedure described by Nsumiwa *et al.*,[138] quinoline **19** was dissolved in a small quantity of toluene and an excess of the chosen diamino alkyl **32** or **33** added in a single portion. The reaction mixture was then heated under reflux for 2 hours or until all of the quinoline was consumed as monitored by TLC. On completion, the mixture was cooled to room temperature and transferred to a

beaker with a minimal amount of water. The aqueous mixture was basified to a pH of approximately 9 using a 1M NaOH solution and the product was extracted with DCM to afford the crude product as a dark brown oil.

In both cases using **32** and **33** with the quinoline analogues **19g–i**, the products were purified by heating the crude oils in hexane, cooling to room temperature and siphoning off the hexane from the product using a pipette. By repeating the process until all traces of the diamine reagent **32** or **33** was removed, the purified compounds were obtained in good yield (43-73%). Compounds **12g–h** and **12g–h** were obtained as yellow powders and compound **13i** as a brown oil. ^{1}H NMR spectroscopy confirmed the formation of the products and examples of the results for two products are given below for the 7-trifluoromethyl-4-amino substituted-quinolines.

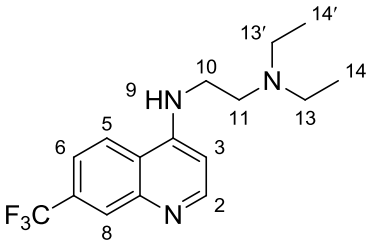

13g–i

The ^{1}H NMR spectroscopic results confirmed the formation of N^{1},N^{1}-diethyl-N^{2}-[7-(trifluoromethyl)quinolin-4-yl]ethane-1,2-diamine. The chemical shift values for the protons are observed as follows. The protons at positions 2 and 3 were observed as two doublets at 8.61 and 6.45 ppm respectively, and each integrating for 1H. The proton at position 8 was observed at 8.26 ppm as a singlet and integrated for 1H. The protons of positions 5 and 6 were observed as a doublet and a doublet of doublets at 7.85 and 7.60 ppm respectively, and both integrated for 1H. The amine proton of position 9 was observed at 6.22 ppm as a broad singlet also integrating for 1H. The protons of positions 14 and 14′ were observed as a triplet at 1.09 ppm integrating for 6H. The protons of positions 13 and 13′ were observed as a quartet at 2.62 and integrating for 4H. The protons of positions 10 and 11 were observed at 3.28 and 2.84 ppm respectively, with each integrating for 2H. The MS spectroscopic analysis reported a value of 312.1681 *m/z* that correlated with the calculated value 312.1688 *m/z*. All the results obtained from MS, IR and NMR spectroscopy coincided well with the literature confirming the successful formation of the compounds.[44,137]

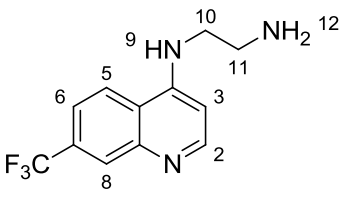

12g–h

The ^{1}H NMR spectroscopic analysis of the N^{1}-[7-(trifluoromethyl)quinolin-4-yl]ethane-1,2-diamine is similar to that of the above compound with regards to the aromatic protons of the quinoline (2, 3, 5, 6 and 8) all being observed at the same chemical shift values. The characteristic differences are observed for the two amines at positions 9 and 12 that were observed at 5.92 and 1.30 ppm as two broad singlets and integrating for 1H and 2H respectively. The protons at position 10 and 11 were observed as a quartet and a triplet at 3.33 and 3.13 ppm respectively, and each integrating for 2H. The MS spectroscopic analysis reported a value of 256.1068 *m/z* that

correlated with the calculated value 256.1062 *m/z*. All the results obtained from MS, IR and NMR spectroscopy coincided well with the literature confirming the successful formation of the compounds.[138]

Table 6 given below summarizes the isolated yields of the compounds **12** and **13** that were synthesized using the quinolines **19g–i** that were available.

Table 6 – Results for the synthesis of the six quinoline derivatives **13g–i** and **12g–h**

Substrate	Substituent	Isolated yields (%)	
		13	**12**
19g	7-CF_3	79	73
19h	7-Cl	88	43
19i	7-H	73	

3.5 CONCLUSIONS

In conclusion, we identified three methodologies, the Gould-Jacobs, Skraup and Doebner-Miller for the synthesis of the desired quinoline compounds **19**. Having utilized all the methods and investigated whether one of them would be the more effective and efficient method of quinoline synthesis, we came to the conclusion that the Gould-Jacobs methodology is the most suitable. Having investigated the Skraup method in detail, the low yields and difficulties faced with regards to by-product formation, which lead to extraction procedures being dirty, tedious and wasteful (i.e. solvents) the decision was made to forgo the use of this method. Purification of the crude products was also time consuming and not economical for the time and resources spent to obtain the low amounts of product, it was clear that the Gould-Jacobs method was the better alternative. Unfortunately, due to the delay in obtaining fresh acrolein, the investigation into the Doebner-Miller reaction was severely hindered, although the short period of time spent on the reaction showed some promise as a suitable alternative to the Gould-Jacobs.

However, further investigation in the future may prove the Doebner-Miller method to be the better method of synthesizing quinoline structures such as **19a–i**. The Doebner-Miller method satisfies the criteria of fewer synthetic steps, lower cost and improved yields. The investigation required a lot of technical skills, time and chemistry insight because of the difficulties faced and solutions that had to be found to progress to the next phase of synthesis. Study of the reactions and application of suitable

alterations proved to be beneficial both for improving yields and knowledge gained during the process of optimization. In the case of the Gould-Jacobs, the alterations to the procedures proved to be successful and improved yields of products were obtained. In the case of the Skraup reaction, the attempted improvements were not as successful; however, with more time it may be possible to obtain the desired quinolines **23a–i** more efficiently and in higher yields than those currently obtained in this work. Overall, the investigation was a success as products were synthesized, isolated and comparisons made between the method and identifying the best method, the Gould-Jacobs.

Finally, it should also be noted that these compounds have proved useful to the research efforts of a group investigating the interaction between these quinolines and ferriprotoporphyrin IX (Fe(III)PPIX). These experiments are being carried out by another researcher and are not yet complete. In addition, obtaining these results were not part of the explicit aims of this project and are therefore not included here

CHAPTER 4: INVESTIGATION INTO THE SYNTHESIS OF HYBRID COMPOUNDS

4.1 INTRODUCTION

Having both quinoline and indole compounds in hand from the synthetic investigations discussed in chapters 2 and 3, we considered the use of these compounds to investigate the synthesis of novel hybrid compounds that may provide valuable insight in future work and antimalarial research. In the past few decades, efforts made in developing new classes of antimalarial drugs have only been rewarded with the addition of a few new compounds that include amino alcohols, sesquiterpene trioxanes and naphthoquinones.[68] General approaches in current drug discovery include optimizing the therapy of available drugs (combination therapy), derivatisation of current drugs and the evaluation of natural products obtained from plants.[67,68]

However, a more recent approach is the design and synthesis of hybrid structures that have dual functionality and multiple targets within the parasite's life cycle.[67,68] Hybrid compounds, classically described as the combination of two or more compounds into a single structure through a covalent bond, may be the perfect response to the current problems faced with drug supply, drug resistance and cost.[67,68] In brief, hybrid antimalarials can be classified into one of four classes by the construction of the framework and intended function, namely: *conjugates*, *cleavage conjugates*, *merged hybrids* and *fused hybrids*.[68] In conjugate and cleavage conjugates, the hybrid compound is constructed from two pharmacophores that have separate modes of action coupled by a distinct linker.[68] In the case of the cleavage conjugates, the linker is metabolically unstable and can be metabolized to release the two drugs that function independently with their intended targets.[68] The fused hybrids are constructed by coupling the two pharmacophores with such a short that the two drugs are essentially touching.[68] And finally, the merged hybrids are constructed by utilizing commonalities in the two pharmacophores structures to couple them to give a smaller and simpler molecule.[68]

Scheme 39 illustrates the rational synthetic approach of synthesizing compound **H3g–h** by an amidation reaction that couples the indole **11** and quinoline **12g–h** pharmacophores together with the incorporated amine linker of compound **12g–h**. Scheme 39 also indicates the two functionalities (carboxylic acid and amine) that were incorporated into compounds **11** and **12g–h** during the investigation of indole and quinoline synthesis and would thus facilitate the amidation that was envisaged.

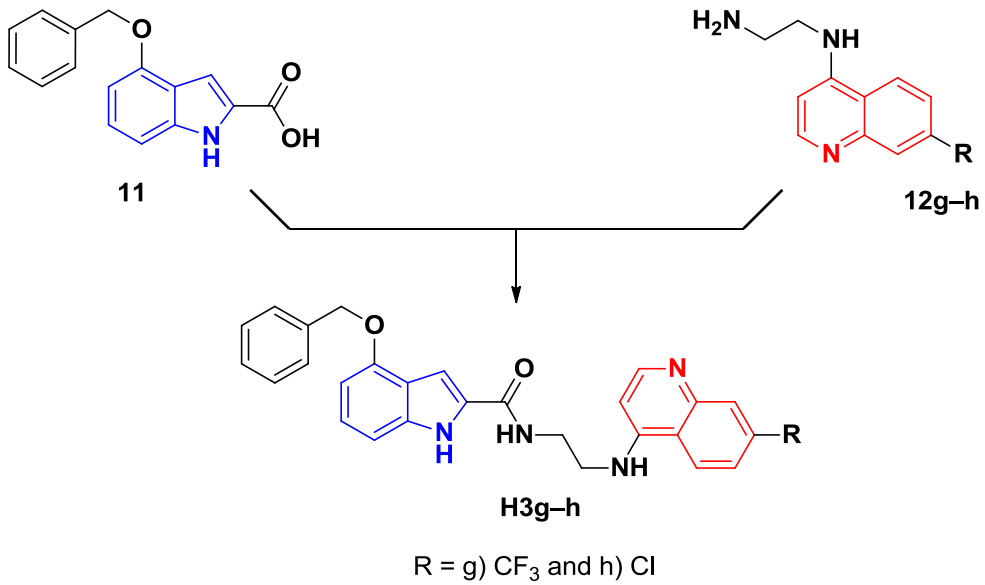

Scheme 39 – Rational approach to synthesis of novel compounds **H3g** and **H3h** by coupling the indole (blue) and quinoline (red) substructures via a stable linker chain.

With the rational synthesis for a hybrid coupling via an amidation reaction established, we proceeded to investigate the available amidation methods to identify the most suitable and effective method for coupling the compounds **11** and **12g–h**.

4.2 SYNTHESIS OF NOVEL HYBRIDS

The amide functionality plays an important role for medicinal chemists because it is ubiquitous in life, specifically in proteins, that play a crucial role in virtually every biological process.[177] The amino carbonyl group is stable, neutral and is both a hydrogen-bond accepter and donor that makes it an attractive functional group for pharmacological drug development.[177] A study by Ghose *et al.*,[178] of the Comprehensive Medicinal Chemistry database revealed that more than 25% of the known drugs contain the amino carbonyl group.[178]

An amidation reaction is a condensation reaction between a carboxylic acid and an amine that forms an amide bond. Unlike esterification, where the reaction is an equilibrium reaction between a carboxylic acid and an alcohol, amidation is initially an acid-base reaction where the acid and amine first form a stable salt. This means that the formation of the amide bond goes against thermodynamics that favor the hydrolysis rather than the amide bond formation.[177] However, the carbonyl components can be activated as acyl azides, acyl chlorides, anhydrides, acylimidazoles etc. to facilitate the attack of the amine to form the amide.[177] Although there are many activation methods,[177] we were interested

in identifying a method that was synthetically simple, cost effective, had mild reaction conditions and was highly efficient at producing amides.

Upon further investigation of the literature,[177,179-185] a simple and efficient method of amidation was identified that readily gives access to amides via the use of a coupling reagent and very mild reaction conditions.[177,179-185] The method we decided to focus our attention on the acylimidazole methodology of activating the carboxylic acid of **11**. The method utilizes *N*,*N*′-carbonyldiimidazole (CDI) to mediate the coupling of amines to carboxylic acids to afford amides in a simple one-pot reaction.[177,179,180,186]

CDI is one of the most commonly used coupling reagents for *N*-acylation reactions, both in industry and academic research, because it is inexpensive, readily available in large quantities and easy to handle.[179,180,182] Other advantages of using CDI for amidation reactions is that the isolation and purification of the desired amide product is very simple because of the by-products, carbon dioxide and imidazole, that are benign and water soluble.[180,186] CDI is also an excellent reagent for up scaling and allows for amidation reaction to be carried out on a larger scale without adverse effects occurring as the by-products do not take part in the reaction.[177,179] The function of the CDI is to activate the less reactive carbonyl OH-group of carboxylic acids and facilitate the coupling with the weakly nucleophilic amines to form amides in a single reaction step with little to no side-reactions occurring.[179,182]

The mechanism for the CDI-mediated reaction is given in Scheme 40 and illustrates the role of the CDI in the reaction and how it facilitates the formation of the desired amide product.[177,182] It is reported that the reaction proceeds via an anhydride intermediate **11b (**that is formed from the deprotonation of **11** by one of the CDI (**A**) molecules, resulting in the formation of the carboxylate anion **11a**.[179,180,182] This is followed by the nucleophilic attack of **11a** on the now more electron-deficient carbonyl carbon of the CDI molecule (**B**), releasing an imidazole molecule and forming the mixed-anhydride intermediate **11b**.[179,180,182] A nucleophilic attack then occurs on **11b** by the released imidazole to form the activated carbonyl **10c** and releases a molecule of carbon dioxide and a second imidazole molecule. Finally, the nucleophilic attack of the primary amine (**12g–h**) occurs at the carbonyl of **11c,** again releasing an imidazole that picks up a proton from the amine to afford the desired amide product **H3g–h**.[179,180,182]

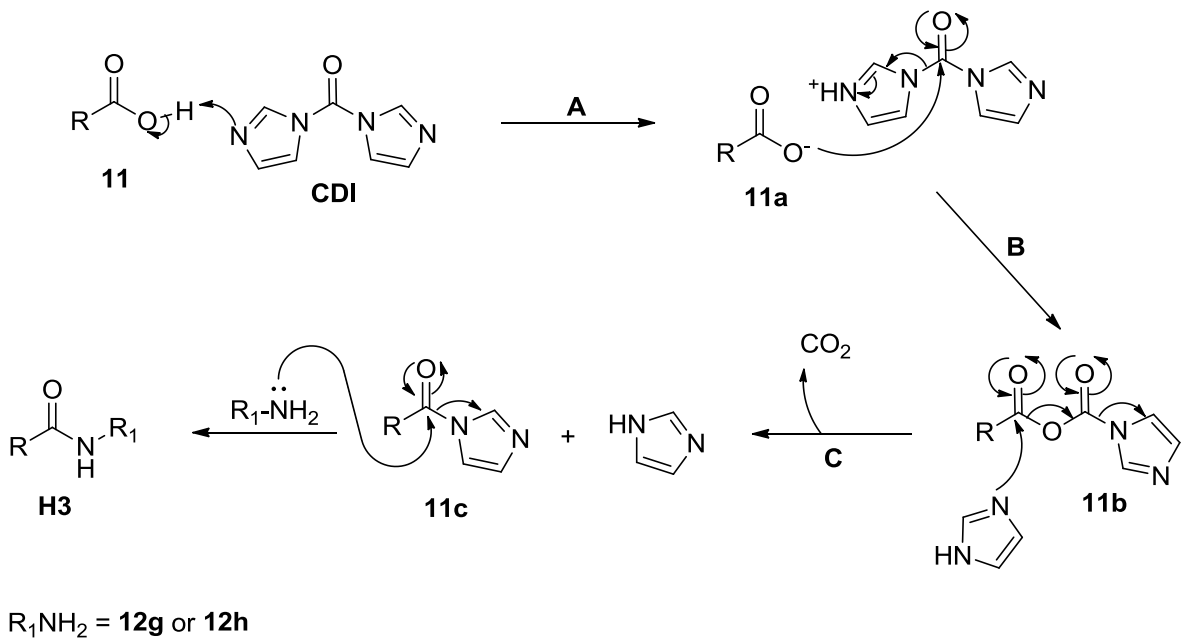

Scheme 40 – Reaction mechanism for the CDI-mediated amidation of indole **11** with quinoline **12g–h**.[177,179,180,182]

Having synthesized compounds **11** and **12g–h,** a coupling reaction could be carried out by making use of the identified CDI-reaction method described above and further illustrated by Scheme 41.[186-188]

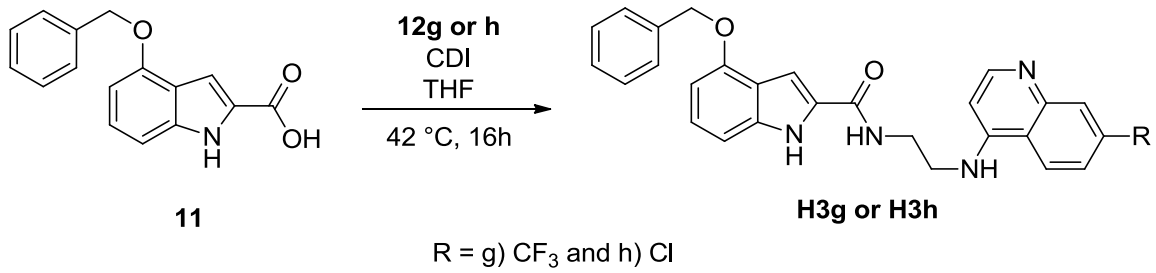

Scheme 41 – General reaction scheme for the attempted synthesis of **H3g** and **H3h**.[187]

A literature procedure reported by Rennard *et al.*,[187] was followed; however, a modification was made to the procedure that made use of THF as reaction solvent instead of the prescribed toluene, and a decrease in reaction temperature from 60 to 42 ºC as a result of the instability of the indole at temperatures above 50 ºC at which point decomposition occurs.[187] Following the procedure, **11** was dissolved in dry THF and the flask sealed under nitrogen. After 10 minutes of stirring, the CDI was added in a single portion and the mixture warmed to 42 ºC and stirred for a further 10 minutes. Once the time had passed, the chosen amine compound **12g** was added in a single portion and the reaction flask sealed and left to stir for 16 hours under nitrogen atmosphere at 42 ºC. After the 16 hours, no

change was observed in product formation or amine consumption, which led us to believe that the reaction had not proceeded as planned. Nevertheless, the reaction was cooled to room temperature and EtOAc added to the mixture. A yellow precipitate formed on the addition of the EtOAc which was collected on filter paper by vacuum filtration. The yellow material was collected in a glass vial, wrapped in foil and placed in a vacuum desiccator to dry. ^{1}H NMR spectroscopic analysis of the yellow material revealed that the desired product had indeed not formed, but that an unknown organic by-product had formed that could not be identified by NMR or IR spectroscopy. Having collected the organic filtrate during the filtration, an aqueous workup was performed and the combined organic layers concentrated to afford a solid residue. TLC of the residue indicated two spots similar to those of the starting materials **11** and **12g** and we suspected that was recovered starting material. The residue was purified by column chromatography and ^{1}H NMR spectroscopic analysis, to our dismay, confirmed the suspicion that the starting materials were indeed recovered as 62% of the original amount of **11** and 48% of **12g** with no trace of any product **H3g**.

Having recovered some of the starting materials from the first attempt, a second attempt was performed on compound **11** but replacing amine **12g** with of **12h** and repeating the reaction using the same reaction procedure. This, however, was also unsuccessful as the reaction again did not proceed to form the desired amide product **H3h**. At this point, a closer inspection of the literature was carried out in order to find some form of an explanation for what could be causing the reaction failure, as the reaction is reported to work consistently and provide good to excellent yields for multiple substrates.[179-184]

4.3 PROBLEM IDENTIFICATION, EXPLANATION AND RESOLUTION

A report by Sharma *et al*.,[182] indicated that steric hindrance of the amine may play an important role in the formation of the desired product.[182] They observed that in a reaction between diphenylamine and arginine that 95% of the starting materials were recovered with trace amount of the amide product being isolated.[182] However, in our case the amines (**12g–h**) employed, contained primary amines situated at the end of an ethylene linker, which is able to move freely in space and thus steric hindrance from the bulky quinoline should have minimal effect in this regard. The structure of **11**, however, provided some evidence with regards to steric hindrance playing a role in the reaction. Studying the structure of **11** (Scheme 41), it can be seen that the carboxylic acid moiety of the compound is substituted directly onto the 2-position of the indole substructure and may possibly be the cause of the hindrance during the reaction.

Referring back to the reaction mechanism of Scheme 40, the steric hindrance of compound **11** can possibly be explained by the formation of the intermediate **11c,** and the attempted attack of the amine

(bulky in itself) on the electron-deficient carbonyl that is semi-protected by the bulky indole structure.[182] Although there are many conformations that the molecules **11c** and **12g–h** can adopt, Figure 20 only shows two examples for the attack of the amine **12g–h** coming in from the top. In both cases there is some form of hindrance restricting the approach of the amine from the freely rotating benzyl group. Not completely satisfied with this explanation, we scoured through the literature for further explanations for our failed reactions.

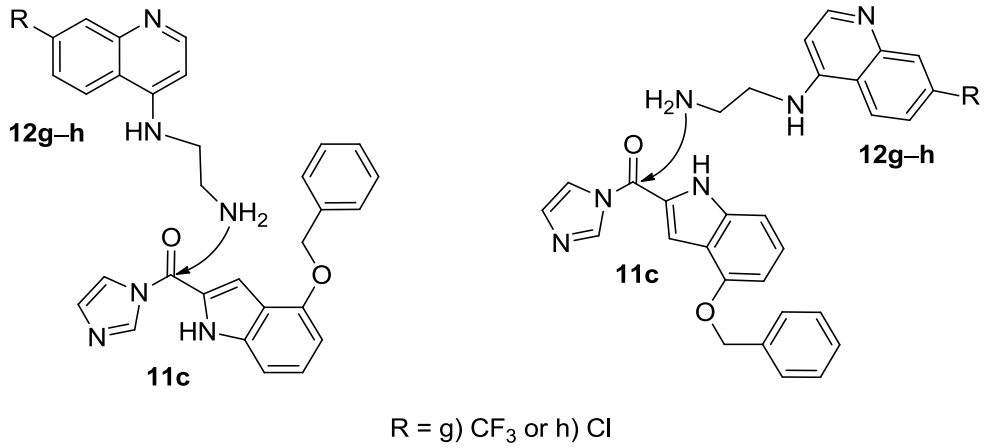

Figure 20 – Two spatial conformations illustrating two pathways of amine (**12g–h**) attack on the electron-deficient carbonyl of **11c**. [179,180,186,189,190]

A second possibility that was identified has to do with the reaction mechanism of aromatic acyl imidazole intermediate **11c**.[179,180,186,189,190] Albeit that the intermediates (i.e. **11b** and **11c**) are more stable than the equivalent activated carbonyls (acyl chlorides and acyl azides), the reaction mechanism is reported to be very slow due to the intermediates being less reactive.[179,180,186,189,190] A possible reason for the lower reactivity of compounds **11b** and **11c** may be as a result of the neighboring aromatic ring system and the conjugation thereof that can make the carbonyl carbon less electrophilic making the reaction less prone to take place.[88] However, the lower reactivity can be combined with the steric hindrance factors mentioned above to decrease the possibility of nucleophilic attack occurring effectively thus inhibiting the formation of the amide product.[189,190] Oakenfall *et al.*[189,190] reported two studies on the structure-reactivity relationship and mechanism of imidazole intermediates and confirmed that the size and basicity of the nucleophile, as well as the size of the intermediate, all have an effect on the rate of reaction and reactivity of the intermediate.

Currently, we are still unsure as to what the reason may be that is causing the reaction not to proceed as desired. The most favorable explanation at this point is the steric hindrance effects and induced stability of the carbonyl by aromaticity, but the investigation into the cause and plausible explanations is still ongoing. Due to limited availability of CDI reagent in the laboratory, starting material that had

to be recovered, additional material needing to be synthesized and the time pressure, the investigation was placed on hold and scheduled to be continued in future work.

4.4 CONCLUSION

In conclusion, this chapter aimed to synthesize a small library of hybrid compounds, utilizing the quinoline and indole precursors obtained during the course of this project. Making use of CDI as a coupling reagent, we aimed to combine the two compounds through an amidation reaction; however, this was unsuccessful, most likely because of the steric hindrance. Despite this however, insight was gained during the investigation as a starting point for future study, modifications of the reaction conditions were identified that may prove to be beneficial at a later stage. The most promising of the alternatives is the modification reported by Larrivée-Aboussafy *et al.*[186] that proposes the use of diazabicycloundecene (DBU) as a catalyst to enhance the rate of reaction when larger carboxylic acid compounds are used.[186] A similar alteration also utilizes a catalyst, imidazole·HCl, to act as a proton source for acid catalysis of CDI-mediated amide coupling that shows increased reaction rates.[179] The last alternative that has some appeal to an organic chemist in search of less toxic and greener methods, is the solvent-free green chemistry methodology reported by Verma *et al.*[180] that utilizes mechanochemistry and water as a reaction medium.[180] However, before attempting the prementioned alterations, two more commonly used methods can be tested apart from the CDI methods; 1) making use of thionyl chloride to convert the carboxylic acid into an acid chloride and then reacting the amine **12** with the acid chloride, 2) investigate an ammonolysis reaction whereby the indole **8** and quinoline amine **12** are reacted directly using an appropriate solvent.

CHAPTER 5: CONCLUSIONS AND FUTURE WORK

5.1 CONCLUSION

The aim of this project was to synthesize a conjugate hybrid dual-activity *Plasmodium* inhibitor by studying, investigating and optimizing the synthetic procedures currently employed for the synthesis of novel antiplasmodial compounds based on the indole **8** and quinoline scaffolds **12** (Figure 21). During the research these indole and quinoline compounds, these individual scaffolds were to be combined into a hybrid structure to afford a novel indole-quinoline hybrid (**H3g–h**). This project also focused on the reactions used to synthesize starting materials, precursors and indoles, as well as, the synthesis of known quinoline antimalarial compounds to assist a fellow student in their research.

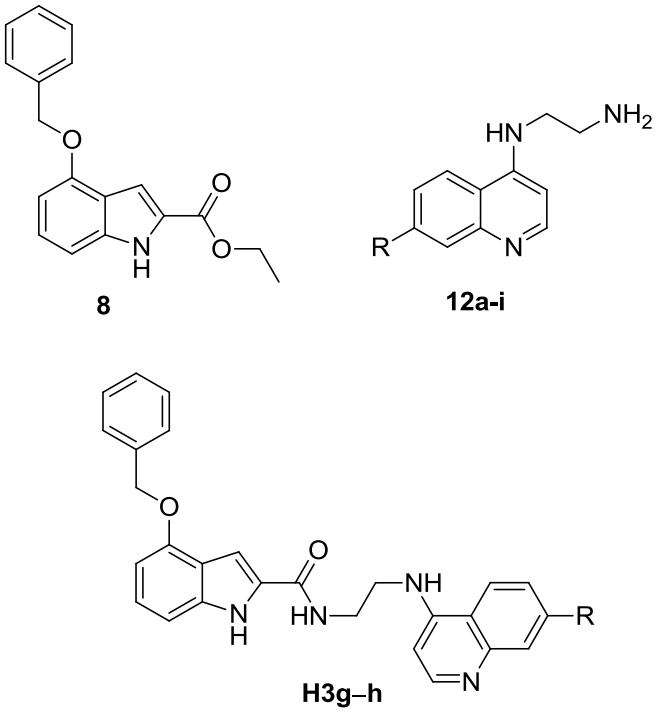

R = a) F, b) Br, c) NO_2, d) CH_3, e) OCH_3, f) I, g) CF_3, h) Cl and i) H

Figure 21 – Illustration of three of the major compound for indole, quinoline and the intended hybrid structure.

Initially we set out to study and optimize the reactions that we were employing for the synthesis of the desired indole **8** namely: the benzylation of the starting material (salicylaldehyde), synthesis of ethyl azidoacetate, the Knoevenagel-condensation reaction to obtain the azido ester precursor to **5** and finally the Hemmetsberger thermal cyclization. Success was attained with the optimization of the starting material 2-benzyloxy benzaldehyde and ethyl azidoacetate reactions and dramatically improving the yields from below 70% to over 95% for both the reactions. An interesting optimization

that was conducted to improve the reaction for ethyl azidoacetate **4a**, was the introduction of a phase transfer catalyst to facilitate the transfer of reactive species from an aqueous to an organic phase and thereby improving the yield. However, the precursor synthesis via the Knoevenagel reaction unfortunately could not be successfully optimized and inconsistency in obtaining the precursor still plagues the synthesis with low to average yields. However, an alternative route was investigated and the synthesis of a unsaturated ester **7** via the Horner-Wadsworth-Emmons reaction and cerium(IV) ammonium nitrate-mediated azide addition reaction proved to be a more suitable and effective method of obtaining the desired indole precursor **5** giving higher yields more consistently. Optimization of the Hemmetsberger cyclization reaction was also successfully achieved and the indole scaffold **8** could readily be accessed even when using unpurified precursor **5** in the reaction. By using the unpurified precursor product from the CAN reaction, we were able to expedite the synthetic process by removing the lengthy isolation and purification step before the cyclization reaction.

Having faced difficulties with the debenzylation of compound **8** using hydrogen and Pd/C, we investigated a recently developed method for the debenzylation of ethers, under mild conditions, which proved to be successful in affording compound **9**. However, this reaction warrants further optimization to improve the yield, as the reaction may prove to be very useful in future work due to its very mild reaction conditions used to debenzylate OH-groups. Having obtained compound **9**, we were unfortunately not able to successfully derivatise **9** to obtain compound **2** using the Mitsunobu reaction. However, the study and optimization of the reaction has not been completed but the foundation laid will provide a useful starting point for the next phase of the larger project. The reaction will prove useful in future work on similar novel antiplasmodial compounds.

During our research of the quinoline compounds, we identified three methodologies for the synthesis of our desired quinoline scaffolds. The Gould-Jacobs, Skraup and Doebner-Miller reactions were all investigated and attempts made to optimize them and identify the most efficient method to obtain the intended quinoline compounds. The Gould-Jacobs and Doebner-Miller methods were identified as the most suitable and efficient methods and successfully afforded the quinoline products. The Gould-Jacobs reaction was successfully optimized to give the desired quinolines consistently regardless of the substituent on the m-substituted aniline starting material. Successful improvements were also made to make the hazardous procedures safer. For example, the decarboxylation of the carboxylic acid quinoline posed a very dangerous situation that was circumvented by introducing an alternative method of adding the acid quinoline to the high temperature refluxing solvent. Our alternative method gave more control over the dangerous gas forming reaction by adding the acid quinoline in flake form instead of as a powder. The Doebner-Miller reaction, although a suitable candidate, was unfortunately not investigated fully due to time pressure. The preliminary results of the investigation showed promise in that the reaction produced the desired quinoline compounds in a more efficient method,

simpler procedure, easier isolation and purification procedures, less by-product formation and very good yields when compare to the Skraup method on which the Doebner-Miller is based. Having studied the Skraup reaction in detail and attempts made to improve the reaction and optimize the yields, the overall result was unsuccessful. Too many problems were faced that made the reaction unsuitable and unfavorable for use as a method to obtain the desired quinolines. The reaction was 'dirty', producing too many by-products, decomposed reagents and difficult and tedious purification procedures with little to no product formation and/or isolation. Nevertheless, a lot of useful chemistry insight and experience was gained during the investigation of the Skraup method which will not go to waste in future when similarly difficult situations are faced and solutions to problems have to be found.

We were able to successfully synthesize a small library of known quinoline antimalarial compounds for a fellow student to use in the research into improving β-hematin inhibition assays. The synthetic procedures were successfully applied to the synthesis of quinoline derivatives using the quinoline compounds obtained from the Gould-Jacobs reaction. These compounds were also intended for use as pharmacophores for the synthesis of a hybrid compound. Having obtained both the desired indole scaffold **11** and the derivatised quinolines, two attempts were made to investigate the synthesis of novel indole-quinoline hybrids. Both attempts were unsuccessful at producing a hybrid compound. Unfortunately, due to a lack of time and resources the investigation and continued synthesis attempts of the hybrid compounds were placed on hold with the intent to continue the research in future.

5.2 FUTURE WORK

For future endeavors, focus should be placed on the continuation of the hybrid concept for antiplasmodial compounds and the synthesis of hybrid compounds. The hybrid indole-quinoline compounds may yet prove to be effective antiplasmodials and warrants further research to ascertain whether this type of compound will be suitable as an alternative to the currently employed mono-therapy compounds. As previously mentioned in the concluding remarks of Chapter 4, the synthesis of the hybrid could be further investigated by attempting to synthesize the hybrid using one or both of the two methods that were mentioned. The first synthesis of an acid chloride of compound **8** or **11** followed by reacting it with the amine **12** to possibly afford the indole-quinoline hybrid, or secondly, making use of an ammonolysis reaction and combine the indole and quinoline in an appropriate solvent. Further investigation into the use of the milder CDI methods as well as the solvent-free CDI method may also prove to be worthwhile future work. However, at present this project has only scratched the surface with regards to combining an indole and quinoline to form novel structures with the possibility of being effective antiplasmodials.

The initial research and synthesis attempts at the Doebner-Miller reaction had shown some success at being a suitable reaction for the synthesis of quinoline structures. It stands to reason that the research into the synthesis via this method is warranted as the reaction may prove to be useful in future quinoline synthesis research. It would be beneficial to make use of this method for future attempts at synthesizing 4,7-substituted quinolines and may well be the preferred method for any further work on this topic.

Although the indole scaffold played a major role in this project, this however is not a limiting factor with regards to continuing with the topic of hybrid synthesis as using different heterocyclic compounds to design new hybrid compounds is possible and worth investigating. Future endeavors into the design and synthesis of hybrids can include the benzofuran scaffold, benzothiophene, different quinoline scaffolds and indole analogues (isoindole and indazoles) all of which can be coupled to form hybrids. However, with the benzofuran, benzothiophene and indoles showing the most positive results as *Plasmodium* inhibitors in hybrid compounds, it stands to reason that any future work will be to continue to investigate the synthesis of hybrids containing a combination of these scaffolds and their derivatives. Another aspect would be to target not only two targets in a single disease but to take full advantage of what a hybrid represents and design a hybrid compound capable of targeting two different diseases i.e. malaria and/or cancer, using a single compound. By broadening the scope of any future work into a dual-activity/disease hybrid inhibitor, the work may serve to aid in the search for a cure or vaccine for these life threatening diseases.

Therefore, new goals can be laid out from the groundwork in this project for the future work that may lie ahead; 1) continue to investigate the dual-activity hybrid inhibitor for the plasmodium parasite, 2) investigate the possibility of a dual-disease targeting hybrid inhibitor being plausible, 3) identify suitable compounds that shown favorable activity towards the *Plasmodium* parasite (benzofuran, indole, benzothiophene etc.), 4) identify structures/compounds with structural similarities that may have the capability of being modified to function as possible antiplasmodial and/or anti-cancer agents, 5) design and synthesize novel compounds for the aforementioned purposes of dual-activity/disease hybrids, 6) test any synthesized novel compounds for their activity towards the *Plasmodium* parasite and, if applicable, as anti-cancer agents, 7) continue to investigate the mechanistic workings of the CDI amidation to afford the desired amide-amine functionality linker for hybrid coupling and lastly, synthesize dual-activity/dual-disease hybrid compounds as inhibitors for *β*-hematin and *Plasmodium vivax* N-myristoyltransferase and possibly malaria and cancer.

Overall the project was a success, although we were not able to obtain the novel indole derivative **2** or the hybrid compounds **H3g–h**, we did achieve our objectives with regards to: optimizing the currently used reactions for synthesis of indole scaffolds, identification of more suitable and effective alternatives to obtain the indole precursors, investigate and identify suitable reactions for the synthesis

of quinoline scaffolds and optimize them, attempts were also made to synthesize the hybrid compound and finally a wealth of chemistry knowledge, experience (theoretical and practical) and insight was gained that will prove to be of benefit in any future chemistry research.

CHAPTER 6: EXPERIMENTAL DATA

6.1 GENERAL PROCEDURES AND INSTRUMENTATION

Purification of Reagents and Solvents

The chemical reagents used in the synthesis procedures that follow were either obtained from the chemicals store or purchased from Sigma Aldrich and Merck. Reaction solvents were also purchased from Sigma Aldrich and Merck with a purity grade ≥ 98%. Before use, the reaction solvents were dried over the appropriate drying agents by refluxing for 30 minutes then distilling under nitrogen gas, and used either directly from the collection vessel or stored in glass bottles over activated molecular sieves. Methanol and ethanol were distilled from magnesium turnings and iodine, dichloromethane from calcium hydride, tetrahydrofuran from sodium metal using benzophenone as indicator, acetonitrile from anhydrous potassium carbonate granules, toluene from calcium hydride and acetone from anhydrous calcium chloride. Diphenyl ether and xylene were purchased from Sigma Aldrich with purity >95% and used directly from the bottles they arrived in without further drying. Solvents used for chromatographic purposes (hexane, ethyl acetate, dichloromethane, methanol and ethanol) were obtained from the chemical store and distilled by conventional distillation procedures to remove impurities.

Chromatography

Thin layer chromatography (TLC) was performed using Macherey-Nagel Alugram® Xtra SIL G/UV_{254} silica gel 60 coated aluminum sheets. Visualization was carried out using a UV lamp and staining the TLC plates with either, iodine on silica, potassium permanganate ($KMnO_4$), bromocresol green or ninhydrin solution followed by heating. Flash chromatography was carried out by either conventional methods or on a Teledyne Isco CombiFlash Rf150 automated purification instrument fitted with a variable 200–400 nm UV detector. All column chromatography was performed using Merck silica gel (230-400 mesh).

Spectroscopic and Physical Data

NMR spectra (^{1}H, ^{13}C, ^{31}P and NOESY) were recorded on a 300 MHz Varian VNMRS (75 MHz for ^{13}C), a 400 MHz Varian Unity Inova (101 MHz for ^{13}C, 162 MHz for ^{31}P), or a 600 MHz Varian Unity Inova (151 MHz for ^{13}C). All chemical shifts (δ) are reported in parts per million (ppm) and coupling constants (*J*-values) are reported in Hertz (Hz). The spectra were processed using MestReNova software. Deuterated chloroform ($CDCl_3$) and dimethyl sulfoxide (DMSO-d_6) were used as internal reference and purchased from Sigma Aldrich.

Infrared (IR) spectroscopy was performed on a Nexus Thermo Nicolet 470 in Attenuated Total Reflectance (ATR) mode and the data processed using OMNIC software. Mass spectroscopy was carried out on a Waters SYNAPT G2 mass spectrometer using a Time-of-Flight mass analyzer in either Electrospray positive (ES+) or Electrospray negative (ES-) ionization method. Melting point analysis was carried out using a Gallenkamp Melting Point Apparatus and results are uncorrected.

Additional Procedures

Injections – In cases were precise injection rates were required a Harvard Apparatus Model 11 single syringe pump was used to control the rate of reagent injection.

High temperature heating (T = 150–260 °C) – For the heating of high boiling solvents and reactions requiring temperature above 150 °C, an electric heating mantle was used to avoid hazardous situations that may have occurred using oil or sand baths for heating to the extreme temperatures. Paraffin oil was used in oil baths for temperatures below 140 °C.

Low temperature cooling – For cooling to -10 °C a cooling bath was made by combining crushed ice with potassium chloride in a 3 to 1 ration by mass, mixed to form a slush and placed in a low form dewar flask to maintain the temperature for extended periods of time.

Solvent degassing [Freeze-Pump-Thaw (FPT)] – Solvent and/or reaction solution was added to a Schlenk tube and sealed. The tube was placed in liquid nitrogen and the solvent/solution frozen. Once frozen vacuum was created in the tube using a high vacuum pump for 5 minutes whilst the tube was kept in the liquid nitrogen. The tube was closed off from the vacuum line and the flask carefully warmed in lukewarm water until the solvent/solution was completely thawed. The freezing, vacuum and thawing process was repeated a minimum of 3 times or until the evolution of gas bubbles ceases during thawing. Once completed the vacuum in the flask was filled with nitrogen gas to create an inert atmosphere to avoid air from entering the flask.

6.2 EXPERIMENTAL DATA PERTAINING TO CHAPTER 2

6.2.1 Synthesis of Starting Materials and Reagents

2-(benzyloxy)benzaldehyde (3b).[62]

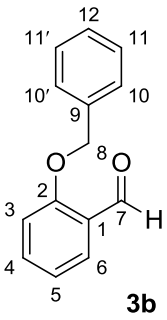

3b

To a 250 mL, two-neck, round-bottom flask was added dry acetone (80 mL) and, under vigorous stirring, anhydrous potassium carbonate (6.22 g, 44.9 mmol). The flask was connected to a condenser and the side neck sealed with a septum stopper after which salicylaldehyde (4.36 mL, 5.00 g, 40.9 mmol) was added in a single portion to the reaction flask. The reaction mixture was heated to 75 °C and began to boil, at which point benzyl bromide (6.75 mL, 9.71 g, 56.8 mmol) was added dropwise over 20 minutes with a noted change in color from yellow to reddish-brown with a white precipitate being formed. The temperature was decreased to 75 ºC and the reaction left to stir under reflux for 18 hours. On completion, the reaction mixture was cooled to room temperature and the acetone removed *in vacuo*. The solid residue that remained was diluted with water (100 mL) and excess potassium carbonate neutralized with 1N HCl. The aqueous mixture was extracted with DCM (3 × 100 mL), the organic layers combined and washed with brine (100 mL) and dried over anhydrous magnesium sulfate for 10 minutes. The magnesium sulfate was removed by filtration, the DCM collected and removed *in vacuo* to afford the crude product as a yellow oil that solidified on standing. The crude product was purified by flash chromatography (R_f = 0.49, 15% EtOAc/Hex) and the pure product was obtained as white crystalline material (8.20 g, 38.6 mmol, 95%).

Mp 46.3 – 47.2 °C; **IR (ATR,cm^{-1})** 3062, 3033, 2873 (ald C-H str.), 1681 (conj. ald C=O str.), 1595, 1482, 1466, 1455, 1381, 1286, 1237 (C-O str.), 1188, 1160 (ether C-O-C str.), 1100, 993, 986, 861, 835, 760, 746, 700, 657; **^{1}H NMR (600 MHz, $CDCl_3$) δ** 10.58 (s, 1H, CHO), 7.87 (dd, J^3 = 7.6 Hz, J^4 = 1.8 Hz, 1H, H-6), 7.56-7.52 (m, 1H, H-4), 7.45 (d, J^3 = 7.0 Hz 2H, H-10, H-10′), 7.43-7.39 (m, 2H, H-11, H-11′), 7.36 (t, J^3 = 7.2 Hz, 1H, H-12), 7.06 (d, J^3 = 8.4 Hz, 1H, H-3), 7.05 (t, J^3 = 8.4 Hz, 1H, H-5), 5.20 (s, 2H, H-8); **^{13}C NMR (151 MHz, $CDCl_3$) δ** 189.9 (C-7), 161.2 (C-2), 136.2 (C-9), 136.0 (C-4), 128.9 (C11, C-11′), 128.6 (C-6), 128.4 (C-12), 127.4 (C-10, C-10′), 125.4 (C-1), 121.2 (C-5), 113.2 (C-3), 70.6 (C-8); **HRMS-TOF MS ES+: *m/z* [M+H]$^+$** calculated for $C_{14}H_{13}O_2$: 213.0916; found: 213.0920. This corresponds well with the reported values.[90,91]

Ethyl 2-azidoacetate (4a).[92,93]

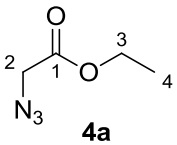

4a

To a 150 mL round-bottom flask was added water (50 mL), DCM (50 mL) and tetrabutylammonium hydrogen sulfate (0.53 g, 2.3 mmol) and the mixture stirred until all dissolved. The flask was lowered into a 30 ºC oil bath and the reaction mixture vigorously stirred to form a single phase solution to which ethyl chloroacetate (0.87 mL, 1.0 g, 8.1 mmol) was added slowly in a single portion. The flask was sealed and left to stir for 48 hours after which the reaction was cooled to room temperature and the aqueous layer removed using a separating funnel. The organic layer was washed with water (3 × 50 mL) and a single portion of brine (50 mL). The organic layer was dried over anhydrous magnesium sulfate, filtered and concentrated under reduced pressure to afford the product as a pale orange liquid in 95% yield. Used further without purification.

IR (ATR,cm^{-1}) 2986 (sp^3 C-H str.), 2104 (N_3 str.), 1741 (C=O str.), 1426, 1372, 1348, 1287, 1193 (C-O str.), 1097, 1026 (C-O str.), 949, 735; **^{1}H NMR (300 MHz, $CDCl_3$) δ** 4.19 (q, J^3 = 7.2 Hz, 2H, H-3), 3.80 (s, 2H, H-2), 1.24 (t, J^3 = 7.1 Hz, 3H, H-4); **^{13}C NMR (75 MHz, $CDCl_3$) δ** 168.2 (C-1), 61.7 (C-3), 50.2 (C-2), 13.9 (C-4); **HRMS-TOF MS ES+: *m/z* [M+H]$^+$** calculated for $C_4H_8N_3O_2$: 130.0572; found: 130.0512. This corresponds well with the reported values.[80,92,97,98]

(*Z*)-Ethyl 2-azido-3-[2-(benzyloxy)phenyl]acrylate (5).

Method 1 – Knoevenagel condensation.[80-82]

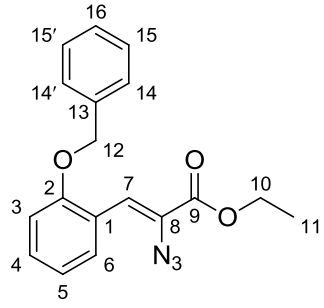

5

A 250 mL, three-neck, round-bottom flask was fitted with a nitrogen-line (side-neck 1), a drying tube (upper-neck) filled with a mixture of anhydrous calcium chloride/silica gel crystals and a rubber septum (side-neck 2). Nitrogen was allowed to flow into the flask and out through the drying tube whilst dry EtOH (45 mL) was added to the flask followed by sodium metal (1.93 g, 84.8 mmol). After the addition of the sodium to the flask, the flask was kept cool in an ice bath (0 ºC) to slow the vigorous release of hydrogen gas. The nitrogen flow was maintained through the flask to force any ethanol vapors and hydrogen gas from the flask that had formed during the dissolving of the sodium. 2-Benzyloxy benzaldehyde (6.00 g, 28.3 mmol) was placed in a glass vial and melted in an oven at 130 ºC and added to the ethanol solution in a single portion. Ethyl trifluoroacetate (10.1 mL, 12.0 g, 84.8 mmol) and ethyl azidoacetate (9.7 mL, 10 g, 84 mmol) were combined and added dropwise to the reaction mixture over 30 minutes. The reaction was kept at 0 ºC for 1 hour and then warmed to room temperature and stirring continued under nitrogen

flow for a further 4 hours. On completion, the reaction mixture was neutralized with saturated NH_4Cl solution (100 mL) and water (100 mL). The aqueous mixture was extracted with EtOAc)3 × 100 mL), the organic layers combined, washed with H_2O (2 × 100 mL) and brine (100 mL). The organic layer was dried over anhydrous magnesium sulfate for 15 minutes, the magnesium sulfate filtered off using a sinter-glass funnel and the collected EtOAc was concentrated *in vacuo* to obtain the crude product as a yellow oil. Purification of the crude product was carried out by flash chromatography (R_f = 0.63, 15% EtOAc/Hex) and the desired product was obtained as a pale yellow oil that solidified into a yellow solid under high vacuum (3.97 g, 12.3 mmol, 43%).

Mp 96.9 – 98.2 °C; **IR (ATR,cm^{-1})** 3323, 3098, 3067, 3033, 2985, 2909, 2871, 2113 (N_3 str.), 1745, 1698 (C=O str.), 1646, 1620, 1595, 1585, 1572, 1498, 1484, 1478, 1448, 1381, 1366, 1313, 1242 (C-O str.), 1199, 1169, 1115 (ether C-O-C str.), 1081, 1052, 1038, 1025, 937, 902, 847 (C=C bend), 828, 762, 752, 731, 692, 655; **^{1}H NMR (600 MHz, $CDCl_3$) δ** 8.23 (dd, J^3 = 7.8 Hz, J^4 = 1.6 Hz, 1H, H-6), 7.53 (s, 1H, H-7), 7.46-7.43 (m, H-14, H-14′), 7.41-7.37 (m, 2H, H-15, H-15′), 7.35-7.31 (m, 1H, H-16), 7.23-7.27 (m, 1H, H-4), 7.04-7.00 (m, 1H, H-5), 6.95 (d, J^3 = 8.3 Hz, 1H, H-3), 5.14 (s, 2H, H-12), 4.35 (q, J^3 = 7.1 Hz, 2H, H-10), 1.38 (t, J^3 = 7.1 Hz, 3H, H-11); **^{13}C NMR (151 MHz, $CDCl_3$) δ** 163.9 (C-9), 156.8 (C-2), 136.8 (C-13), 130.8 (C-8), 130.7 (C-6), 128.6 (C-15, C-15′), 128.0 (C-4), 127.0 (C-14, C-14′), 125.4 (C-16), 122.8 (C-5), 120.9 (C-7), 119.5 (C-1), 112.3 (C-3), 70.6 (C-12), 62.2 (C-10), 14.3 (C-11); **HRMS-TOF MS ES+: *m/z* [M+H]$^+$** calculated for $C_{18}H_{18}N_3O_3$: 324.1303; found: 324.1348. This corresponds well with the reported values in the literature.[101]

Ethyl 2-(diethoxyphosphoryl)acetate (6b).[108,109,119]

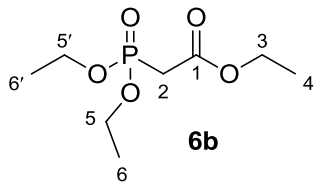

6b

Ethyl chloroacetate (26.1 mL, 30.0 g, 24.0 mmol) and triethyl phosphite (50.9 mL, 48.8 g, 293 mmol) were combined in a 250 mL, one-neck, round-bottom flask equipped with a Teflon-coated magnetic stirbar. The reaction flask was connected to a condenser and heated in an oil-bath to 170 ºC and heated under reflux for 8 hours. The mixture was then cooled to room temperature, the flask equipped with a distillation manifold and the reaction re-heated and the product collected by distillation at atmospheric pressure (142 – 145 ºC). The desired product was obtained as a pale yellow liquid (46.1 mL, 52.1 g, 232 mmol, 95%) and stored in an air tight glass bottle at a temperature of 2 ºC.

IR (ATR, cm^{-1}) 2984 (sp^3 C-H str.), 2936, 1736 (C=O str.), 1446, 1393, 1372, 1238 (P=O str.), 1164, 1115, 1024 (P-OR str.), 970, 797; **^{1}H NMR (400 MHz, $CDCl_3$) δ** 4.17-4.03 (m, 6H, H-3, H-5, H-5′), 2.85 (d, J^2 = 21.5 Hz, 2H, H-2), 1.24 (t, J^3 = 7.1 Hz, 6H, H-6, H-6′), 1.18 (t, J^3 = 7.1 Hz, 3H, H-4); **^{13}C NMR (101 MHz, $CDCl_3$) δ** 165.7 (d, J^2 = 6.0 Hz, C-1), 62.6 (d, J^2 = 6.3 Hz, C-5, C-5′), 61.5 (C-3), 34.9 (d, J^1 = 134.2 Hz, C-2), 16.3 (d, J^2 = 6.3 Hz, C-6, C-6′), 14.1 (C-4); **^{31}P NMR (10 MHz, $CDCl_3$)**

δ 19.8 (s, 1P); **HRMS-TOF MS ES+: *m/z* [M+H]$^+$** calculated for $C_8H_{18}O_5P$: 225.0892; found: 225.0883. This corresponds well with the reported values in the literature.[108,109]

(*E*)-Ethyl 3-[2-(benzyloxy)phenyl]acrylate (7).[104,118,191]

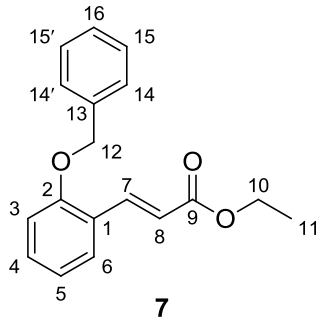

7

To a 250 mL 2-neck, round-bottom flask was added dry toluene (120 mL) and 2-(benzyloxy)benzaldehyde (5.00 g, 23.6 mmol) in a single portion and stirred until thoroughly dissolved. To the reaction mixture was added granular anhydrous potassium carbonate (8.14 g, 58.9 mmol) and the solution was vigorously stirred to prevent sticking and clumping from occurring. The flask was equipped with a condenser, the side neck sealed with a rubber septum and the solution heated to 125 ºC to reflux. Once the mixture started to reflux ethyl 2-(diethoxyphosphoryl)acetate (13.2 g, 58.9 mmol) was slowly added to the refluxing mixture over 15 minutes and the reaction was left to reflux for 2 – 3 hours, monitoring completion by TLC (R_f = 0.60, 15% EtOAc/Hex). On completion, the reaction mixture was cooled to room temperature and saturated NH_4Cl (150 mL) solution was added to the flask. The toluene was separated and the aqueous layer extracted EtOAc (3 × 75 mL). All the organic layers were combined and washed with H_2O (150 mL) then with brine (150 mL). The organic layer was collected and dried over anhydrous magnesium sulfate for 15 minutes, followed by filtration to remove the solids using a sinter-glass funnel. The filtrate was concentrated *in vacuo* to give the crude product as a light-brown oil. The crude product was purified by flash chromatography (R_f = 0.60, 15% EtOAc/Hex) to afford the title product as a white crystalline material (5.91 g, 20.9 mmol, 89%).

Mp 55.1 – 56.9 °C; **IR (ATR,cm^{-1})** 3065, 3034, 2980 (sp^3 C-H str.), 1704 (conj. ester C=O str.), 1630 (conj. C=C str.), 1597, 1578, 1486, 1451, 1380, 1366, 1317, 1268, 1239, 1160 (ester C-O str.), 1123 (ether C-O-C str.), 1104, 1024 (alkoxy C-O str.), 988, 868, 748, 695; **^{1}H NMR (600 MHz, $CDCl_3$) δ** 8.11 (d, J^3 = 16.1 Hz, 1H, H-7), 7.55 (dd, J^3 = 7.6 Hz, J^4 = 1.5 Hz, 1H, H-6), 7.45 (d, J^3 = 7.3 Hz, 2H, H-14, H-14′), 7.42-7.38 (m, 2H, H-15, H-15′), 7.36-7.29 (m, 2H, H-16, H-4), 7.00-6.94 (m, 2H, H-3, H-5), 6.55 (d, J^3 = 16.1 Hz, 1H, H-8), 5.17 (s, 2H, H-12), 4.26 (q, J^3 = 7.1 Hz, 2H, H-10), 1.34 (t, J^3 = 7.1 Hz, 3H, H-11); **^{13}C NMR (151 MHz, $CDCl_3$) δ** 167.5 (C-9), 157.4 (C-2), 139.9 (C-7), 136.7 (C-13), 131.4 (C-6), 128.8 (C-4), 128.7 (C-15, C-15′), 128.0 (C-16), 127.2 (C-14, C-14′), 124.0 (C-1), 121.1 (C-5), 118.9 (C-8), 112.9 (C-3), 70.4 (C-12), 60.4 (C-10), 14.4 (C-11); **HRMS-TOF MS ES+: *m/z* [M+H]$^+$** calculated for $C_{18}H_{19}O_3$: 283.1334; found: 283.1338. This corresponds well with the reported values in the literature.[120,121]

(*Z*)-Ethyl 2-azido-3-[2-(benzyloxy)phenyl]acrylate (5).

Method 2 – Cerium(IV) ammonium nitrate (CAN) mediated azide addition.[86,87]

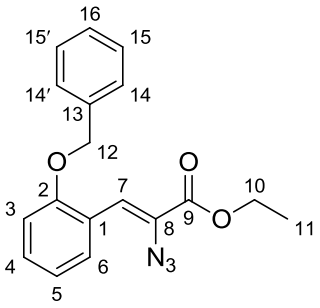

5

In separate 200 mL Schlenk tubes, two solutions, **(***E***)**-ethyl 3-(2-(benzyloxy)phenyl)phenyl)acrylate (7.50 g, 26.6 mmol) and sodium azide (6.91 g, 106 mmol) in dry acetonitrile (50 mL) and cerium(IV) ammonium nitrate (43.6 g, 79.6 mmol) in the same solvent were respectively made. The tube was sealed and the solution deoxygenated using the freeze-pump-thaw method described in the beginning of this chapter. Once the deoxygenation process was completed, the Schlenk tubes were kept under vacuum, charged with nitrogen and kept so for the remainder of the reaction procedure. The tube containing the acrylate solution was placed into a cooling bath at -10 ºC to -15 ºC and the CAN solution tube was placed in an ice bath (0 ºC). Both tubes were left to stir for 10 minutes to cool sufficiently. A 60 mL syringe was filled under N_2 atmosphere with CAN solution (50 mL) and the solution was added dropwise to the acrylate solution – initially very slowly (1 mL/min) and after 20 mL had been added the rate was increased to 2.5 mL/min. The reaction mixture was left to stir in the cooling bath under nitrogen for 14 hours while warming naturally to room temperature. On completion, the reaction mixture was concentrated *in vacuo* and the resulting residue was diluted with H_2O (400 mL). The product was extracted with 4 × 150 mL EtOAc. The combined organic layers were dried over anhydrous magnesium sulfate for 20 minutes. The magnesium sulfate was then filtered off and the filtrate concentrated *in vacuo*. The dark oily residue was diluted with dry acetone (40 mL), transferred to a 100 mL round bottom flask with minimal amounts of dry acetone and anhydrous sodium acetate (6.54 g, 79.7 mmol) was added. The flask was sealed and the reaction left to stir at 30 ºC for 48 hours (covered in aluminium foil to reduce the exposure to light and retain heat). On completion, the acetone was removed *in vacuo*, the dark oily residue redissolved into EtOAc (150 mL) and the resulting solution washed 2 × 50 mL H_2O. The organic layer was separated, dried over anhydrous magnesium sulfate, filtered and the solvent evaporated under reduced pressure. The crude dark oil was purified by flash chromatography (R_f = 0.62, 15% EtOAc/Hex) and the product obtained as a pale yellow solid (5.84 g, 18.0 mmol, 68%)

Mp 96.1 – 98.5 °C; **IR (ATR,cm^{-1})** 3099, 3033, 2986, 2909, 2870, 2115 (N_3 str.), 1698 (C=O str.), 1595, 1572, 1498, 1484, 1477, 1448, 1381, 1366, 1313, 1242 (C-O str.), 1199, 1169, 1119 (ether C-O-C str.), 1077, 1052, 1038, 1025, 846 (C=C bend), 762, 752, 731, 692; **^{1}H NMR (400 MHz, $CDCl_3$) δ** 8.23 (dd, J^3 = 7.8 Hz, J^4 = 1.6 Hz, 1H, H-6), 7.53 (s, 1H, H-7), 7.47-7.42 (m, 2H, H-14, H-14′), 7.42-7.37 (m, 2H, H-15, H-15′), 7.36-7.32 (m, 1H, H-16), 7.32-7.27 (m, 1H, H-4), 7.04-7.00 (m, 1H, H-5), 6.95 (dd, J^3 = 8.3 Hz, J^4 = 0.75 Hz, 1H, H-3), 5.14 (s, 2H, H-12), 4.35 (q, J^3 = 7.1 Hz, 2H, H-10), 1.38 (t, J^3 = 7.1 Hz, 3H, H-11); **^{13}C NMR (101 MHz, $CDCl_3$) δ** 163.9 (C-9), 156.9 (C-2), 137.0 (C-13),

130.9 (C-8), 130.8 (C-6), 128.7 (C-15, C-15′), 128.0 (C-4), 127.1 (C-14, C-14′), 125.4 (C-16), 122.8 (C-5), 120.9 (C-7), 119.5 (C-1), 112.4 (C-3), 70.5 (C-12), 62.2 (C-10), 14.2 (C-11); **HRMS-TOF MS ES+: *m/z* [M+H]$^+$** calculated for $C_{18}H_{18}N_3O_3$: 324.1303; found: 296.1282. This corresponds well with the reported values in the literature with the exception of the MS value which is explained in Section 2.3.3.[101]

6.2.2 Synthesis of Indoles and Indole-derivatives

Ethyl 4-(benzyloxy)-1*H*-indole-2-carboxylate (8).[62,80,83,131]

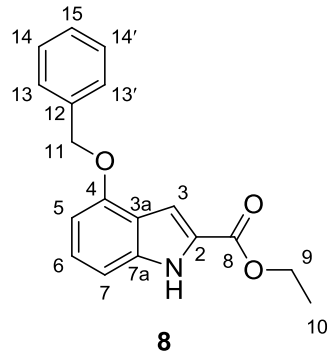

8

To a 50 mL, two-neck, round-bottom flask was added toluene (20 mL) and the flask equipped with a condenser and a rubber septum and was lowered into a 130 ºC oil bath. (*Z*)-ethyl 2-azido-3-(2-(benzyloxy)phenyl)acrylate (716 mg, 2.21 mmol), dissolved into a minimal volume of toluene, was added dropwise to the refluxing toluene over 5 minutes. The reaction was left to stir under reflux at 130 ºC for 2 hours, monitoring reaction completion by TLC (15% EtOAc/Hex) to avoid decomposition from extended reflux times. On completion, the reaction mixture was cooled to room temperature and the solvent removed under reduced pressure. The crude product was purified by flash chromatography (R_f = 0.42, 15% EtOAc/Hex) and afforded the title product as a white powder (412 mg, 1.39 mmol, 63%).

Mp 168.9 – 170.2 °C; **IR (ATR,cm^{-1})** 3321 (N-H str.), 3036, 2997, 2959, 2937, 1726, 1682 (C=O str.), 1584, 1518, 1391, 1377, 1364, 1347, 1300, 1242 (ester C-O str.), 1195 (ether C-O-C str.), 1170, 1114, 1079, 1050, 1011, 970, 918, 824, 755, 727, 698, 676; **^{1}H NMR (600 MHz, $CDCl_3$) δ** 8.96 (br s, 1H, NH), 7.51 (d, J^3 = 7.4 Hz, 2H, H-13, H-13′), 7.44-7.39 (m, 3H, H-14, H-14′, H-3), 7.37-7.32 (m, 1H, H-15), 7.24-7.20 (m, 1H, H-6), 7.03 (d, J^3 = 8.2 Hz, 1H, H-7), 6.58 (d, J^3 = 7.7 Hz, 1H, H-5), 5.22 (s, 2H, H-11), 4.41 (q, J^3 = 7.1 Hz, 2H, H-9), 1.41 (q, J^3 = 7.1 Hz, 3H, H-10); **^{13}C NMR (151 MHz, $CDCl_3$) δ** 162.1 (C-8), 153.8 (C-4), 138.4 (C-7a), 137.2 (C-12), 128.6 (C-14, C-14′), 128.0 (C-6), 127.5 (C-13, C-13′), 126.4 (C-15), 126.3 (C-2), 119.4 (C-3a), 106.6 (C-5), 105.1 (C-3), 101.2 (C-7), 70.0 (C-11), 61.0 (C-9), 14.2 (C-10); **HRMS-TOF MS ES+: *m/z* [M+H]$^+$** calculated for $C_{18}H_{18}NO_3$: 296.1287; found: 296.1283. This corresponds well with the reported values.[62,81,101]

Ethyl 4-hydroxy-1*H*-indole-2-carboxylate (9).[130]

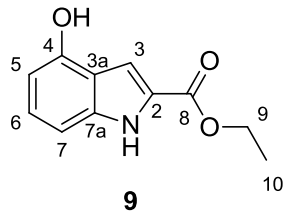

9

Ethyl 4-(benzyloxy)-1*H*-indole-2-carboxylate **7** (456 mg, 1.54 mmol) was added to a 25 mL, round-bottom flask containing a mixture of MeOH (5.0 mL) and nickel(II) chloride hexahydrate (299 mg, 2.31 mmol) at 0 ºC. Sodium borohydride (174 mg, 4.62 mmol) was added to the stirring reaction mixture and left to stir for 10 minutes. The reaction was monitored by TLC until the all the starting material was consumed. On completion, the reaction mixture was quenched with MeOH (10 mL) and stirred for a further 20 minutes and filtered through Celite. The collected methanol was concentrated in vacuo to afford the crude product as a black residue which was purified by flash chromatography (R_f = 0.20, 15% EtOAc/Hex) and yielded the product as a white powder (221 mg, 1.08 mmol, 70%).

Mp 159.0 – 161.3 °C; **IR (ATR,cm^{-1})** 3420 (O-H str.), 3063, 3025, 3006, 2946, 2915, 1686 (N-H str.), 1599 (N-H bend), 1589, 1492, 1450, 1417, 1386, 1361, 1283, 1235 (C-O str.), 1209, 1183, 1165, 1114, 1080, 1062, 1043, 1027, 754, 736, 696; **^{1}H NMR (600 MHz, $CDCl_3$) δ** 8.90 (br s, 1H, NH), 7.34 (s, 1H, H-3), 7.19-7.15 (m, 1H, H-6), 7.01 (d, J^3 = 8.3 Hz, 1H, H-7), 7.50-6.54 (m, 1H, H-5), 5.31 (br s, 1H, OH), 4.41 (q, J^3 = 7.1 Hz, 2H, H-9) 1.42 (t, J^3 = 7.1 Hz, 3H, H-10); **^{13}C NMR (150 MHz, $CDCl_3$) δ** 161.9 (C-8), 150.4 (C-4), 138.7 (C-7a), 126.7 (C-2), 126.5 (C-6), 118.1 (C-3a), 105.5 (C-3), 104.8 (C-5), 104.6 (C-7), 61.2 (C-9), 14.5 (C-10); **HRMS-TOF MS ES+: *m/z* [M+H]$^+$** calculated for $C_{11}H_{12}NO_3$: 206.0818; found: 206.0848. This corresponds well with the reported values.[62]

4-(benzyloxy)-1*H*-indole-2-carboxylic acid (11).[54,58,62]

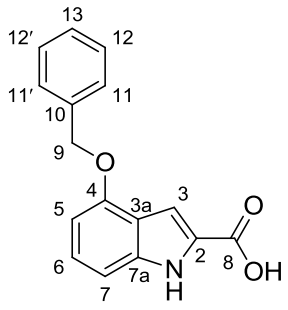

11

To a 20 mL, two-neck, round-bottom flask was added methanol (1.5 mL), THF (4.5 mL) and ethyl 4-(benzyloxy)-*1H*-indole-2-carboxylate (500 mg, 1.69 mmol). The mixture was stirred at room temperature until the indole had completely dissolved. In a separate 10 mL glass vial, lithium hydroxide (89.2 mg, 3.72 mmol) was dissolved in water (2.5 mL) and was added dropwise to the stirring reaction mixture. Once the solution was added, the flask was equipped with a condenser, flushed with nitrogen and the flask sealed. The reaction mixture was heated to 60 ºC and left to stir for 12 hours. On completion, the reaction was cooled to room temperature, transferred to a 50 mL beaker with a minimal amount of water and the solution acidified with 2N HCl solution (10 mL) to a pH of ~2. The precipitate that formed was removed by filtration and washed with H_2O (2 × 20 mL), then dried in a vacuum desiccator to give the product as a pale-brown solid (280 mg, 10.5 mmol, 62%). Used without further purification.

Mp 244.8 – 247.9 °C; **IR (ATR,cm^{-1})** 3320 (N-H str.), 3033 (br, O-H str.), 2914, 2864, 1686 (C=O str.), 1620, 1583, 1516, 1443 (O-H bend), 1428, 1364, 1257 (C-O str.), 1234, 1197 (ether C-O-C str.), 1120, 1083, 827, 779, 746, 695, 631; **^{1}H NMR (400 MHz, CDCl$_3$) δ** 11.77 (br s, 1H, COOH), 7.51 (d, J^3 = 7.2 Hz, 2H, H-11, H-11′), 7.44-7.38 (m, 2H, H-12, 1H-2′), 7.36-7.30 (m, 1H, H-13), 7.17-7.11 (m, 1H, H-6), 7.10-7.07 (m, 1H, H-3), 7.02 (d, J^3 = 8.3 Hz, 1H, H-7), 6.62 (d, J^3 = 7.6 Hz, 1H, H-5), 5.23 (s, 2H, H-9); **^{13}C NMR (101 MHz, CDCl$_3$) δ** 162.6 (C-8), 152.6 (C-4), 138.6 (C-7a), 137.3 (C-10), 128.4 (C-12, C-12′), 127.7 (C-12), 127.3 (C-11, C-11′), 127.1 (C-6), 125.3 (C-2), 118.3 (C-3a), 105.6 (C-5), 104.5 (C-3), 100.8 (C-7), 69.0 (C-9); **HRMS-TOF MS ES+: *m/z* [M+H]$^+$** calculated for $C_{16}H_{14}NO_3$: 268.0974; found: 268.0966. This corresponds well with the reported values.[131]

6.3 EXPERIMENTAL DATA PERTAINING TO CHAPTER 3

6.3.1 Synthesis of Diethyl 2-(((3-X-phenyl)amino)methylene)malonate (X = Br, F, NO_2, CH_3 and OCH_3)

General Procedure[140,141,145]

In a round-bottom flask, 3-X-aniline (1 equivalent, X = F, Br, NO_2, CH_3 or OCH_3) was added to a minimum amount of ethanol to dissolve the aniline. While stirring, diethyl ethoxymethylenemalonate (1.1 to 1.3 equivalents) was added to the reaction mixture in a single portion and the reaction mixture heated to 110 ºC for 1 hour, leaving the flask open to allow ethanol to evaporate from the reaction flask. The temperature was then increased to 140 ºC and the reaction left to stir for a further 1 – 2 hours, monitoring completion by TLC. On completion, the reaction mixture was cooled to room temperature and purified either by automated gradient column chromatography (0 – 100% EtOAc/Hex) or conventional flash chromatography (15 – 20% EtOAc/Hex). The products were obtained as crystalline solids, varying in color, with yields ranging from 70 – 95%.

Diethyl 2-{[(3-bromophenyl)amino]methylene}malonate (15a).[140,141,145]

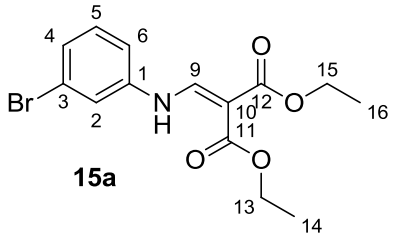

15a

The general procedure described above was followed using 3-bromoaniline (1.00 mL, 1.58 g, 9.19 mmol), 96% ethanol (2.0 mL) and diethyl diethoxymethylenemalonate (2.02 mL, 2.18 g, 10.1 mmol). The reaction mixture was heated for 1 hour at 110 °C and then at 140 °C for 2 hours which on completion, was cooled

to room temperature. The mixture was purified by automated chromatography as described in the general procedure (R_f = 0.26, 15% EtOAc/Hex) and the product was obtained as a white to pale pink crystalline material (2.88 g, 8.41 mmol, 92%).

Mp 61.1 – 62.6 °C; **IR (ATR, cm^{-1})** 3150 (N-H str.), 2984, 2901, 1681 (C=O str.), 1640, 1610, 1587 (N-H bend), 1477, 1457, 1405, 1386, 1345, 1239 (C-O str.), 1119, 1093, 1071, 1026, 993, 975, 859, 799 (2° N-H wag), 769, 672 (C-Br str.); **^{1}H NMR (600 MHz, $CDCl_3$) δ** 10.96 (d, J^3 = 13.2 Hz, 1H, NH), 8.43 (d, J^3 = 13.4 Hz, 1H, H-9), 7.29 (s, 1H, H-2), 7.25 (s, 1H, H-6), 7.21 (t, J^3 = 7.9 Hz, 1H, H-5), 7.04 (d, J^3 = 1.2 Hz, J^4 = 7.9 Hz, 1H, H-4), 4.29 (q, J^3 = 7.1 Hz, 2H, H-13), 4.24 (q, J^3 = 7.1 Hz, 2H, H-15), 1.36 (t, J^3 = 7.1 Hz, 3H, H-14), 1.32 (t, J^3 = 7.1 Hz, 3H, H-14); **^{13}C NMR (151 MHz, $CDCl_3$) δ** 169.1 (C-11), 165.6 (C12), 151.3 (C-9), 140.7 (C-3), 131.2 (C-5), 127.8 (C-2), 123.7 (C-1), 120.2 (C-6), 115.9 (C-4), 94.9 (C-10), 60.7 (C-13), 60.4 (C-15), 14.5 (C-14), 14.4 (C-16); **HRMS-TOF MS ES+: *m/z* [M+H]$^+$** calculated for $C_{14}H_{17}BrNO_4$: 342.0341; found: 342.0336. This corresponds well with the reported values.[192]

Diethyl 2-{[(3-fluorophenyl)amino]methylene}malonate (15b).[140,141,145]

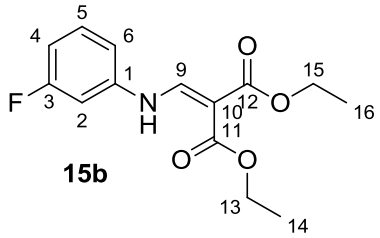

15b

The general procedure described above was followed using 3-fluoroaniline (0.220 mL, 0.250 g, 2.25 mmol), 96% ethanol (2.0 mL) and diethyl diethoxymethylenemalonate (0.50 mL, 0.53 g, 2.48 mmol). The reaction mixture was heated for 1 hour at 110 °C and then at 140 °C for 1 hour, which on completion, was cooled to room temperature. The mixture was purified by automated chromatography as described in the general procedure (R_f = 0.51, 15% EtOAc/Hex) and the product was obtained as a white crystalline material (0.54 g, 1.9 mmol, 84%).

Mp 47.3 – 48.7 °C; **IR (ATR, cm^{-1})** 3177 (N-H str.), 2984, 2930, 2904, 1682 (C=O str.) , 1637, 1606, 1582 (N-H bend), 1496, 1475, 1459, 1425, 1384, 1373, 1343, 1247 (C-O str.), 1219, 1167, 1144, 1100, 1019, 1001, 980, 966, 833, 799 (2° N-H wag), 776, 677; **^{1}H NMR (600 MHz, $CDCl_3$) δ** 10.98 (d, J^3 = 13.3 Hz, 1H, NH), 8.44 (d, J^3 = 13.5 Hz, 1H, H-9), 7.33-7.27 (m, 1H, H-5), 6.88 (dd, J^3 = 8.0 Hz, J^4 = 1.8 Hz, 1H, H-6), 6.86 – 6.79 (m, 2H, H-2, H-4), 4.29 (q, J^3 = 7.1 Hz, 2H, H-13), 4.24 (q, J^3 = 7.1 Hz, 2H, H-15), 1.36 (t, J^3 = 7.1 Hz, 3H, H-14), 1.32 (t, J^3 = 7.1 Hz, 3H, H-14); **^{13}C NMR (151 MHz, $CDCl_3$) δ** 168.9 (C-11), 165.5 (C-12), 164.5 (C-3), 162.9 (C-9) 151.3 (C-1), 131.3 (C-5), 112.9 (C-4), 111.5 (C-2), 104.5 (C-6), 94.6 (C-10), 60.6 (C-13), 60.3 (C-15), 14.4 (C-14), 14.3 (C-16); **HRMS-TOF MS ES+: *m/z* [M+H]$^+$** calculated for $C_{14}H_{17}FNO_4$: 282.1142; found: 282.1141. This corresponds well with the reported values.[144]

Diethyl 2-{[(3-nitrophenyl)amino]methylene}malonate (15c).[140,141,145]

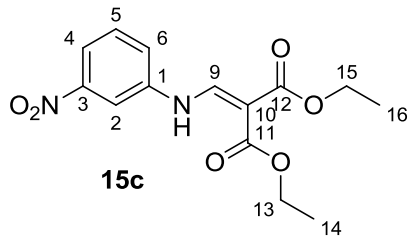

The general procedure described above was followed using 3-nitroaniline (6.00 g, 43.4 mmol), 96% ethanol (15.0 mL) and diethyl diethoxymethylenemalonate (11.3 mL, 12.2 g, 56.5 mmol). The reaction mixture was heated for 1 hour at 100 °C and then at 140 °C for another hour, which on completion, was cooled to room temperature. The mixture was purified by automated chromatography as described in the general procedure (R_f = 0.17, 10% EtOAc/Hex) to afford the desired product as a fine yellow crystalline material (11.12 g, 36.1 mmol, 83%).

Mp 81.3 – 83.6 °C; **IR (ATR, cm^{-1})** 3182 (N-H str.), 2985, 2905, 1677 (C=O str.), 1643, 1602, 1576, 1533 (N-O asym. str.), 1477, 1427, 1391, 1376, 1345 (N-O sym. str.), 1281, 1257, 1235 (C-O str.), 1123, 1097, 1021, 977, 946, 864, 797 (2° N-H wag), 787, 734; **^{1}H NMR (600 MHz, $CDCl_3$) δ** 11.17 (d, J^3 = 13.2 Hz, 1H, NH), 8.51 (d, J^3 = 13.2 Hz, 1H, H-9), 8.02-7.96 (m, 2H, H_2, H-4), 7.55 (t, J^3 = 8.1 Hz, 1H, H-6), 7.43 (dd, J^3 = 8.0 Hz, J^4 = 1.8 Hz, 1H, H-5), 4.32 (q, J^3 = 7.1 Hz, 2H, H-13), 4.28 (q, J^3 = 7.1 Hz, 2H, H-15), 1.38 (t, J^3 = 7.1 Hz, 3H, H-14), 1.34 (t, J^3 = 7.1 Hz, 3H, H-14); **^{13}C NMR (151 MHz, $CDCl_3$) δ** 168.9 (C-11), 165.3 (C-12), 150.7 (C-9) 149.5 (C-3), 140.7 (C-1), 130.9 (C-5), 122.7 (C-4), 119.6 (C-6), 111.6 (C-2), 96.2 (C-10), 60.9 (C-13), 60.6 (C-15), 14.5 (C-14), 14.3 (C-16); **HRMS-TOF MS ES+: *m/z* [M+H]$^+$** calculated for $C_{14}H_{17}N_2O_6$: 309.1087; found: 309.1089. This corresponds well with the reported values.[138,139]

Diethyl 2-[(3-methylamino)methylene]malonate (15d).[140,141,145]

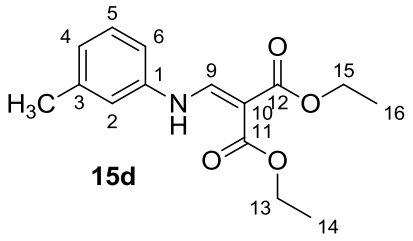

The general procedure described above was followed using 3-bromoaniline (1.00 mL, 1.58 g, 9.19 mmol), 96% ethanol (2.00 mL) and diethyl diethoxymethylenemalonate (2.02 mL, 2.18 g, 10.1 mmol). The reaction mixture was heated for 1 hour at 110 °C and then at 140 °C for 2 hours, which on completion, was cooled to room temperature. The mixture was purified by automated chromatography as described in the general procedure (R_f = 0.26, 15% EtOAc/Hex) and the product was obtained as a white crystalline material (2.88 g, 8.41 mmol, 92%).

Mp 40.4 – 41.9 °C; **IR (ATR, cm^{-1})** 3258, 3209 (N-H str.), 3181, 3052, 2985 (sp^3 C-H str.), 2908, 1682 (C=O str.), 1638, 1612, 1581, 1495, 1478, 1445, 1406, 1384, 1347, 1316, 1302, 1243 (C-O str.), 1226, 1167, 1117, 1097, 1031, 1019, 982, 929, 885, 863, 818, 801 (N-H wag), 760, 683;**^{1}H NMR (600 MHz, $CDCl_3$) δ** 10.96 (d, J^3 = 13.5 Hz, 1H, NH), 8.52 (d, J^3 = 13.7 Hz, 1H, H-9), 7.24 (t, J^3 = 7.6 Hz, 1H, H-5), 6.98-6.91 (m, 3H, H-2, H-4, H-6), 4.30 (q, J^3 = 7.1 Hz, 2H, H-13), 4.25 (q, J^3 = 7.1 Hz, 2H, H-15), 2.36 (s, 3H, H-8), 1.37 (t, J^3 = 7.1 Hz, 3H, H-14), 1.33 (t, J^3 = 7.1 Hz, 3H, H-14); **^{13}C**

NMR (151 MHz, $CDCl_3$) δ 169.1 (C-11), 165.9 (C-12), 152.0 (C-9), 140.0 (C-1), 139.3 (C-3), 129.7 (C-5), 125.8 (C-2), 117.9 (C-6), 114.3 (C-4), 93.4 (C-10), 60.4 (C-13), 60.1 (C-15), 21.5 (C-7) 14.5 (C-14), 14.4 (C-16); **HRMS-TOF MS ES+: *m/z* [M+H]$^+$** calculated for $C_{15}H_{20}NO_4$: 278.1392; found: 278.1400. This corresponds well with the reported values.[138,193,194]

Diethyl 2-{[(3-methoxyphenyl)amino]methylene}malonate (15e).[140,141,145]

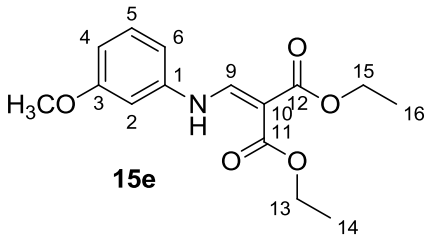

15e

The general procedure described above was followed using *m*-anisidine (1.00 mL, 1.10 g, 8.93 mmol), 96% ethanol (2.00 mL) and diethyl diethoxymethylenemalonate (1.97 mL, 2.12 g, 9.83 mmol). The reaction mixture was heated for 30 minutes at 110 °C and then at 140 °C for 2 hours, which on completion, was cooled to room temperature. The mixture was purified by automated chromatography as described in the general procedure (R_f = 0.16, 15% EtOAc/Hex) and the product was obtained as a white solid (2.37 g, 8.08 mmol, 91%).

Mp 44.9 – 45.9 °C; **IR (ATR, cm^{-1})** 3201 (N-H str.), 2979, 2935, 2904, 1715 (C=O str.), 1689, 1650, 1584, 1497, 1464, 1442, 1412, 1376, 1348, 1293, 1246, 1211 (C-O str.), 1151, 1070 (C-O str.), 1029, 984, 959, 941, 798 (N-H wag), 766, 732, 683; **^{1}H NMR (600 MHz, $CDCl_3$) δ** 11.58 (d, J^3 = 13.5 Hz, 1H, NH), 9.11 (d, J^3 = 13.6 Hz, 1H, H-9), 7.87 (t, J^3 = 8.0 Hz, 1H, H-5), 7.33 (dd, J^3 = 7.9 Hz, J^4 = 1.9 Hz, 1H, H-6), 7.30 (dd, J^3 = 8.2 Hz, J^4 = 2.3 Hz, 1H, H-4), 7.26 (s, 1H, H-2), 4.92 (q, J^3 = 7.1 Hz, 2H, H-13), 4.85 (q, J^3 = 7.1 Hz, 2H, H-15), 4.42 (s, 3H, H-8), 1.99 (t, J^3 = 7.1 Hz, 3H, H-14), 1.93 (t, J^3 = 7.1 Hz, 3H, H-14); **^{13}C NMR (151 MHz, $CDCl_3$) δ** 171.6 (C-11), 168.3 (C-12), 163.5 (C-3), 154.4 (C-9), 143.0 (C-3), 133.2 (C-5), 112.8 (C-6), 112.0 (C-4), 105.9 (C-2), 96.2 (C-10), 62.9 (C-13), 62.7 (C-15), 58.0 (C-7), 17.0 (C-14), 16.9 (C-16); **HRMS-TOF MS ES+: *m/z* [M+H]$^+$** calcd for $C_{15}H_{20}NO_5$: 294.1341; found: 294.1350. This corresponds well with the reported values.[138]

6.3.2 Synthesis of 7-X-4-chloroquinoline – Gould-Jacobs Method (X = Br, F, NO_2, CH_3 and OCH_3)

General Procedure[140,141,145]

To a 250 mL round-bottom flask was added 150 mL of diphenyl ether, boiling chips and the respective 2-(((3-X-phenyl)amino)methylene)malonate (1 equivalent) (X = F, Br, NO_2, CH_3 or OCH_3). The flask was placed in a 250 mL heating mantle and the reaction mixture heated to 260 ºC for 2 hours or until completion of the reaction was observed by TLC (15% EtOAc/Hex). On completion, the mantle was removed and the flask left to cool to room temperature with the condenser

still attached. During cooling, the respective ethyl 7-X-4-hydroxyquinoline-3-carboxylate precipitated out of the solution and once the solution had reached room temperature, hexane was added to the flask to avoid solidification of the diphenyl ether and allow for further precipitation to occur. The precipitate was collected by filtration and the filtrate repeatedly washed with 6 × 100 mL portions of hexane to remove excess diphenyl ether. The crude product was transferred to a 250 mL round-bottom flask containing an excess of 2 M sodium hydroxide solution (160 mL) and thoroughly stirred under reflux at 125 ºC for 4 – 6 hours. The reaction was tested for completion after 3 hours by TLC (50% EtOAc/Hex), visualizing the TLC plate with bromo-cresol green (carboxylic acid stain) to identify the 7-X-4-hydroxyquinoline-3-carboxylic acid products. On completion, the reaction mixture was cooled to room temperature and the pH adjusted to ~4 with 2 M hydrochloric acid that formed the product as a thick white suspension that was collected by filtration. The product was washed once with 100 mL water and completely dried in an oven on the filter paper in a crucible at 75 ºC. Note: All traces of water must be removed to avoid any extremely hazardous exothermic reactions in the next step. The thoroughly dried 7-X-4-hydroxyquinoline-3-carboxylic acid was cooled to room temperature and broken into pieces small enough to fall down the inside of a B29 condenser into a flask that contained refluxing diphenyl ether (Note: highly exothermic reaction occurs on addition of the pieces to the boiling ether). After the addition was completed the reaction mixture was left to reflux for 2 hours and cooled to room temperature resulting in the 7-X-quinolin-4ol product forming as a fine precipitate. Once the ether had cooled, hexane was added to the flask to dilute the ether and avoid solidification and at the same time increase precipitation of the product. The precipitate was collected by filtration and washed with 6 × 100 mL portions of hexane to remove excess diphenyl ether. The crude product was then added to a 25 mL, 2-neck, round-bottom flask equipped with a condenser, the side neck sealed and the flask cooled to 0 ºC in an ice bath. Cold phosphorous oxychloride (8 equivalents) was added dropwise to the stirring quinolin-4-ol after which the ice bath was removed and the flask heated to 140 ºC under reflux for 4 hours. With the condenser still attached, the reaction mixture was cooled to -10 ºC and ammonium hydroxide solution was slowly added to the flask via the side neck (Note: extremely exothermic reaction and gas formation) to neutralize the remaining $POCl_3$. Once gas formation has ceased, a minimal amount of cold water was used to transfer the aqueous mixture to a 100 mL beaker and an extra 25 mL of ammonium hydroxide solution was added. The aqueous mixture was extracted with 3 × 70 mL EtOAc and the organic layers combined, washed with a single portion of 100 mL brine and dried over anhydrous magnesium sulfate. The magnesium sulfate was filtered off and the collected organic solvent concentrated *in vacuo*. The resulting 7-X-4-chloroquinoline compounds were obtained as semi-pure oils or solids and purified by automated linear-gradient column chromatography (0 – 100% EtOAc/Hex) that gave the pure compounds as crystalline materials varying in color and yield (29 – 75%).

7-Bromo-4-chloroquinoline (19a).[140,141,145]

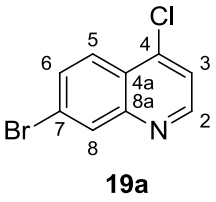

19a

The general procedure described above was followed using diethyl 2-(((3-bromophenyl)amino)methylene)malonate (1.00 g, 2.93 mmol) as starting material and phosphorous oxychloride (2.17 mL, 3.59 g, 23.4 mmol). The mixture was purified as mentioned in general procedure (R_f = 0.45, 15% EtOAc/Hex) and the product was obtained as a fine off-white crystalline material (0.38 g, 1.6 mmol, 54%).

Mp 106.1 – 106.9 °C; **IR (ATR, cm^{-1})** 3874, 3845, 3822, 3789, 3670, 3626, 3603, 3556, 3078, 3052, 2924, 2268, 1602, 1579, 1550, 1483, 1406, 1343, 1294, 1287 (C-N arom. Str.), 1059, 970, 877, 862, 844, 813 (C-Cl str.), 673, 636 (C-Br stch); **^{1}H NMR (600 MHz, $CDCl_3$) δ** 8.78 (d, J^3 = 4.7 Hz, 1H, H-2), 8.31 (d, J^3 = 1.9 Hz, 1H, H-8), 8.10 (d, J^3 = 8.9 Hz, 1H, H-5), 7.73 (dd, J^3 = 8.9 Hz, J^4 = 1.9 Hz, 1H, H-6), 7.50 (d, J^3 = 4.7 Hz, 1H, H-3); **^{13}C NMR (151 MHz, $CDCl_3$) δ** 151.0 (C-2), 149.8 (C-8a), 142.9 (C-4), 132.2 (C-8), 131.3 (C-6), 125.7 (C-4a), 125.4 (C-7), 124.9 (C-5), 121.7 (C-3); **HRMS-TOF MS ES+: *m/z* [M+H]$^+$** calculated for C_9H_6BrClN: 241.9372; found: 241.9373. This corresponds well with the reported values.[195,196]

4-Chloro-7-fluoroquinoline (19b).[140,141,145]

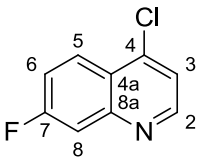

19b

The general procedure described above was followed using diethyl 2-(((3-fluorophenyl)amino)methylene)malonate (2.00 g, 7.11 mmol) and phosphorous oxychloride (5.29 mL, 8.72 g, 56.8 mmol). The mixture was purified by column chromatography as described in the general procedure (R_f = 0.41, 15% EtOAc/Hex) and was obtained as a white crystalline material (0.89 g, 4.9 mmol, 69%).

Mp 74.5 – 75.3 °C; **IR (ATR, cm^{-1})** 3097, 3071, 3046, 2991, 2920, 2849, 1625, 1566, 1497, 1454, 1414, 1367, 1340, 1298 (C-F str.), 1273, 1239, 1222, 1193, 1145, 1125, 1117, 979, 947, 861, 839, 815 (C-Cl str.), 670, 642; **^{1}H NMR (400 MHz, $CDCl_3$) δ** 8.76 (d, J^3 = 4.7 Hz, 1H, H-2), 8.22 (dd, J^3 = 9.2 Hz, J^4 = 5.9 Hz, 1H, H-8), 7.74 (dd, J^3 = 9.7 Hz, J^4 = 2.5 Hz, 1H, H-5), 7.44 (d, J^3 = 4.6 Hz, 1H, H-3), 7.44-7.38 (m, 1H, H-6); **^{13}C NMR (101 MHz, $CDCl_3$) δ** 163.6 (C-7), 151.1 (C-2), 150.3 (C-8a), 142.8 (C-4), 126.6 (C-5), 123.7 (C-4a), 120.7 (C-3), 118.2 (C-6), 113.6 (H-8); **HRMS-TOF MS ES+: *m/z* [M+H]$^+$** calculated for C_9H_6ClFN: 182.0173; found: 182.0180. This corresponds well with the reported values.[197,198]

4-Chloro-7-nitroquinoline (19c).[140,141,145]

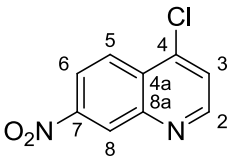

19c

The general procedure described above was followed using diethyl 2-(((3-nitrophenyl)amino)methylene)malonate (1.00 g, 3.24 mmol) and phosphorous oxychloride (2.41 mL, 3.97 g, 25.9 mmol). The mixture was purified by automated column chromatography as described in the general procedure (R_f = 0.32, 15% EtOAc/Hex) and was obtained as a yellow crystalline material (0.13 g, 0.61 mmol, 19%).

Mp 174.3 – 175.3°C; **IR (ATR, cm^{-1})** 3093, 1583, 1570, 1512 (N-O asym. str.), 1444, 1366, 1342 (N-O sym str.), 1293, 1241, 1190, 1081, 1055, 977, 924, 908, 849, 831, 805, 739 (C-Cl str.), 682; **^{1}H NMR (300 MHz, $CDCl_3$) δ** 9.05-9.02 (m, 1H, H-6), 8.98-8.94 (m, 1H, H-2), 8.44-8.41 (m, 2H, H-5, H-8), 7.68 (d, J^3 = 4.6 Hz, 1H, H-3); **^{13}C NMR (75 MHz, $CDCl_3$) δ** 152.3 (C-7), 148.4 (C-8a), 143.0 (C-4), 129.8 (C-4a), 126.4 (C-5), 126.2 (C-3), 123.9 (C-6), 121.1 (C-8); **HRMS-TOF MS ES+: *m/z* [M+H]$^+$** calculated for $C_9H_6ClN_2O_2$: 209.0116; found: 209.0120. This corresponds well with the reported values.[138,139]

4-Chloro-7-methylquinoline (19d).[140,141,145]

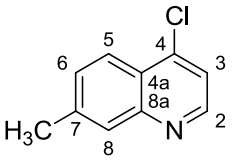

19d

The general procedure described above was followed using diethyl 2-((3-*m*-tolylamino)methylene)malonate (1.00 g, 3.60 mmol) and phosphorous oxychloride (2.68 mL, 4.42 g, 28.8 mmol). The mixture was purified by automated column chromatography as described in the general procedure (R_f = 0.24, 15% EtOAc/Hex) and was obtained as an orange oil (383 mg, 1.58 mmol, 54%).

Mp 23.5 – 26.1°C; **IR (ATR, cm^{-1})** 3049 (sp^3 C-H str.), 2975, 2917, 1626, 1582, 1556, 1498 (C-C arom str.), 1457, 1418, 1368, 1346, 1300, 1194, 1146, 975, 883, 813 (C-Cl str.), 773, 707, 670, 634; **^{1}H NMR (400 MHz, $CDCl_3$) δ** 8.72 (d, J^3 = 4.7 Hz, 1H, H-2), 8.10 (d, J^3 = 8.5 Hz, 1H, H-5), 7.89 (s, 1H, H-8), 7.46 (dd, J^3 = 8.5 Hz, 1H, H-6), 7.40 (d, J^3 = 4.7 Hz, 1H, H-3), 2.57 (s, 3H, CH_3); **^{13}C NMR (101 MHz, $CDCl_3$) δ** 149.9 (C-2), 149.5 (C-8a), 142.5 (C-4), 141.0 (C-7), 129.9 (C-6), 128.8 (C-8), 124.6 (C-4a), 123.9 (C-5), 120.5 (C-3), 21.8 (C-9); **HRMS-TOF MS ES+: *m/z* [M+H]$^+$** calculated for $C_{10}H_9ClN$: 178.0424; found: 178.0429. This corresponds well with the reported values.[138]

4-Chloro-7-methoxyquinoline (19e).[140,141,145]

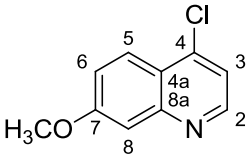

19e

The general procedure described above was followed using diethyl 2-(((3-methoxyphenyl)amino)methylene)malonate (1.00 g, 3.40 mmol) and phosphorous oxychloride (2.53 mL, 4.18 g, 27.2 mmol). The mixture was

purified by purified by automated column chromatography as described in the general procedure (R_f = 0.13, 15% EtOAc/Hex) and the product was obtained as a light brown powder (0.38 g, 1.96 mmol, 57%).

Mp 85.9-86.8 °C; **IR (ATR, cm^{-1})** 3145, 3097, 3064, 3015, 2988, 1623, 1583, 1562, 1501, 1467, 1438, 1418, 1343, 1308, 1259, 1230, 1195, 1161, 1129, 1022 (C-O str.), 971, 937, 844, 814 (C-Cl str.), 677; **^{1}H NMR (600 MHz, $CDCl_3$) δ** 8.68 (d, J^3 = 4.7 Hz, 1H, H-2), 8.10 (d, J^3 = 9.2 Hz, 1H, H-5), 7.42 (d, J^3 = 2.5 Hz, 1H, H-8), 7.33 (d, J^3 = 4.7 Hz, 1H, H-3), 7.28 (dd, J^3 = 9.2 Hz, J^4 = 2.5 Hz 1H, H-6), 3.96 (s, 3H, OCH_3); **^{13}C NMR (151 MHz, $CDCl_3$) δ** 161.4 (C-7), 151.1 (C-2), 150.3 (C-8a), 142.7 (C-4), 125.4 (C-5), 121.7 (C-4a), 120.9 (C-6), 119.3 (C-3), 107.7 (C-8), 55.7 (C-9); **HRMS-TOF MS ES+: *m/z* [M+H]$^+$** calculated for $C_{10}H_9ClNO$: 194.0373; found: 194.0379. This corresponds well with the reported values.[138,199]

6.3.3 Synthesis of 7-X-4-derivative-quinoline - Skraup Method (X = Br, CH_3 and OCH_3,)

General procedure[155,165]

A 25 mL, 2-neck, round-bottom flask was placed in an oven at 75 ºC for 30 minutes, removed and set up over a 140 ºC oil bath and a stirbar added. Glycerol (2-3 equivalents) was added to the flask and left to warm slightly by the residual heat in the glass to make it less viscous. Concentrated sulfuric acid (96% H_2SO_4, 5 equivalents) was added to the stirring glycerol in a single portion over 30 seconds and a condenser connected to the flask. The side neck was sealed with a rubber septum and the flask lowered into the oil bath and the *m*-substituted aniline (Br, CH_3 and OCH_3) injected into the thoroughly-stirring reaction mixture over 30 seconds. The reaction was left to stir for 30 seconds to allow the aniline to be fully mixed into the glycerol/acid mixture. The rubber septum was removed and iron(II) sulfate heptahydrate (0.07 equivalents) in a quickly single portion and the stopper returned to close the neck. The reaction mixture was stirred until it was observed that all of the iron(II) sulfate heptahydrate had dissolved, at which point nitrobenzene (1.1 equivalents) was slowly injected into the mixture. It should be noted that an exothermic reaction occurs and a gas develops in the flask and condenser. 5 – 10 minutes after adding the nitrobenzene, the reaction turned black and the mixture was left to stir at 140 ºC under reflux for 1 – 4 hours. Completion of the reaction was monitored by TLC whereby a few drops of reaction mixture was diluted with the same amount of water and neutralized with 5M NaOH solution. One milliliter of DCM was added and gently shaken to extract the products followed by TLC analysis using 15% EtOAc/Hex as a solvent system. On completion, the reaction was cooled to room temperature. The mixture was diluted with 70 mL of

water and basified with 5M NaOH until the solution had turned from black to a milky brown and a precipitate was suspended in the solution. The solution was carefully extracted using 6 × 100 mL of DCM and the organic layers combined and washed with a single portion (200 mL) of water followed by the same amount of brine. The DCM solution was dried over anhydrous magnesium sulfate, collected by filtration and concentrated *in vacuo* to give the crude product as a dark brown to black oil. The product was purified by column chromatography (30% EtOAc/Hex) and afforded the products as oils with varying colours in yields of 16 – 63%.

7-Bromoquinoline (23a).[155,165]

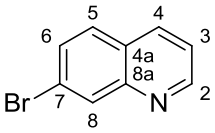

23a

The general procedure described above was followed using 3-bromoaniline (1.89 mL, 3.00 g, 17.4 mmol), 99.5% glycerol (3.26 mL, 4.01 g, 43.6 mmol), 96% sulfuric acid (4.65 mL, 8.55 g, 87.2 mmol), nitrobenzene (1.97 mL, 2.36 g, 19.2 mmol) and iron(II)sulfate heptahydrate (0.34 g, 1.2 mmol). The mixture was purified as described in the general procedure and the product (R_f = 0.13, 100% EtOAc) was obtained as a red-brown oil (0.57 g, 2.7 mmol, 16%).

IR (ATR, cm^{-1}) 3063, 2984, 1610, 1587, 1567, 1486 (C-C in-ring str.), 1445, 1428, 1379, 1311 (C-N str.), 1142, 1125, 1053, 1035, 937, 877, 847, 829, 778, 766 (C-H oop), 633 (C-Br str.); **^{1}H NMR (400 MHz, $CDCl_3$) δ** 8.91 (dd, J^3 = 4.2 Hz, J^4 = 1.6 Hz 1H, H-2), 8.29 (d, J^4 = 1.7 Hz, 1H, H-8), 8.12 (dd, J^3 = 8.3 Hz, J^4 = 0.9 Hz, 1H, H-4), 7.68 (d, J^3 = 8.6 Hz, 1H, H-5), 7.62 (dd, J^3 = 8.6 Hz, J^4 = 1.8 Hz 1H, H-6), 7.41 (dd, J^3 = 8.6 Hz, J^4 = 1.8 Hz 1H, H-3); **^{13}C NMR (101 MHz, $CDCl_3$) δ** 151.4 (C-2), 148.9 (C-8a), 136.0 (C-4), 131.9 (C-8), 130.2 (C-6), 129.1 (C-5), 126.9 (C-4a), 123.6 (C-7), 121.5 (C-3); **HRMS-TOF MS ES+: *m/z* [M+H]$^+$** calculated for C_9H_7BrN: 207.9762; found: 207.9756. This corresponds well with the reported values.[201,202]

7-Methylquinoline (23d).[155,165]

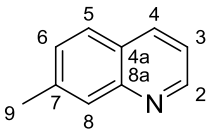

23d

The general procedure described above was followed using *m*-toluidine (0.99 mL, 1.0 g, 9.3 mmol), 99.5% glycerol (1.39 mL, 1.72 g, 18.7 mmol), 96% sulfuric acid (2.48 mL, 4.57 g, 46.7 mmol), nitrobenzene (0.96 mL, 1.15 g, 9.33 mmol) and iron(II)sulfate heptahydrate (0.16 g, 0.56 mmol). The mixture was purified as described in the general procedure and the product (R_f = 0.23, 12% EtOAc/Hex) was obtained as a light brown oil (0.83 g, 5.79 mmol, 63%).

IR (ATR, cm^{-1}) 3360 (sp^3 C-H str.) , 3050, 2971, 1699, 1626, 1595, 1573, 1502 (C-C in-ring str.), 1459, 1361, 1318 (C-N str.), 1146, 1120, 832, 803, 785, 771, 638, 613; **^{1}H NMR (400 MHz, $CDCl_3$) δ** 8.86 (dd, J^3 = 4.2 Hz, J^4 = 1.7 Hz 1H, H-2), 8.05 (dd, J^3 = 8.2 Hz, J^4 = 1.6 Hz, 1H, H-4), 7.89 (d, J^3 = 8.6 Hz, 1H, H-8), 7.67 (d, J^3 = 8.6 Hz, 1H, H-5), 7.34 (dd, J^4 = 8.4 Hz, J^4 = 1.8 Hz, 1H, H-6), 7.29

(m, 1H, H-3), 2.54 (s, 3H, H-9); **^{13}C NMR (101 MHz, $CDCl_3$) δ** 150.3 (C-2), 149.9 (C-8a), 139.6 (C-7), 135.6 (C-4), 128.7 (C-8), 128.4 (C-6), 127.4 (C-5), 126.9 (C-4a), 120.2 (C-3), 21.8 (C-9); **HRMS-TOF MS ES+: *m/z* [M+H]$^+$** calculated for $C_{10}H_{10}N$: 144.0813; found: 144.0806. This corresponds well with the reported values.[136,203,204]

7-Methoxyquinoline (23e).[155,165]

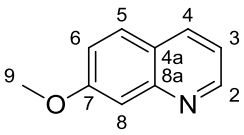

23e

The general procedure described above was followed using *m*-anisidine (1.82 mL, 2.00 g, 16.2 mmol), 99.5% glycerol (2.4 mL, 2.99 g, 32.5 mmol), 96% sulfuric acid (4.5 mL, 8.21 g, 81.2 mmol), nitrobenzene (2.00 mL, 2.40 g, 19.5 mmol) and iron(II)sulfate heptahydrate (0.28 g, 0.97 mmol). The mixture was purified as described in the general procedure and the product (R_f = 0.20, 30% EtOAc/Hex) was obtained as a brown oil (0.67 g, 4.24 mmol, 26%).

IR (ATR, cm^{-1}) 3381 (sp^3 C-H str.), 3055, 3004, 2962, 2835, 1621, 1596, 1578, 1502, 1459, 1445, 1433, 1392, 1356, 1319, 1265 (C-O str.), 1208, 1163, 1133, 1115, 1025 (C-O str.), 951, 850, 830 (C-H oop), 767, 706, 660, 617; **^{1}H NMR (600 MHz, $CDCl_3$) δ** 8.82 (dd, J^3 = 4.2 Hz, J^4 = 1.6 Hz 1H, H-2), 8.05 (dd, J^3 = 8.0 Hz, J^4 = 1.0 Hz, 1H, H-4), 7.68 (d, J^3 = 8.9 Hz, 1H, H-5), 7.42 (d, J^4 = 2.4 Hz, 1H, H-8), 7.27-7.23 (m, 1H, H-3), 7.19 (dd, J^3 = 8.9 Hz, J^4 = 2.5 Hz, 1H, H-6), 3.94 (s, 3H, OCH_3); **^{13}C NMR (151 MHz, $CDCl_3$) δ** 160.7 (C-2), 150.6 (C-7), 150.0 (C-8a), 135.7 (C-4), 128.9 (C-5), 123.6 (C-4a), 119.9 (C-3), 119.0 (C-6), 107.4 (C-8), 55.6 (C-9); **HRMS-TOF MS ES+: *m/z* [M+H]$^+$** calculated for $C_{10}H_{10}NO$: 160.0762; found: 160.0756. This corresponds well with the reported values.[136,200]

6.3.4 Synthesis of 7-Methoxyquinoline – Doebner-Miller Method

General Procedure[164]

To a 150 mL, 2-neck, round-bottom flask equipped with a condenser and rubber septum, was added 6M HCl (60 equivalents) and heated to 70 ºC followed by the addition of the respective *m*-substituted aniline (1 equivalent, OCH_3) in a single portion. The reaction mixture was stirred under reflux at 70 ºC until the evolution of gas had ceased and no white vapor was visible in the flask. Toluene was added to the reaction flask in a single portion followed by the dropwise addition of acrolein (3 equivalents). The reaction temperature was increased to 85 ºC and held at this temperature for 15 minutes after which the temperature was increased to 105 ºC for a further 45 minutes. Once the time had elapsed, the reaction temperature was decreased to 90 ºC and the reaction heated under reflux for a further 45 minutes, monitoring the completion of the reaction by TLC. On completion, the reaction

mixture was cooled to room temperature and transferred to a 600 mL beaker using a small amount of water. The mixture was carefully neutralized with cold saturated sodium bicarbonate solution (excessive bubbling and overflow possible). Once a pH of ~8 was obtained, the aqueous mixture was extracted 3 × 150 mL EtOAc and 2 × 100 mL DCM and the organic layers combined. The combined organic layers were dried over anhydrous magnesium sulfate for 15 minutes, the organic solvent collected by filtration and concentrated *in vacuo*. The dark oily crude product was purified by automated gradient column chromatography (0 – 100% ethyl acetate/Hex) and the pure product was collected as a brown oil good yield.

7-Methoxyquinoline (23e).[164]

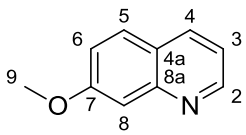

23e

The general procedure described above was followed using *m*-anisidine (1.82 mL, 2.00 g, 16.2 mmol), acrolein (3.26 mL, 2.73 g, 48.7 mmol), 6M HCl (30.8 mL, 35.5 g, 974 mmol) and 20.0 mL of toluene. The mixture was purified as described in the general procedure (R_f = 0.14, 15% EtOAc/Hex) and the product obtained as a red-brown oil (1.77 g, 11.2 mmol, 69%).

IR (ATR, cm^{-1}) 3200 (sp^3 C-H str.), 3004, 2937, 2835, 1621, 1596, 1578, 1502, 1459, 1445, 1433, 1393, 1356, 1319, 1265 (C-O str.), 1208, 1163, 1133, 1115, 1025 (C-O str.), 951, 850, 831 (C-H oop), 767, 706, 617; **^{1}H NMR (300 MHz, $CDCl_3$) δ** 8.81 (dd, J^3 = 4.3 Hz, J^4 = 1.7 Hz 1H, H-2), 8.05 (dd, J^3 = 8.1 Hz, J^4 = 1.3 Hz, 1H, H-4), 7.67 (d, J^3 = 8.9 Hz, 1H, H-5), 7.41 (d, J^4 = 2.5 Hz, 1H, H-8), 7.27-7.22 (m, 1H, H-3), 7.19 (dd, J^3 = 8.9 Hz, J^4 = 2.5 Hz, 1H, H-6), 3.94 (s, 3H, C-9); **^{13}C NMR (75 MHz, $CDCl_3$) δ** 160.7 (C-2), 150.6 (C-8a), 150.0 (C-7), 135.7 (C-4), 128.9 (C-5), 123.6 (C-4a), 119.9 (C-3), 119.0 (C-6), 107.4 (C-8), 55.6 (C-9); **HRMS-TOF MS ES+: *m/z* [M+H]$^+$** calculated for $C_{10}H_9NO_2$: 160.0762; found: 160.0757 This corresponds well with the reported values.[136,200]

6.3.5 Synthesis of 7-X-Quinoline *N*-Oxides (X =H and OCH_3)

General procedure[171]

To a 25 mL, 2-neck, round-bottom flask was added glacial acetic acid (11 equivalents) and 7-X-quinoline (1 equivalent). The flask was equipped with a condenser and the side-neck sealed with a rubber septum and the solution stirred at 70 ºC. 30% hydrogen peroxide (7 equivalents) was added dropwise over 1 minute to the reaction mixture and heated under reflux at 70 ºC for 24 hour. On completion, the reaction was cooled to room temperature and quenched with 10% sodium metasulfite. The aqueous solution was extracted with 3 × 100 mL of DCM and the combined organic layers dried over anhydrous magnesium sulfate for 15 minutes. The magnesium sulfate was collected by filtration

and the DCM removed *in vacuo* to give the crude product as a yellow oil. The crude product purified by automated gradient column chromatography using 0 – 100 % of 5% MeOH:EtOAc/Hex as solvent system. [The ethyl acetate was a 5% methanol/ethyl acetate mixture and facilitates effective separation of the oxide product from the baseline at 100% Ethyl acetate]

7-Methoxyquinoline 1-oxide (31e).[171]

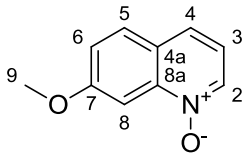

31e

The general procedure described above was followed using 7-methoxy-quinoline (1.00 g, 6.98 mmol), glacial acetic acid (4.39 mL, 4.61 g, 76.8 mmol) and 30% hydrogen peroxide (1.51 mL, 1.66 g, 48.8 mmol). The mixture was purified as described in the general procedure and the product obtained as a pale orange oil (R_f = 0.13, 100% EtOAc) that crystallized under vacuum (1.06 g, 6.07 mmol, 87%).

IR (ATR, cm^{-1}) 3400, 3060 (arom. C-H str.), 2917, 1567, 1510 (N-O pendulum str.), 1406, 1396, 1379, 1363, 1297 (N-O deform str.), 1255 (C-O str.), 1229, 1193, 1136, 1089 (C-O str.), 1070, 913, 862, 825, 812, 798, 783, 763, 745, 732; **^{1}H NMR (600 MHz, $CDCl_3$) δ** 8.69 (d, J^3 = 8.8 Hz, 1H, H-8), 8.50 (dd, J^3 = 6.0 Hz, J^4 = 0.7 Hz, 1H, H-2), 7.82 (dd, J^3 = 8.2 Hz, J^4 = 0.5 Hz, 1H, H-5), 7.71 (m, 1H, H-7, H-6), 7.59 (ddd, J^3 = 8.1 Hz, J^3 = 7.1 Hz, J^4 = 1.0 Hz 1H, H-4), 7.25 (t, J^3 = 8.4 Hz, 1H, H-3); **^{13}C NMR (151 MHz, $CDCl_3$) δ** 141.5 (C-8a), 140.6 (C-2), 135.7 (C-7), 130.5 (C-4a), 128.8 (C-5), 128.1 (C-6), 126.3 (C-4), 120.9 (C-3), 119.7 (C-8); **HRMS-TOF MS ES+: *m/z* [M+H]$^+$** calculated for $C_{10}H_9NO_2$: 176.0712; found: 176.0704. This corresponds well with the reported values.[156,175,205,206]

Quinoline 1-oxide (31i).[171]

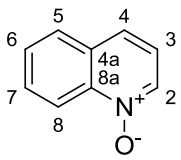

31i

The general procedure described above was followed using quinoline (0.910 mL, 1.00 g, 7.74 mmol), glacial acetic acid (4.86 mL, 5.11 g, 85.2 mmol) and 30% hydrogen peroxide (1.66 mL, 1.84 g, 54.2 mmol). The mixture was purified as described in the general procedure and the product was obtained as a yellow oil (R_f = 0.13, 100% EtOAc) that crystallized under vacuum (887 mg, 6.10 mmol, 79%).

Mp 60.3 – 62.2 °C; **IR (ATR, cm^{-1})** 3391, 3096, 3072, 1566, 1509 (N-O pendulum str.), 1439, 1393, 1305 (N-O deform. str.), 1261 (N-O pendulum), 1225, 1206, 1179, 1135, 1090, 1056, 1012, 878 (C-H arom. str.), 792, 783, 761, 723; **^{1}H NMR (400 MHz, $CDCl_3$) δ** 8.69 (d, J^3 = 8.8 Hz, 1H, H-8), 8.53-8.48 (m, 1H, H-2), 7.82 (dd, J^3 = 8.2 Hz, J^4 = 0.5 Hz, 1H, H-5), 7.75-7.67 (m, 1H, H-7, H-6), 7.63-7.56 (m, 1H, H-4), 7.28-7.21 (m, 1H, H-3); **^{13}C NMR (101 MHz, $CDCl_3$) δ** 141.5 (C-8a), 140.6 (C-2), 135.7 (C-7), 130.5 (C-4a), 128.8 (C-5), 128.1 (C-6), 126.3 (C-4), 120.9 (C-3), 119.7 (C-8); **HRMS-TOF MS ES+: *m/z* [M+H]$^+$** calculated for C_9H_8NO: 146.0608; found 146.0600. This corresponds well with the reported values.[156,175,205-208]

6.3.6 Synthesis of 4-cloro-quinoline from *N*-oxides

4-Chloro-7-methoxyquinoline (19e)

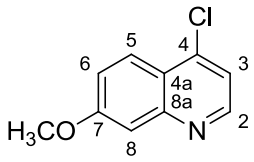

19e

The chlorination of the *N*-oxide **30e** was done by following the general procedure for chlorination described in the Gould-Jacobs method above, section 6.3.2. The procedure was followed using **30e** (0.332 g, 1.89 mmol) and phosphorous oxychloride (1.41 mL, 2.32 g, 15.2 mmol). The pure product was obtained as pale brown powder (0.137 g, 0.708 mmol, 37%).

Mp 85.1-86.4 °C; **^{1}H NMR (600 MHz, $CDCl_3$) δ** 8.68 (d, J^3 = 4.8 Hz, 1H, H-2), 8. 09 (d, J^3 = 9.2 Hz, 1H, H-5), 7.41 (d, J^3 = 2.5 Hz, 1H, H-8), 7.33 (d, J^3 = 4.8 Hz, 1H, H-3), 7.27 (dd, J^3 = 9.3 Hz, J^4 = 2.5 Hz 1H, H-6), 3.95 (s, 3H, OCH_3); **^{13}C NMR (151 MHz, $CDCl_3$) δ** 161.4 (C-7), 151.0 (C-2), 150.3 (C-8a), 142.5 (C-4), 125.3 (C-5), 121.7 (C-4a), 120.8 (C-6), 119.3 (C-3), 107.7 (C-8), 55.8 (C-9).[138,199]

6.3.7 Synthesis of 7-X-4-derivative-quinoline (X = CF_3, Cl and H)

General Procedure[38,138]

To a mixture of 7-X-4-chloroquinoline (X = F, Br, NO_2, CH_3 or OCH_3) and a minimal amount of toluene in a 25 mL round-bottom flask was added an excess of either ethane-1,2-diamine (5 equivalents) or N^1,N^1-diethylethane-1,2-diamine (5-10 equivalents) and heated to 160 ºC under reflux for 2 hours. The consumption of the 7-X-4-chloroquinoline was monitored by TLC (20% EtOAc/Hex) until completion was reached. The reaction mixture was cooled to room temperature and transferred to 100 mL beaker with a minimal amount of distilled water and then basified with 1 M sodium hydroxide to a pH of ~9. The aqueous mixture was extracted with DCM (3 × 60 mL), the organic layers were combined and washed with water (5 × 50 mL) to remove any excess diamine followed by washing with brine (100 mL). The combined organic layers were dried over magnesium sulfate for 20 minutes, filtered and the DCM removed *in vacuo*. The purification methods for the crude products varied depending on the substrate used and the diamine reagent that was substituted onto the 4 position.

N^1-[7-(Trifluoromethyl)quinolin-4-yl]ethane-1,2-diamine (12g).[38,138]

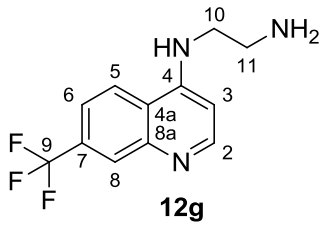

12g

The general procedure described above was followed using 4-chloro-(trifluoromethyl)quinoline (523 mg, 2.26 mmol) and ethane-1,2-diamine (0.75 mL, 0.67 g, 11 mmol). The crude product was obtained as a solid that was purified by heating the solid in hexane, cooling the mixture and removing the hexane via a Pasteur pipette. This process was repeated three times to remove the excess diamine. After drying for 48 hours in a vacuum desiccator, the product was obtained as a pale yellow powder (382 mg, 1.49 mmol, 73%).

Mp 87.3 – 88.9 °C; **IR (ATR, cm^{-1})** 3083 (1° N-H str.), 3056, 3031, 1608, 1578, 1553 (1° N-H scissor), 1485 (C-C in-ring str.), 1412, 1368, 1344, 1296, 1290, 1187, 1072 (1° N-H str.), 973, 876 (1° N-H wag), 844, 814, 679; **^{1}H NMR (400 MHz, $CDCl_3$) δ** 8.60 (d, J^3 = 5.3 Hz, 1H, H-2), 8.25 (s, 1H, H-8), 7.91 (d, J^3 = 8.7 Hz, 1H, H-5), 7.57 (s, J^3 = 8.7 Hz, J^4 = 1.8 Hz 1H, H-6), 6.48 (d, J^3 = 5.3 Hz, 1H, H-3), 5.92 (br s, 1H, NH), 3.39-3.27 (m, 2H, H-10) 3.17-3.08 (m, 2H, H-11), 1.35 (br s, J^2 = 30.8 Hz, 2H, NH_2);**^{13}C NMR (101 MHz, $CDCl_3$) δ** 152.4 (C-4), 149.8 (C-2), 147.8 (C-8a), 130.7 (C-7), 127.7 (q, J^1 = 4.3 Hz, C-9), 125.5 (C-8), 121.2 (C-5), 120.8 (C-4a), 120.1 (C-6), 100.3 (C-3), 44.8 (C-10), 40.2 (C-11); **HRMS-TOF MS ES+: *m/z* [M+H]$^+$** calculated for $C_{12}H_{13}F_3N_3$: 256.1062; found: 256.1068. This corresponds well with the reported values.[138]

N^1-(7-Chloroquinolin-4-yl)ethane-1,2-diamine (12h).[38,138]

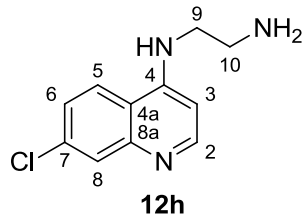

12h

The general procedure described above was followed using 4,7-dichloroquinoline (1.00 g, 5.05 mmol) and ethane-1,2-diamine (1.69 mL, 1.52 g, 25.25 mmol). The crude product was obtained as a solid that was purified by heating the solid in hexane, cooling the mixture and removing the hexane via a Pasteur pipette. This process was repeated three times to remove the excess diamine. After drying for 48 hours in a vacuum desiccator, the product was obtained as a pale yellow powder (0.47 g, 2.15 mmol, 43%).

Mp 131.4 – 132.3 °C; **IR (ATR, cm^{-1})** 3379, 3258 (1° N-H str.), 2961, 2941, 2904, 2864, 1593 (1° N-H scissor), 1541, 1471, 1458, 1432, 1376, 1322 (2° C-N str.), 1284, 1205, 1156, 1113, 1070 (1° C-N str.), 895 (1° N-H wag), 809, 738; **^{1}H NMR (400 MHz, $CDCl_3$) δ** 8.38 (d, J^3 = 5.4 Hz, 1H, H-2), 8.28 (d, J^3 = 9.0 Hz, 1H, H-5), 7.77 (d, J^4 = 2.2 Hz 1H, H-8), 7.44 (dd, J^3 = 8.9 Hz, J^4 = 2.2 Hz 1H, H-6), 7.23 (m, 1H, NH), 6.49 (d, J^3 = 5.4 Hz, 1H, H-3), 3.25 (dd, J^3 = 11.7 Hz, J^3 = 6.3 Hz, 2H, H-9), 2.82 (t, J^3 = 6.4 Hz, J^3 = 6.4 Hz, 2H, H-10); **^{13}C NMR (151 MHz, $CDCl_3$) δ** 152.2 (C-4), 150.0 (C-2), 149.2 (C-8a), 134.7 (C-7), 128.8 (C-8), 125.3 (C-5), 121.3 (C-6), 117.5 (C-4a), 99.4 (C-3), 46.6 (C-9), 39.8 (C-10); **HRMS-TOF MS ES+: *m/z* [M+H]$^+$** calculated for $C_{11}H_{13}ClN_3$: 222.0798; found: 222.0795. This corresponds well with the reported values.[38,63,66,138,211]

N^1,N^1-diethyl-N^2-[7-(trifluoromethyl)quinolin-4-yl]ethane-1,2-diamine (13g).[38,138]

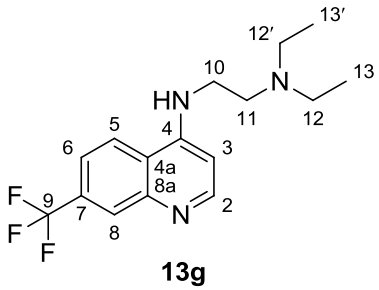

13g

The general procedure described above was followed using 4-chloro-(trifluoromethyl)quinoline (1.01 g, 4.32 mmol) and N^1,N^1-diethylethane-1,2-diamine (4.25 mL, 3.51 g, 30.2 mmol). The crude product was obtained as a solid that was purified by heating the solid in hexane, cooling the mixture and removing the hexane via a Pasteur pipette. This process was repeated three times to remove the excess diamine. After drying for 48 hours in a vacuum desiccator, the product was obtained as a yellow solid (1.07 g, 34.3 mmol, 79%).

Mp 98.8 – 100.0 °C; **IR (ATR, cm^{-1})** 3219 (2° N-H str.) , 3074, 2975 (sp^3 C-H str.), 2940, 2806, 1587 (N-H bend), 1568, 1552, 1465, 1430, 1376, 1323, 1277, 1204, 1182, 1160, 1136, 1119 (C-F str.), 1069 (C-N str.), 901, 811 (N-H oop bend), 739, 681; **^{1}H NMR (300 MHz, $CDCl_3$) δ** 8.61 (d, J^3 = 5.3 Hz, 1H, H-2), 8.26 (s, 1H, H-8), 7.85 (d, J^3 = 8.7 Hz, 1H, H-5), 7.60 (dd, J^3 = 8.7 Hz, J^4 = 1.8 Hz, 1H, H-6), 6.45 (d, J^3 = 5.3 Hz, 1H, H-3), 6.22 (br s, NH), 3.32-3.23 (m, 2H, H-10), 2.84 (t, J^3 = 5.7 Hz, 2H, H-11), 2.62 (q, J^3 = 7.1 Hz, 4H, H-12, H-12′), 1.09 (t, J^3 = 7.1 Hz, 6H, H-13, H-13′); **^{13}C NMR (75 MHz, $CDCl_3$) δ** 152.5 (C-4), 149.8 (C-2), 147.8 (C-8a), 131.1 (C-7), 130.7 (C-8), 127.7 (q, J^1 = 4.3 Hz, C-9), 122.4 (C-5), 121.1 (C-6), 120.9 (C-4a), 100.4 (C-3), 50.7 (C-11), 46.6 (C-12, C-12′), 39.8 (C-10), 12.2 (C-13, C-13′); **HRMS-TOF MS ES+: *m/z* [M+H]$^+$** calculated for $C_{16}H_{21}F_3N_3$: 312.1688; found: 312.1681. This corresponds well with the reported values.[44,137]

N^1-(7-chloroquinolin-4-yl)-N^2,N^2-diethylethane-1,2-diamine (13h).[38,138]

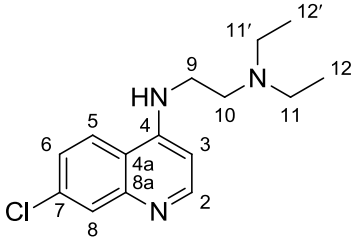

13h

The general procedure described above was followed using 4,7-dichloroquinoline (300 mg, 1.51 mmol) and N^1,N^1-diethylethane-1,2-diamine (1.10 mL, 0.88 mg, 54.5 mmol). The crude product was obtained as a solid that was purified by heating the solid in hexane, cooling the mixture and removing the hexane via a Pasteur pipette. This process was repeated three times to remove the excess diamine. After drying for 48 hours in a vacuum desiccator, the product was obtained as a yellow crystalline material (369 mg, 1.33 mmol, 88%).

Mp 103.4 – 103.9 °C; **IR (ATR, cm^{-1})** 3230 (2° N-H str.), 3065, 2968 (sp^3 C-H str.), 2934, 2801, 1611, 1577 (N-H bend), 1551, 1449, 1428, 1370, 1312, 1282, 1256, 1201, 1138, 1078 (C-N str.), 877, 848, 804 (N-H oop bend); **^{1}H NMR (600 MHz, $CDCl_3$) δ** 8.51 (d, J^3 = 5.3 Hz, 1H, H-2), 7.94 (d, J^4 = 2.1 Hz, 1H, H-8), 7.65 (d, J^3 = 8.9 Hz, 1H, H-5), 7.35 (dd, J^3 = 8.9 Hz, J^4 = 2.1 Hz, 1H, H-6), 6.35 (d, J^3 = 5.3 Hz, 1H, H-3), 6.11 (br s, NH), 3.27-3.23 (m, 2H, H-9), 2.81 (t, J^3 = 5.9 Hz, 2H, H-10), 2.59 (q, J^3 = 7.1 Hz, 4H, H-11, H-11′), 1.07 (t, J^3 = 7.1 Hz, 6H, H-12, H-12′); **^{13}C NMR (151 MHz,**

$CDCl_3$) δ 152.2 (C-4), 150.0 (C-2), 149.2 (C-8a), 134.9 (C-7), 128.8 (C-8), 125.4 (C-5), 121.3 (C-6), 117.6 (C-4a), 99.4 (C-3), 50.7 (C-10), 46.6 (C-11, C-11′), 39.9 (C-9), 12.2 (C-12, C-12′); **HRMS-TOF MS ES+: *m/z* [M+H]$^+$** calculated for $C_{15}H_{21}ClN_3$: 274.1424; found: 278.1419. This corresponds well with the reported values.[38,142,209,210]

***N*^{1},*N*^{1}-diethyl-*N*^{2}-(quinolin-4-yl)ethane-1,2-diamine (13i).**[38,138]

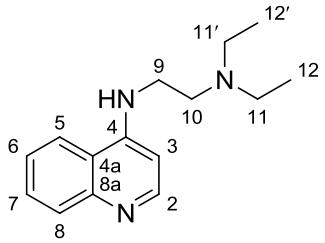

13i

The general procedure described above was followed using 4-chloroquinoline (500 mg, 3.05 mmol) and *N*^{1},*N*^{1}-diethylethane-1,2-diamine (3.00 mL, 2.49 g, 21.4 mmol). The crude product was obtained as a solid that was purified by heating the solid in hexane, cooling the mixture and removing the hexane via a Pasteur pipette. This process was repeated three times to remove the excess diamine. After drying for 48 hours in a vacuum desiccator, the product was obtained as a brown oil (542 mg, 2.22 mmol, 73%).

IR (ATR, cm^{-1}) 3259 (2° N-H str.), 3068, 2967 (sp^3 C-H str.), 2933, 2871, 2811, 1581 (N-H bend), 1529, 1454, 1372, 1335, 1238, 1201, 1126, 1066, 1040, 809 (N-H oop bend), 760; **^{1}H NMR (600 MHz, $CDCl_3$) δ** 8.52 (d, J^3 = 5.3 Hz, 1H, H-2), 7.96 (d, J^3 = 8.4 Hz, J^4 = 0.7 Hz, 1H, H-5), 7.74 (dd, J^3 = 8.3 Hz, J^4 = 0.7 Hz, 1H, H-8), 7.64-7.58 (m, 1H, H-7), 7.42 (ddd, J^3 = 8.2 Hz, J^3 = 6.8 Hz, J^4 = 1.2 Hz 1H, H-6), 6.37 (d, J^3 = 5.3 Hz, 1H, H-3), 6.09 (br s, NH), 3.26 (q, J^2 = 10.4 Hz, J^3 = 5.8 Hz, 2H, H-9), 2.83-2.79 (m, 2H, H-10), 2.59 (q, J^3 = 7.1 Hz, 4H, H-11, H-11′), 1.07 (t, J^3 = 7.1 Hz, 6H, H-12, H-12′); **^{13}C NMR (151 MHz, $CDCl_3$) δ** 151.1 (C-4), 150.0 (C-2), 148.4 (C-8a), 129.8 (C-7), 129.0 (C-8), 124.6 (C-6), 119.7 (C-5), 119.6 (C-4a), 99.0 (C-3), 50.8 (C-10), 46.6 (C-11, C-11′), 39.9 (C-9), 12.2 (C-12, C-12′); **HRMS-TOF MS ES+: *m/z* [M+H]$^+$** calculated for $C_{15}H_{22}N_3$: 244.1814; found: 244.1802. This corresponds well with the reported values.[38,44]

6.4 EXPERIMENTAL DATA PERTAINING TO CHAPTER 4

6.4.1 Synthesis of Novel Indole-Quinoline Hybrid Compounds

Hybrid Compounds H3g and H3h.

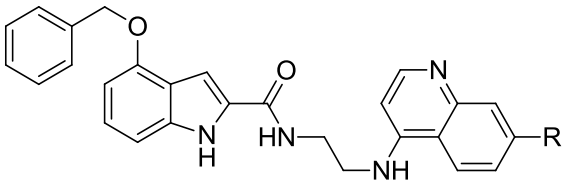

H3g–h

Although the reactions did not successfully form the desired hybrid compounds **H3g** and **H3h**, the procedure followed is described below for review purposes.

A 15 mL, 2-neck, round-bottom flask was equipped with a condenser and a nitrogen line followed by addition of dry THF (5 mL) and compound **10** (50 mg, 0.18 mmol) and stirred for 10 minutes to allow the indole **10** to dissolve. While the reaction mixture was stirring, the flask was flushed with nitrogen gas and sealed to maintain the inert atmosphere. CDI (33 mg, 0.21 mmol) was dissolved in the same solvent (2 mL) and drawn into a syringe in preparation for injection. After 10 minutes the indole **10** was dissolved and the CDI solution injected dropwise into the flask and the flask lowered into a 42 °C oil bath. The mixture was stirrer for a further 10 minutes followed by the addition of the amine **12g** (95 mg, 0.37 mmol) and the reaction left to stir for 16 hours. After the time had passed the reaction was cooled to room temperature and EtOAc (15 mL) added to the mixture, a yellow precipitate formed and was collected by vacuum filtration. The yellow precipitate was transferred to a glass vial, wrapped in foil and placed in a vacuum desiccator to dry for 24 hours.

The collected filtrate was collected and evaporated to remove the solvents giving a pale white residue which was dissolved in EtOAc and transferred to a separating funnel and water (20 mL) added. An extraction was performed and the water separated from the EtOAc followed by water (2 × 20 mL) to wash the EtOAc. The EtOAc was collected and dried over magnesium sulfate, filtered and evaporated to give a white residue. The residue was purified by column chromatography that afforded 2 white solids. The yellow precipitate and the two unknown white solids were all analyzed by NMR spectroscopy and found to be an unknown product (yellow solid) and recovered starting materials (white solids) with 62% of compound **10** and 48% of **2g** original amounts. The reaction procedure was repeated for amine 12h; however, similar results were obtained. The unknown yellow compound could not be characterized by NMR, MS or IR spectroscopy so the product remains unidentified.

CHAPTER 7: REFERENCES

References

1. Bell, A. S.; Mills, J. E.; Williams, G. P.; Brannigan, J. A.; Wilkinson, A. J.; Parkinson, T.; Leatherbarrow, R. J.; Tate, E. W.; Holder, A. A.; Smith, D. F. Selective inhibitors of protozoan protein *N*-myristoyltransferases as starting points for tropical disease medicinal chemistry programs. *PLoS. Negl. Trop. Dis.* **2012**, *6*.

2. AnonymousWHO | World Malaria Report 2014. http://www.who.int/malaria/publications/world_malaria_report_2014/report/en/ (accessed 11/23/2015).

3. AnonymousWHO | Achieving the malaria MDG target: reversing the incidence of malaria 2000–2015. http://www.who.int/malaria/publications/atoz/9789241509442/en/ (accessed 11/23/2015).

4. Nafo Traore, F. Rolling back malaria: opportunities and challenges. *Trans. R. Soc. Trop. Med. Hyg.* **2005**, *99*, 403-406.

5. AnonymousWHO | Global report on antimalarial efficacy and drug resistance: 2000-2010. http://www.who.int/malaria/publications/atoz/9789241500470/en/ (accessed 11/29/2015).

6. Bhatt, S.; Weiss, D. J.; Cameron, E.; Bisanzio, D.; Mappin, B.; Dalrymple, U.; Battle, K. E.; Moyes, C. L.; Henry, A.; Eckhoff, P. A.; Wenger, E. A.; Briët, O.; Penny, M. A.; Smith, T. A.; Bennett, A.; Yukich, J.; Eisele, T. P.; Griffin, J. T.; Fergus, C. A.; Lynch, M.; Lindgren, F.; Cohen, J. M.; Murray, C. L. J.; Smith, D. L.; Hay, S. I.; Cibulskis, R. E.; Gething, P. W. The effect of malaria control on *Plasmodium falciparum* in Africa between 2000 and 2015. *Nature* **2015**, *526*, 207-211.

7. Mendis, K.; Rietveld, A.; Warsame, M.; Bosman, A.; Greenwood, B.; Wernsdorfer, W. H. From malaria control to eradication: The WHO perspective. *Trop. Med. Int. Health* **2009**, *14*, 802-809.

8. Garcia, L. S. Malaria. *Clin. Lab. Med.* **2010**, *30*, 93-129.

9. Beadle, C.; Hoffman, S. L. History of malaria in the United States naval forces at War: World War I through the Vietnam conflict. *Clin. Infect. Dis.* **1993**, *16*, 320-329.

10. Baird, J. K. Resurgent malaria at the millennium: Control strategies in crisis. *Drugs* **2000**, *59*, 719-743.

11. Prajapati, S. M.; Patel, K. D.; Vekariya, R. H.; Panchal, S. N.; Patel, H. D. Recent advances in the synthesis of quinolines: A review. *RSC Adv.* **2014**, *4*, 24463-24476.

12. Kouznetsov, V. V.; Vargas Méndez, L. Y.; Meléndez Gómez, C. M. Recent progress in the synthesis of quinolines. *Curr. Org. Chem.* **2005**, *9*, 141-161.

13. Klein, E. Y. Antimalarial drug resistance: A review of the biology and strategies to delay emergence and spread. *Int. J. Antimicrob. Agents* **2013**, *41*, 311-317.

14. Hyde, J. E. Mechanisms of resistance of *Plasmodium falciparum* to antimalarial drugs. *Microbes Infect.* **2002**, *4*, 165-174.

15. Buller, R.; Peterson, M. L.; Almarsson, Ö; Leiserowitz, L. Quinoline binding site on malaria pigment crystal: A rational pathway for antimalaria drug design. *Cryst. Growth Des.* **2002**, *2*, 553-562.

16. Lee, S. J.; Seo, E.; Cho, Y. Proposal for a new therapy for drug-resistant malaria using *Plasmodium* synthetic lethality inference. *Int. J. Parasitol Drugs Drug Resist.* **2013**, *3*, 119-128.

17. Goncalves, V.; Brannigan, J. A.; Whalley, D.; Ansell, K. H.; Saxty, B.; Holder, A. A.; Wilkinson, A. J.; Tate, E. W.; Leatherbarrow, R. J. Discovery of *Plasmodium vivax N* -myristoyltransferase inhibitors: Screening, synthesis, and structural characterization of their binding mode. *J. Med. Chem.* **2012**, *55*, 3578-3582.

18. Waters, A. P. Guilty until proven otherwise. *Science* **2003**, *301*, 1487-1488.

19. Phillips, R. S. Current status of malaria and potential for control. *Clin. Microbiol. Rev.* **2001**, *14*, 208-226.

20. Klonis, N.; Dilanian, R.; Hanssen, E.; Darmanin, C.; Streltsov, V.; Deed, S.; Quiney, H.; Tilley, L. Hematin-hematin self-association states involved in the formation and reactivity of the malaria parasite pigment, hemozoin. *Biochemistry* **2010**, *49*, 6804-6811.

21. Tuteja, R. Malaria - An overview. *FEBS J.* **2007**, *274*, 4670-4679.

22. Cooke, B. M.; Mohandas, N.; Coppel, R. L. Malaria and the Red Blood Cell Membrane. *Semin. Hematol.* **2004**, *41*, 173-188.

23. Hall, N.; Karras, M.; Raine, J. D.; Carlton, J. M.; Kooij, T. W. A.; Berriman, M.; Florens, L.; Janssen, C. S.; Pain, A.; Christophides, G. K.; James, K.; Rutherford, K.; Harris, B.; Harris, D.; Churcher, C.; Quail, M. A.; Ormond, D.; Doggett, J.; Trueman, H. E.; Mendoza, J.; Bidwell, S. L.; Rajandream, M..; Carucci, D. J.; Yates III, J. R.; Kafatos, F. C.; Janse, C. J.; Barrell, B.; Turner, C. M. R.; Waters, A. P.; Sinden, R. E. A comprehensive survey of the *Plasmodium* life cycle by genomic, transcriptomic, and proteomic analyses. *Science* **2005**, *307*, 82-86.

24. Rasti, N.; Wahlgren, M.; Chen, Q. Molecular aspects of malaria pathogenesis. *FEMS Immunol. Med. Microbiol.* **2004**, *41*, 9-26.

25. Le Roch, K. G.; Zhou, Y.; Blair, P. L.; Grainger, M.; Moch, J. K.; Haynes, J. D.; De la Vega, P.; Holder, A. A.; Batalov, S.; Carucci, D. J.; Winzeler, E. A. Discovery of gene function by expression profiling of the malaria parasite life cycle. *Science* **2003**, *301*, 1503-1508.

26. Teguh, S. C.; Klonis, N.; Duffy, S.; Lucantoni, L.; Avery, V. M.; Hutton, C. A.; Baell, J. B.; Tilley, L. Novel conjugated quinoline-indoles compromise *Plasmodium falciparum* mitochondrial function and show promising antimalarial activity. *J. Med. Chem.* **2013**, *56*, 6200-6215.

27. Navarro, M.; Castro, W.; Biot, C. Bioorganometallic compounds with antimalarial targets: Inhibiting hemozoin formation. *Organometallics* **2012**, *31*, 5715-5727.

28. Müller, I. B.; Hyde, J. E. Antimalarial drugs: Modes of action and mechanisms of parasite resistance. *Future Microbiol.* **2010**, *5*, 1857-1873.

29. Olliaro, P. Mode of action and mechanisms of resistance for antimalarial drugs. *Pharmacol. Ther.* **2001**, *89*, 207-219.

30. Egan, T. J. Haemozoin (malaria pigment): A unique crystalline drug target. *Drug Discov. Today Targets* **2003**, *2*, 115-124.

31. Egan, T. J. Haemozoin formation. *Mol. Biochem. Parasitol.* **2008**, *157*, 127-136.

32. Kumar, S.; Guha, M.; Choubey, V.; Maity, P.; Bandyopadhyay, U. Antimalarial drugs inhibiting hemozoin (ß-hematin) formation: A mechanistic update. *Life Sci.* **2007**, *80*, 813-828.

33. Gamo, F. Antimalarial drug resistance: New treatments options for *Plasmodium*. *Drug Discov. Today Techn.* **2014**, *11*, 81-88.

34. Blackie, M. A. L.; Beagley, P.; Croft, S. L.; Kendrick, H.; Moss, J. R.; Chibale, K. Metallocene-based antimalarials: An exploration into the influence of the ferrocenyl moiety on in vitro antimalarial activity in chloroquine-sensitive and chloroquine-resistant strains of *Plasmodium falciparum*. *Bioorg. Med. Chem.* **2007**, *15*, 6510-6516.

35. Combrinck, J. M.; Mabotha, T. E.; Ncokazi, K. K.; Ambele, M. A.; Taylor, D.; Smith, P. J.; Hoppe, H. C.; Egan, T. J. Insights into the role of heme in the mechanism of action of antimalarials. *ACS Chem. Biol.* **2013**, *8*, 133-137.

36. Gildenhuys, J.; Roex, T. L.; Egan, T. J.; de Villiers, K. A. The single crystal X-ray structure of ß-hematin DMSO solvate grown in the presence of chloroquine, a ß-hematin growth-rate inhibitor. *J. Am. Chem. Soc.* **2013**, *135*, 1037-1047.

37. Slater, A. F. G.; Swiggard, W. J.; Orton, B. R.; Flitter, W. D.; Goldberg, D. E.; Cerami, A.; Henderson, G. B. An iron-carboxylate bond links the heme units of malaria pigment. *Proc. Natl. Acad. Sci. U. S. A.* **1991**, *88*, 325-329.

38. Egan, T. J.; Hunter, R.; Kaschula, C. H.; Marques, H. M.; Misplon, A.; Walden, J. Structure-function relationships in aminoquinolines: Effect of amino and chloro groups on quinoline-hematin complex formation, inhibition of ß- hematin formation, and antiplasmodial activity. *J. Med. Chem.* **2000**, *43*, 283-291.

39. Pagola, S.; Stephens, P. W.; Bohle, D. S.; Kosar, A. D.; Madsen, S. K. The structure of malaria pigment ß-haematin. *Nature* **2000**, *404*, 307-310.

40. Le Bras, J.; Durand, R. The mechanisms of resistance to antimalarial drugs in *Plasmodium falciparum*. *Fundam. Clin. Pharmacol.* **2003**, *17*, 147-153.

41. Egan, T. J. Structure-function relationships in chloroquine and related 4-aminoquinoline antimalarials. *Mini Rev. Med. Chem.* **2001**, *1*, 113-123.

42. Egan, T. J. Quinoline antimalarials. *Expert Opin. Ther. Pat.* **2001**, *11*, 185-209.

43. Biot, C.; Taramelli, D.; Forfar-Bares, I.; Maciejewski, L. A.; Boyce, M.; Nowogrocki, G.; Brocard, J. S.; Basilico, N.; Olliaro, P.; Egan, T. J. Insights into the mechanism of action of ferroquine. Relationship between physicochemical properties and antiplasmodial activity. *Mol. Pharm.* **2005**, *2*, 185-193.

44. Kaschula, C. H.; Egan, T. J.; Hunter, R.; Basilico, N.; Parapini, S.; Taramelli, D.; Pasini, E.; Monti, D. Structure-activity relationships in 4-aminoquinoline antiplasmodials. The role of the group at the 7-position. *J. Med. Chem.* **2002**, *45*, 3531-3539.

45. Cui, L.; Su, X. Discovery, mechanisms of action and combination therapy of artemisinin. *Expert Rev. Anti-Infect. Ther.* **2009**, *7*, 999-1013.

46. White, N. J. Qinghaosu (artemisinin): The price of success. *Science* **2008**, *320*, 330-334.

47. Chang, Z. The discovery of Qinghaosu (artemisinin) as an effective anti-malaria drug: A unique China story. *Sci. China Life Sci.* **2015**, 1-8.

48. Meshnick, S. R.; Taylor, T. E.; Kamchonwongpaisan, S. Artemisinin and the antimalarial endoperoxides: From herbal remedy to targeted chemotherapy. *Microbiol. Rev.* **1996**, *60*, 301-315.

49. Olliaro, P. L.; Haynes, R. K.; Meunier, B.; Yuthavong, Y. Possible modes of action of the artemisinin-type compounds. *Trends Parasitol.* **2001**, *17*, 122-126.

50. Hong, Y.; Yang, Y.; Meshnick, S. R. The interaction of artemisinin with malarial hemozoin. *Mol. Biochem. Parasitol.* **1994**, *63*, 121-128.

51. Asawamahasakda, W.; Ittarat, I.; Pu, Y.; Ziffer, H.; Meshnick, S. R. Reaction of antimalarial endoperoxides with specific parasite proteins. *Antimicrob. Agents Chemother.* **1994**, *38*, 1854-1858.

52. Pandey, A. V.; Tekwani, B. L.; Singh, R. L.; Chauhan, V. S. Artemisinin, an endoperoxide antimalarial, disrupts the hemoglobin catabolism and heme detoxification systems in malarial parasite. *J. Biol. Chem.* **1999**, *274*, 19383-19388.

53. Fisher, N.; Majid, R. A.; Antoine, T.; Al-Helal, M.; Warman, A. J.; Johnson, D. J.; Lawrenson, A. S.; Ranson, H.; O'Neill, P. M.; Ward, S. A.; Biagini, G. A. Cytochrome *b* mutation Y268S conferring atovaquone resistance phenotype in malaria parasite results in reduced parasite *bc1* catalytic turnover and protein expression. *J. Biol. Chem.* **2012**, *287*, 9731-9741.

54. Rackham, M. D.; Brannigan, J. A.; Moss, D. K.; Yu, Z.; Wilkinson, A. J.; Holder, A. A.; Tate, E. W.; Leatherbarrow, R. J. Discovery of novel and ligand-efficient inhibitors of *Plasmodium falciparum* and *Plasmodium vivax N*-myristoyltransferase. *J. Med. Chem.* **2013**, *56*, 371-375.

55. Wright, M. H.; Heal, W. P.; Mann, D. J.; Tate, E. W. Protein myristoylation in health and disease. *J. Chem. Biol.* **2010**, *3*, 19-35.

56. Wright, M. H.; Clough, B.; Rackham, M. D.; Rangachari, K.; Brannigan, J. A.; Grainger, M.; Moss, D. K.; Bottrill, A. R.; Heal, W. P.; Broncel, M.; Serwa, R. A.; Brady, D.; Mann, D. J.; Leatherbarrow, R. J.; Tewari, R.; Wilkinson, A. J.; Holder, A. A.; Tate, E. W. Validation of *N*-myristoyltransferase as an antimalarial drug target using an integrated chemical biology approach. *Nature Chem.* **2014**, *6*, 112-121.

57. Goncalves, V.; Brannigan, J. A.; Thinon, E.; Olaleye, T. O.; Serwa, R.; Lanzarone, S.; Wilkinson, A. J.; Tate, E. W.; Leatherbarrow, R. J. A fluorescence-based assay for *N*-myristoyltransferase activity. *Anal. Biochem.* **2012**, *421*, 342-344.

58. Yu, Z.; Brannigan, J. A.; Moss, D. K.; Brzozowski, A. M.; Wilkinson, A. J.; Holder, A. A.; Tate, E. W.; Leatherbarrow, R. J. Design and synthesis of inhibitors of *Plasmodium falciparum N*-myristoyltransferase, a promising target for antimalarial drug discovery. *J. Med. Chem.* **2012**, *55*, 8879-8890.

59. Sheng C.; Ji H.; Miao Z.; Che X.; Yao J.; Wang W.; Dong G.; Guo W.; Lü J.; Zhang W. Homology modeling and molecular dynamics simulation of *N*-myristoyltransferase from protozoan parasites: Active site characterization and insights into rational inhibitor design. *J. Comp. -Aided Mol. Des.* **2009**, *23*, 375-389.

60. Price, H. P.; Menon, M. R.; Panethymitaki, C.; Goulding, D.; McKean, P. G.; Smith, D. F. Myristoyl-CoA:Protein *N*-myristoyltransferase, an essential enzyme and potential drug target in kinetoplastid parasites. *J. Biol. Chem.* **2003**, *278*, 7206-7214.

61. Gordon, J. I.; Duronio, R. J.; Rudnick, D. A.; Adams, S. P.; Gokel, G. W. Protein *N*-myristoylation. *J. Biol. Chem.* **1991**, *266*, 8647-8650.

62. Sheng, C.; Xu, H.; Wang, W.; Cao, Y.; Dong, G.; Wang, S.; Che, X.; Ji, H.; Miao, Z.; Yao, J.; Zhang, W. Design, synthesis and antifungal activity of isosteric analogues of benzoheterocyclic *N*-myristoyltransferase inhibitors. *Eur. J. Med. Chem.* **2010**, *45*, 3531-3540.

63. Sunduru, N.; Sharma, M.; Srivastava, K.; Rajakumar, S.; Puri, S. K.; Saxena, J. K.; Chauhan, P. M. S. Synthesis of oxalamide and triazine derivatives as a novel class of hybrid 4-aminoquinoline with potent antiplasmodial activity. *Bioorg. Med. Chem.* **2009**, *17*, 6451-6462.

64. Kumar, A.; Srivastava, K.; Raja Kumar, S.; Puri, S. K.; Chauhan, P. M. S. Synthesis of new 4-aminoquinolines and quinoline-acridine hybrids as antimalarial agents. *Bioorg. Med. Chem. Lett.* **2010**, *20*, 7059-7063.

65. Singh, K.; Kaur, H.; Smith, P.; De Kock, C.; Chibale, K.; Balzarini, J. Quinoline-pyrimidine hybrids: Synthesis, antiplasmodial activity, SAR, and mode of action studies. *J. Med. Chem.* **2014**, *57*, 435-448.

66. Pinheiro, L. C. S.; Boechat, N.; Ferreira, M. D. L. G.; Júnior, C. C. S.; Jesus, A. M. L.; Leite, M. M. M.; Souza, N. B.; Krettli, A. U. Anti-*Plasmodium falciparum* activity of quinoline-sulfonamide hybrids. *Bioorg. Med. Chem.* **2015**, *23*, 5979-5984.

67. Oliveira, R.; Miranda, D.; Magalhães, J.; Capela, R.; Perry, M. J.; O'Neill, P. M.; Moreira, R.; Lopes, F. From hybrid compounds to targeted drug delivery in antimalarial therapy. *Bioorg. Med. Chem.* **2015**, *23*, 5120-5130.

68. Muregi, F. W.; Ishih, A. Next-generation antimalarial drugs: Hybrid molecules as a new strategy in drug design. *Drug Dev. Res.* **2010**, *71*, 20-32.

69. Anderson, J.; Forssberg, H.; Zierath, J. R. Avermectin and Artemisinin - Revolutionary Therapies against Parasitic Diseases. *http://www.nobelprize.org/nobel_prizes/medicine/laureates/2015/advanced-medicineprize2015.pdf* (accessed 12/29,2015).

70. Kaur, K.; Jain, M.; Kaur, T.; Jain, R. Antimalarials from nature. *Bioorg. Med. Chem.* **2009**, *17*, 3229-3256.

71. Morphy, R.; Rankovic, Z. Designed multiple ligands. An emerging drug discovery paradigm. *J. Med. Chem.* **2005**, *48*, 6523-6543.

72. Vandekerckhove, S.; D'Hooghe, M. Quinoline-based antimalarial hybrid compounds. *Bioorg. Med. Chem.* **2015**, *23*, 5098-5119.

73. Baeyer, A. Ueber die Reduction aromatischer Verbindungen mittelst Zinkstaub. *Ann* **1866**, *140*, 295-296.

74. Inman, M.; Moody, C. J. Indole synthesis-something old, something new. *Chem. Sci.* **2013**, *4*, 29-41.

75. Taber, D. F.; Tirunahari, P. K. Indole synthesis: A review and proposed classification. *Tetrahedron* **2011**, *67*, 7195-7210.

76. Park, J.; Kim, S.; Kim, J.; Cho, C. Intramolecular fischer indole synthesis in combination with alkyne hydroarylation: Synthesis of tetracyclic chromeno-indoles. *Org. Lett.* **2014**, *16*, 178-181.

77. Inman, M.; Moody, C. J. A two step route to indoles from haloarenes - A versatile variation on the Fischer indole synthesis. *Chem. Commun.* **2011**, *47*, 788-790.

78. Vicente, R. Recent advances in indole syntheses: New routes for a classic target. *Org. Biomol. Chem.* **2011**, *9*, 6469-6480.

79. Quin, L. D.; Tyrell, J. A. *Fundamentals of heterocyclic chemistry : importance in nature and in the synthesis of pharmaceuticals;* John Wiley & Sons, Inc. Hoboken, New Jersey, 2010; pp 357.

80. Heaner IV, W. L.; Gelbaum, C. S.; Gelbaum, L.; Pollet, P.; Richman, K. W.; Dubay, W.; Butler, J. D.; Wells, G.; Liotta, C. L. Indoles via Knoevenagel-Hemetsberger reaction sequence. *RSC Adv.* **2013**, *3*, 13232-13242.

81. Al-Said, N. H.; Shawakfeh, K. Q.; Abdullah, W. N. Cyclization of free radicals at the C-7 position of ethyl indole-2-carboxylate derivatives: An entry to a new class of duocarmycin analogues. *Molecules* **2005**, *10*, 1446-1457.

82. Ranasinghe, N.; Jones, G. B. Extending the versatility of the Hemetsberger-Knittel indole synthesis through microwave and flow chemistry. *Bioorg. Med. Chem. Lett.* **2013**, *23*, 1740-1742.

83. Lehmann, F.; Holm, M.; Laufer, S. Rapid and easy access to indoles via microwave-assisted Hemetsberger-Knittel synthesis. *Tetrahedron Lett.* **2009**, *50*, 1708-1709.

84. Stokes, B. J.; Dong, H.; Leslie, B. E.; Pumphrey, A. L.; Driver, T. G. Intramolecular C-H amination reactions: Exploitation of the Rh 2(II)-catalyzed decomposition of azidoacrylates. *J. Am. Chem. Soc.* **2007**, *129*, 7500-7501.

85. Larock, R. C.; Yum, E. K.; Refvik, M. D. Synthesis of 2,3-disubstituted indoles via palladium-catalyzed annulation of internal alkynes. *J. Org. Chem.* **1998**, *63*, 7652-7662.

86. Nair, V.; George, T. G. A novel synthesis of α-azidocinnamates, α-azido-α,ß-unsaturated ketones and ß-azidostyrenes mediated by cerium(IV) ammonium nitrate. *Tetrahedron Lett.* **2000**, *41*, 3199-3201.

87. Chang, M.; Lin, C.; Sun, P. Synthesis of phenylalanine analogs. *J. Chin. Chem. Soc.* **2005**, *52*, 1061-1067.

88. Clayden, J.; Greeves, N.; Warren, S. *Organic chemistry;* Oxford University Press: Oxford; New York, 2001 .

89. Wuts, P. G. M. Greene's Protective Groups in Organic Synthesis: Fifth Edition. In *Greene's Protective Groups in Organic Synthesis: Fifth Edition* 2014; pp 1-1360.

90. Wang, Z.; Li, Z.; Liu, T.; Ren, J. A new synthesis for methyl 2-benzyloxylphenylacetate. *Synthetic Communications* **1999**, *29*, 2361-2364.

91. Nakamura, K.; Ohmori, K.; Suzuki, K. The flavan-isoflavan rearrangement: Bioinspired synthetic access to isoflavonoids via 1,2-shift-alkylation sequence. *Chem. Commun.* **2015**, *51*, 7012-7014.

92. Golas, P. L.; Tsarevsky, N. V.; Matyjaszewski, K. Structure-reactivity correlation in "Click" chemistry: Substituent effect on azide reactivity. *Macromol. Rapid Commun.* **2008**, *29*, 1167-1171.

93. Zheng, H.; McDonald, R.; Hall, D. G. Boronic acid catalysis for mild and selective [3+2] dipolar cycloadditions to unsaturated carboxylic acids. *Chem. Eur. J.* **2010**, *16*, 5454-5460.

94. Albanese, D. Liquid-Liquid Phase Transfer Catalysis: Basic Principles and Synthetic Applications. *Catal. Rev. Sci. Eng.* **2003**, *45*, 369-395.

95. Senthamizh, S. R.; Nanthini, R.; Sukanyaa, G. The basic principle of phase-transfer catalysis, some mechanistic aspects and important applications. *IJSTR* **2012**, *1*, 21 December 2015.

96. Makosza, M.; Fedorynski, M. Phase transfer catalysis. *Catal. Rev. Sci. Eng.* **2003**, *45*, 321-367.

97. Bergman J.A.; Hahne K.; Song J.; Hrycyna C.A.; Gibbs R.A. *S*-farnesyl-thiopropionic acid triazoles as potent inhibitors of isoprenylcysteine carboxyl methyltransferase. *ACS Med. Chem. Lett.* **2012**, *3*, 15-19.

98. Smith, C. J.; Smith, C. D.; Nikbin, N.; Ley, S. V.; Baxendale, I. R. Flow synthesis of organic azides and the multistep synthesis of imines and amines using a new monolithic triphenylphosphine reagent. *Org. Biomol. Chem.* **2011**, *9*, 1927-1937.

99. Menegatti Chapter 2, R. Green Chemistry - Environmentally Benign Approaches; Green Chemistry – Aspects for the Knoevenagel Reaction. **2012**.

100. Bigi, F.; Quarantelli, C. The Knoevenagel condensation in water. *Curr. Org. Synth.* **2012**, *9*, 31-39.

101. Henn, L.; Hickey, D. M. B.; Moody, C. J.; Rees, C. W. Formation of indoles, isoquinolines, and other fused pyridines from azidoacrylates. *J. Chem. Soc. [Perkin 1]*. **1984**, 2189-2196.

102. Ando, K. A mechanistic study of the Horner-Wadsworth-Emmons reaction: Computational investigation on the reaction pass and the stereochemistry in the reaction of lithium enolate derived from trimethyl phosphonoacetate with acetaldehyde. *J. Org. Chem.* **1999**, *64*, 6815-6821.

103. Ando, K.; Yamada, K. Solvent-free Horner-Wadsworth-Emmons reaction using DBU. *Tetrahedron Lett.* **2010**, *51*, 3297-3299.

104. Ando, K.; Yamada, K. Highly *E*-selective solvent-free Horner-Wadsworth-Emmons reaction catalyzed by DBU. *Green Chem.* **2011**, *13*, 1143-1146.

105. Harwood, H. J.; Grisley Jr., D. W. The unexpected course of several Arbuzov-Michaelis reactions; an example of the nucleophilicity of the phosphoryl group. *J. Am. Chem. Soc.* **1960**, *82*, 423-426.

106. Gerrard, W.; Green, W. J. Mechanism of the formation of dialkyl alkylphosphonates. *J. Chem. Soc. [Resumed]* **1951**, 2550-2553.

107. Garner, A. Y.; Chapin, E. C.; Scanlon, P. M. Mechanism of the Michaelis-Arbuzov reaction: Olefin formation. *J. Org. Chem.* **1959**, *24*, 532-536.

108. Johnson, J. W.; Evanoff, D. P.; Savard, M. E.; Lange, G.; Ramadhar, T. R.; Assoud, A.; Taylor, N. J.; Dmitrienko, G. I. Cyclobutanone mimics of penicillins: Effects of substitution on conformation and hemiketal stability. *J. Org. Chem.* **2008**, *73*, 6970-6982.

109. Kartha, K. K.; Praveen, V. K.; Babu, S. S.; Cherumukkil, S.; Ajayaghosh, A. Pyridyl-amides as a multimode self-assembly Driver for the design of a stimuli-responsive *p*-gelator. *Chem. Asian J.* **2015**, *10*, 2250-2256.

110. Byrne, P. A.; Gilheany, D. G. The modern interpretation of the Wittig reaction mechanism. *Chem. Soc. Rev.* **2013**, *42*, 6670-6696.

111. Vedejs, E.; Snoble, K. A. J. Direct observation of oxaphosphetanes from typical wittig reactions [15]. *J. Am. Chem. Soc.* **1973**, *95*, 5778-5780.

112. Vedejs, E.; Marth, C. F. Oxaphosphetane pseudorotation: Rates and mechanistic significance in the Wittig reaction. *J. Am. Chem. Soc.* **1989**, *111*, 1519-1520.

113. Vedejs, E. Georg Wittig and the Betaine: What Controversy? *Phosphorus Sulfur Silicon Relat. Elem.* **2015**, *190*, 612-618.

114. Vedejs, E.; Marth, C. F. Mechanism of the Wittig reaction: The role of substituents at phosphorus. *J. Am. Chem. Soc.* **1988**, *110*, 3948-3958.

115. Vedejs, E.; Fleck, T. J. Kinetic (not equilibrium) factors are dominant in Wittig reactions of conjugated ylides. *J. Am. Chem. Soc.* **1989**, *111*, 5861-5871.

116. Robiette, R.; Richardson, J.; Aggarwal, V. K.; Harvey, J. N. Reactivity and selectivity in the Wittig reaction: A computational study. *J. Am. Chem. Soc.* **2006**, *128*, 2394-2409.

117. Robiette, R.; Richardson, J.; Aggarwal, V. K.; Harvey, J. N. On the origin of high E selectivity in the Wittig reaction of stabilized ylides: Importance of dipole-dipole interactions. *J. Am. Chem. Soc.* **2005**, *127*, 13468-13469.

118. Seguineau, P.; Villieras, J. The Wittig-Horner reaction in heterogeneous media: Synthesis of α-deuterated functional olefins using potassium carbonate with deuterium oxide. *Tetrahedron Lett.* **1988**, *29*, 477-480.

119. Li, D.; Zhang, Y. Applications of mesoporous titanium phosphonate functionalized with carboxylic groups. *RSC Adv.* **2014**, *4*, 44229-44233.

120. Aeluri, M.; Pramanik, C.; Chetia, L.; Mallurwar, N. K.; Balasubramanian, S.; Chandrasekar, G.; Kitambi, S. S.; Arya, P. 14-membered macrocyclic ring-derived toolbox: The identification of

small molecule inhibitors of angiogenesis and early embryo development in zebrafish assay. *Org. Lett.* **2013**, *15*, 436-439.

121. Dong, L.; Miller, M. J. Total synthesis of exochelin MN and analogues. *J. Org. Chem.* **2002**, *67*, 4759-4770.

122. Pavia, D. L. *Introduction to spectroscopy;* Brooks/Cole Cengage Learning: Australia; Belmont, CA, 2009.

123. Hwu, J. R.; King, K. Versatile reagent ceric ammonium nitrate in modern chemical synthesis. *Curr. Sci.* **2001**, *81*, 1043-1053.

124. Dincturk, S.; Ridd, J. H. - Reactions of cerium(IV) ammonium nitrate with aromatic compounds in acetonitrile. Part 1. The mechanism of side-chain substitution. *J. Chem. Soc., Perkin Trans. 2* , 961.

125. Dincturk, S.; Ridd, J. H. - Reactions of cerium(IV) ammonium nitrate with aromatic compounds in acetonitrile. Part 2. Nitration; comparison with reactions of nitric acid. *J. Chem. Soc., Perkin Trans. 2* , 965.

126. Nair, V.; Panicker, S. B.; Augustine, A.; George, T. G.; Thomas, S.; Vairamani, M. An efficient bromination of alkenes using cerium(IV) ammonium nitrate (CAN) and potassium bromide. *Tetrahedron* **2001**, *57*, 7417-7422.

127. Nair, V.; Nair, L. G.; George, T. G.; Augustine, A. Cerium(IV) ammonium nitrate mediated addition of thiocyanate and azide to styrenes: Expeditious routes to phenacyl thiocyanates and phenacyl azides. *Tetrahedron* **2000**, *56*, 7607-7611.

128. Chawla, H. M.; Sharma, S. K.; Chakrabarty, K.; Bhanumati, S. A novel cerium(IV)-based conjunction catalyst for aromatic hydroxylation. *Journal of Molecular Catalysis* **1988**, *48*, 349-363.

129. Huang, W.; Zhang, X.; Liu, H.; Shen, J.; Jiang, H. New selective *O*-debenzylation of phenol with Mg/MeOH. *Tetrahedron Lett.* **2005**, *46*, 5965-5967.

130. Chouhan, M.; Kumar, K.; Sharma, R.; Grover, V.; Nair, V. A. $NiCl_2 \cdot 6H_2O/NaBH_4$ in methanol: A mild and efficient strategy for chemoselective deallylation/debenzylation of aryl ethers. *Tetrahedron Lett.* **2013**, *54*, 4540-4543.

131. Gray, N. M.; Dappen, M. S.; Cheng, B. K.; Cordi, A. A.; Biesterfeldt, J. P.; Hood, W. F.; Monahan, J. B. Novel indole-2-carboxylates as ligands for the strychnine-insensitive *N*-methyl-*D*-aspartate-linked glycine receptor. *J. Med. Chem.* **1991**, *34*, 1283-1292.

132. Lins, G. O. W.; Campo, L. F.; Rodembusch, F. S.; Stefani, V. Novel ESIPT fluorescent benzazolyl-4-quinolones: Synthesis, spectroscopic characterization and photophysical properties. *Dyes Pigm.* **2010**, *84*, 114-120.

133. Salon, J.; Milata, V.; Prónayová, N.; Leško, J. The Gould-Jacobs reaction of 5-aminoquinoxaline. *Monatsh. Chem.* **2000**, *131*, 293-299.

134. Li, J.; Kung, D. W.; Griffith, D. A. Synthesis of 5-hydroxyquinolines. *Tetrahedron Lett.* **2010**, *51*, 3876-3878.

135. Zibaseresht, R.; Amirlou, M. R.; Karimi, P. An Efficient Two-step selective synthesis of 7-methyl-8-nitroquinoline from *m*-toluidine as a Key Starting Material in Medicinal Chemistry. *J. Arch. Mil. Med.* **2014**, *2*, e15957.

136. Saggadi, H.; Luart, D.; Thiebault, N.; Polaert, I.; Estel, L.; Len, C. Toward the synthesis of 6-hydroxyquinoline starting from glycerol via improved microwave-assisted modified Skraup reaction. *Cat. Comm.* **2014**, *44*, 15-18.

137. De, D.; Krogstad, F. M.; Byers, L. D.; Krogstad, D. J. Structure-activity relationships for antiplasmodial activity among 7 substituted 4-aminoquinolines. *J. Med. Chem.* **1998**, *41*, 4918-4926.

138. Nsumiwa, S.; Kuter, D.; Wittlin, S.; Chibale, K.; Egan, T. J. Structure-activity relationships for ferriprotoporphyrin IX association and ß-hematin inhibition by 4-aminoquinolines using experimental and ab initio methods. *Bioorg. Med. Chem.* **2013**, *21*, 3738-3748.

139. Vippagunta, S. R.; Dorn, A.; Matile, H.; Bhattacharjee, A. K.; Karle, J. M.; Ellis, W. Y.; Ridley, R. G.; Vennerstrom, J. L. Structural specificity of chloroquine-hematin binding related to inhibition of hematin polymerization and parasite growth. *J. Med. Chem.* **1999**, *42*, 4630-4639.

140. Gould Jr., R. G.; Jacobs, W. A. The synthesis of certain substituted quinolines and 5,6-benzoquinolines. *J. Am. Chem. Soc.* **1939**, *61*, 2890-2895.

141. Price, C. C.; Roberts, R. M. The synthesis of 4-hydroxyquinolines. I. Through ethoxymethylenemalonic ester. *J. Am. Chem. Soc.* **1946**, *68*, 1204-1208.

142. De, D.; Byers, L. D.; Krogstad, D. J. Antimalarials: Synthesis of 4-Aminoquinolines that circumvent drug resistance in malaria parasites. *J. Heterocycl. Chem.* **1997**, *34*, 315-320.

143. Riegel, B.; Lappin, G. R.; Adelson, B. H.; Jackson, R. I.; Albisetti Jr., C. J.; Dodson, R. M.; Baker, R. H. The synthesis of some 4-quinolinols and 4-chloroquinolines by the ethoxymethylenemalonic ester method. *J. Am. Chem. Soc.* **1946**, *68*, 1264-1266.

144. Leyva, E.; Monreal, E.; Hernández, A. Synthesis of fluoro-4-hydroxyquinoline-3-carboxylic acids by the Gould-Jacobs reaction. *J. Fluor. Chem.* **1999**, *94*, 7-10.

145. Price, C. C.; Snyder, H. R.; Bullitt Jr., O. H.; Kovacic, P. Synthesis of 4-hydroxyquinolines. IX. 4-chloro-7-cyanoquinoline and 4-chloro-5-cyanoquinoline. *J. Am. Chem. Soc.* **1947**, *69*, 374-376.

146. England C.; Funk J. E. Reduced product yield in chemical processes by second law effects. *Energy* **1979**, *5*, 941-947.

147. Gilmore R.; Levine R.D. Le Chateliers principle with multiple relaxation channels. *Phys. Rev. A* **1986**, *33*, 3328-3332.

148. Desai, N. D. The Gould-Jacob type of reaction for the synthesis of novel pyrimidopyrrolopyrimidines: A comparison of classical heating *vs* solvent free microwave irradiation. *J. Heterocycl. Chem.* **2006**, *43*, 1343-1348.

149. Yamashkin, S. A.; Oreshkina, E. A. Traditional and modern approaches to the synthesis of quinoline systems by the Skraup and Doebner-Miller methods. (Review). *Chem. Hetero. Comp.* **2006**, *42*, 701-718.

150. Leir, C. M. An improvement in the Doebner-Miller synthesis of quinaldines. *J. Org. Chem.* **1977**, *42*, 911-913.

151. Cohn, E. W. A modification of the Skraup synthesis of quinoline. *J. Am. Chem. Soc.* **1930**, *52*, 3685-3688.

152. Cohn, B. E. A modification of the Skraup synthesis of quinoline. *J. Am. Chem. Soc.* **1928**, *50*, 2709-2711.

153. Bartow, E. Syntheses of derivatives of quinoline. *J. Am. Chem. Soc.* **1904**, *26*, 700-705.

154. Tomisek, A.; Graham, B.; Griffith, A.; Pease, C. S.; Christensen, B. E. Syntheses of certain 8-nitroquinolines. *J. Am. Chem. Soc.* **1946**, *68*, 1587-1589.

155. Rodríguez, J. G.; de los Rios, C.; Lafuente, A. Synthesis of n-chloroquinolines and n-ethynylquinolines (n=2, 4, 8): homo and heterocoupling reactions. *Tetrahedron* **2005**, *61*, 9042-9051.

156. Heitman, L. H.; Göblyös, A.; Zweemer, A. M.; Bakker, R.; Mulder-Krieger, T.; van Veldhoven, J. P. D.; De Vries, H.; Brussee, J.; Ijzerman, A. P. A series of 2,4-disubstituted quinolines as a new class of allosteric enhancers of the adenosine A3 receptor. *J. Med. Chem.* **2009**, *52*, 926-931.

157. Ott, L.; Bicker, M.; Vogel, H. Catalytic dehydration of glycerol in sub- and supercritical water: A new chemical process for acrolein production. *Green Chem.* **2006**, *8*, 214-220.

158. Park, H.; Yun, Y. S.; Kim, T. Y.; Lee, K. R.; Baek, J.; Yi, J. Kinetics of the dehydration of glycerol over acid catalysts with an investigation of deactivation mechanism by coke. *Appl. Catal. B Environ.* **2015**, *176-177*, 1-10.

159. Nimlos, M. R.; Blanksby, S. J.; Qian, X.; Himmel, M. E.; Johnson, D. K. Mechanisms of glycerol dehydration. *J. Phys. Chem. A* **2006**, *110*, 6145-6156.

160. Kongpatpanich, K.; Nanok, T.; Boekfa, B.; Probst, M.; Limtrakul, J. Structures and reaction mechanisms of glycerol dehydration over H-ZSM-5 zeolite: A density functional theory study. *Phys. Chem. Chem. Phys.* **2011**, *13*, 6462-6470.

161. Delgado, M.; Desroches, M.; Ganachaud, F. Ionic oligomerization of acrolein in water. *RSC Adv.* **2013**, *3*, 23057-23065.

162. Schulz, R. C. Acrolein Polymers. *Angew. Chem. Int. Ed. Engl.* **1964**, *3*, 416-423.

163. Harless, M. L. Method and apparatus for remotely monitoring acrolein temperature in storage tanks. **2015**.

164. Matsugi, M.; Tabusa, F.; Minamikawa, J. Doebner-Miller synthesis in a two-phase system: Practical preparation of quinolines. *Tetrahedron Lett.* **2000**, *41*, 8523-8525.

165. Castellano, S.; Santoriello, M.; Campiglia, P.; Cardillo, G.; Bertamino, A.; Gomez-Monterrey, I.; Novellino, E.; Sbardella, G. A regioselective approach toward the synthesis of pharmacologically important quinone-containing heterocyclic systems. *Tetrahedron Lett.* **2009**, *50*, 6869-6871.

166. Madugula, S. R. M.; Thallapelly, S.; Bandarupally, J.; Yadav, J. S. Process for the synthesis of quinoline derivatives. **2010**.

167. Billah M.; Buckley G. M.; Cooper N.; Dyke H. J.; Egan R.; Ganguly A.; Gowers L.; Haughan A. F.; Kendall H. J.; Lowe C.; Minnicozzi M.; Montana J. G.; Oxford J.; Peake J. C.; Picken C. Louise; Piwinski J. J.; Naylor R.; Sabin V.; Shih N. Y.; Warneck J. B. H. 8-Methoxyquinolines as PDE4 inhibitors. *Bioorg. Med. Chem. Lett.* **2002**, *12*, 1617-1619.

168. Oleynik, I. I.; Shteingarts, V. D. Partially halogenated heterocycles. Synthesis of 5,7-difluoro, 5,6,7-trifluoro- and 7-chloro-6,8-difluoroquinolines. *J. Fluor. Chem.* **1998**, *91*, 25-26.

169. Bradford, L.; Elliott, T. J.; Rowe, F. M. 88. The Skraup reaction with *m*-substituted anilines. *J. Chem. Soc.*, 437.

170. Caillol, S.; Boutevin, B.; David, G.; Burguiere, C. Novel phenolic plastic resins obtained from phenolic compounds and macromolecular hardeners having aldehyde functions. **2012**.

171. Vörös, A.; Timári, G.; Baán, Z.; Mizsey, P.; Finta, Z. Preparation of pyridine *N*-oxide derivatives in microreactor. *Period. Polytech. Chem. Eng.* **2014**, *58*, 195-205.

172. Gubarev, Y. A.; Lebedeva, N. S.; Andreev, V. P.; Girichev, G. V. Thermal behavior of quinoline *N*-oxide hydrates and deuterohydrate. *Russ. J. Gen. Chem.* **2009**, *79*, 1183-1190.

173. Bernier, D.; Wefelscheid, U. K.; Woodward, S. Properties, preparation and synthetic uses of amine *N*-oxides. An update. *Organic Preparations and Procedures International* **2009**, *41*, 175-210.

174. Ochiai, E. Recent Japanese work on the chemistry of pyridine 1-oxide and related compounds. *J. Org. Chem.* **1953**, *18*, 534-551.

175. Zhong, P.; Guo, S.; Song, C. A Simple and Efficient Method for the Preparation of Heterocyclic *N*-Oxide. *Synth. Commun.* **2004**, *34*, 247-253.

176. Yokoyama, A.; Ohwada, T.; Saito, S.; Shudo, K. Nitration of quinoline 1-oxide: Mechanism of regioselectivity. *Chem. Pharm. Bull.* **1997**, *45*, 279-283.

177. Montalbetti, C. A. G. N.; Falque, V. Amide bond formation and peptide coupling. *Tetrahedron* **2005**, *61*, 10827-10852.

178. Ghose A. K.; Viswanadhan V. N.; Wendoloski J. J. A knowledge-based approach in designing combinatorial or medicinal chemistry libraries for drug discovery. 1. A qualitative and quantitative characterization of known drug databases. *J. Comb. Chem.* **1999**, *1*, 55-68.

179. Woodman, E. K.; Chaffey, J. G. K.; Hopes, P. A.; Hose, D. R. J.; Gilday, J. P. *N*,*N*-carbonyldiimidazole-mediated amide coupling: Significant rate enhancement achieved by acid catalysis with imidazole - HCI. *Org. Process. Res. Dev.* **2009**, *13*, 106-113.

180. Verma, S. K.; Ghorpade, R.; Pratap, A.; Kaushik, M. P. Solvent free, *N*,*N*'-carbonyldiimidazole (CDI) mediated amidation. *Tetrahedron Lett.* **2012**, *53*, 2373-2376.

181. Sharma, R. K. 1,1'-Carbonyldiimidazole (CDI). *Synlett* **2007**, 3073-3074.

182. Sharma, R. K.; Jain, R. Unprecedented 1,1'-carbonyldiimidazole-mediated amidation of unprotected a-amino acids in water. *Synlett* **2007**, 603-606.

183. Tukulula M.; Klein R.; Kaye P. T. Indolizine studies, part 5: Indolizine-2-carboxamides as potential HIV-1 protease inhibitors. *Synth. Commun.* **2010**, *40*, 2018-2028.

184. Métro, T.; Bonnamour, J.; Reidon, T.; Duprez, A.; Sarpoulet, J.; Martinez, J.; Lamaty, F. Comprehensive Study of the Organic-solvent-free CDI-mediated acylation of various nucleophiles by mechanochemistry. *Chem. Eur. J.* **2015**, *21*, 12787-12796.

185. Ivanov A.S.; Shishkov S.V. Synthesis of imatinib: A convergent approach revisited. *Monatsh. Chem.* **2009**, *140*, 619-623.

186. Larrlvée-Aboussafy C.; Jones B.P.; Price K.E.; Hardink M.A.; McLaughlin R.W.; Lillie B.M.; Hawkins J.M.; Vaidyanathan R. DBU catalysis of *N*,*N*'-carbonyldiimidazole-mediated amidations. *Org. Lett.* **2010**, *12*, 324-327.

187. Rannard, S. P.; Davis, N. J. The selective reaction of primary amines with carbonyl imidazole containing compounds: Selective amide and carbamate synthesis. *Org. Lett.* **2000**, *2*, 2117-2120.

188. Rannard, S. P.; Davis, N. J. Controlled synthesis of asymmetric dialkyl and cyclic carbonates using the highly selective reactions of imidazole carboxylic esters. *Org. Lett.* **1999**, *1*, 933-936.

189. Oakenfull, D. G.; Jencks, W. P. Reactions of acetylimidazole and acetylimidazolium ion with nucleophilic reagents. Structure-reactivity relationships. *J. Am. Chem. Soc.* **1971**, *93*, 178-188.

190. Oakenfull, D. G.; Salvesen, K.; Jencks, W. P. Reactions of acetylimidazole and acetylimidazolium ion with nucleophilic reagents. Mechanisms of catalysis. *J. Am. Chem. Soc.* **1971**, *93*, 188-194.

191. Villieras, J.; Rambaud, M.; Graff, M. La reaction de wittig-horner en milieu heterogene VI1. Selectivite de la reaction sur des composes bifonctionnels. *Tetrahedron Lett.* **1985**, *26*, 53-56.

192. Chen, Y.; Zacharias, J.; Vince, R.; Geraghty, R. J.; Wang, Z. C-6 aryl substituted 4-quinolone-3-carboxylic acids as inhibitors of hepatitis C virus. *Bioorg. Med. Chem.* **2012**, *20*, 4790-4800.

193. Singh, K.; Kaur, H.; Chibale, K.; Balzarini, J. Synthesis of 4-aminoquinoline - pyrimidine hybrids as potent antimalarials and their mode of action studies. *Eur. J. Med. Chem.* **2013**, *66*, 314-323.

194. Deshmukh, A. R. A. S.; Panse, D. G.; Bhawal, B. M. A clay catalyzed method for diethyl 2,2,2-trichloroethylidenepropanedioate, an efficient intermediate for the synthesis of enamino esters. *Synth. Commun.* **1999**, *29*, 1801-1809.

195. Devine, W.; Woodring, J. L.; Swaminathan, U.; Amata, E.; Patel, G.; Erath, J.; Roncal, N. E.; Lee, P. J.; Leed, S. E.; Rodriguez, A.; Mensa-Wilmot, K.; Sciotti, R. J.; Pollastri, M. P. Protozoan parasite growth inhibitors discovered by cross-screening yield potent scaffolds for lead discovery. *J. Med. Chem.* **2015**, *58*, 5522-5537.

196. Hwang, J. Y.; Kawasuji, T.; Lowes, D. J.; Clark, J. A.; Connelly, M. C.; Zhu, F.; Guiguemde, W. A.; Sigal, M. S.; Wilson, E. B.; Derisi, J. L.; Guy, R. K. Synthesis and evaluation of 7-substituted 4-aminoquinoline analogues for antimalarial activity. *J. Med. Chem.* **2011**, *54*, 7084-7093.

197. Illuminati, G.; Marino, G. Electronic transmission through condensed-ring systems. II. The kinetics of methoxydechlorination of some 6- and 7-substituted 1-aza-4-chloronaphthalenes. *J. Am. Chem. Soc.* **1958**, *80*, 1421-1424.

198. Matthews, R. S. ^{19}F NMR spectroscopy of polyhalonaphthalenes. Part IV. Halex reactions of polychloroquinolines. *J. Fluor. Chem.* **1998**, *91*, 203-205.

199. Lauer, W. M.; Arnold, R. T.; Tiffany, B.; Tinker, J. The synthesis of some chloromethoxyquinolines. *J. Am. Chem. Soc.* **1946**, *68*, 1268-1269.

200. Mash, E. A.; Aavula, B. R. Synthesis of 7-alkoxyquinolines, coumarins, and resorufins. *Synth. Commun.* **2000**, *30*, 367-375.

201. Palmer, M. H. 710. The Skraup reaction. Formation of 5- and 7-substituted quinolines. *J. Chem. Soc. [Resumed]* **1962**, 3645-3652.

202. Petasis, N. A.; Butkevich, A. N. Synthesis of ^{2}H-chromenes and 1,2-dihydroquinolines from aryl aldehydes, amines, and alkenylboron compounds. *J. Organomet. Chem.* **2009**, *694*, 1747-1753.

203. Shields, J. D.; Ahneman, D. T.; Graham, T. J. A.; Doyle, A. G. Enantioselective, nickel-catalyzed Suzuki cross-coupling of quinolinium ions. *Org. Lett.* **2014**, *16*, 142-145.

204. Washburn, L. C.; Barbee Jr., T. G.; Pearson, D. E. Potential antimalarials. V. 2-*p*-chlorophenyl-7-quinolinemethanols. *J. Med. Chem.* **1970**, *13*, 1004-1005.

205. Londregan, A. T.; Burford, K.; Conn, E. L.; Hesp, K. D. Expedient synthesis of *α*-(2-azaheteroaryl) acetates via the addition of silyl ketene acetals to azine- *N* -oxides. *Org. Lett.* **2014**, *16*, 3336-3339.

206. Zhang, H.; Huang, C. Reactivity and transformation of antibacterial *N*-oxides in the presence of manganese oxide. *Environ. Sci. Technol.* **2005**, *39*, 593-601.

207. Larionov, O. V.; Stephens, D.; Mfuh, A.; Chavez, G. Direct, catalytic, and regioselective synthesis of 2-alkyl-, aryl-, and alkenyl-substituted *N*-Heterocycles from *N*-oxides. *Org. Lett.* **2014**, *16*, 864-867.

208. Gopiraman, M.; Bang, H.; Babu, S. G.; Wei, K.; Karvembu, R.; Kim, I. S. Catalytic *N*-oxidation of tertiary amines on RuO_2NPs anchored graphene nanoplatelets. *Catal. Sci. Technolog.* **2014**, *4*, 2099-2106.

209. Nachod, F. C.; Surrey, A. R.; Lesher, G. Y.; Martini, C. M.; Mayer, J. R.; Priznar, M.; Webb, W. G. Intramolecular hydrogen bonding in 7-chloro-4-diethylaminoethylaminoquinoline. *J. Am. Chem. Soc.* **1959**, *81*, 2897-2898.

210. Nguyen, T.; Yang, T.; Go, M. Functionalized acridin-9-yl phenylamines protected neuronal HT22 cells from glutamate-induced cell death by reducing intracellular levels of free radical species. *Bioorg. Med. Chem. Lett.* **2014**, *24*, 1830-1838.

211. Pretorius, S. I.; Breytenbach, W. J.; de Kock, C.; Smith, P. J.; N'Da, D. D. Synthesis, characterization and antimalarial activity of quinoline-pyrimidine hybrids. *Bioorg. Med. Chem.* **2013**, *21*, 269-277.